Review

# Homoleptic transition metal acetylides

Roy Buschbeck[a], Paul J. Low[b], Heinrich Lang[a,*]

[a] Technische Universität Chemnitz, Fakultät für Naturwissenschaften, Institut für Chemie, Lehrstuhl für Anorganische Chemie, Straße der Nationen 62, 09111 Chemnitz, Germany
[b] Department of Chemistry, Durham University, South Rd, Durham DH1 3LE, UK

## Contents

### ARTICLE INFO

### ABSTRACT

The synthesis, structure, bonding motifs, reaction chemistry, and some potential applications of homoleptic metal alkynides, as well as current trends in this field of chemistry, are reported.

© 2010 Elsevier B.V. All rights reserved.

## 1. Introduction

A homoleptic transition metal complex may be defined as a metal complex in which all of the ligands bound to the d-block metal atom are identical. Common examples include $Ti(NMe_2)_4$, $WMe_6$, $Fe(CO)_5$, $Pd(PPh_3)_4$, and $[Ag(C\equiv N)_4]^{3-}$. Cyanide is perhaps one of the most common ligands in transition metal chemistry, and forms homoleptic complexes with every metal of the d-block [1]. The first example of a homoleptic cyanide complex, Prussian blue, was prepared, albeit serendipitously, over 300 years ago in Berlin, and this dark blue and non-toxic pigment has been widely used throughout the ensuing centuries [2]. This family of homoleptic compounds was enriched as early as in 1884 by the discovery of transition metal alkynides such as $[Hg(C\equiv CMe)_2]$ by Kutscheroff [3], and much of the early work has been summarized, albeit briefly [4].

Systematic studies of the alkynide ligand started in 1953 with the recognition that alkynides $[RC\equiv C]^-$ (R = H, single bonded

* Corresponding author.
  E-mail address: heinrich.lang@chemie.tu-chemnitz.de (H. Lang).
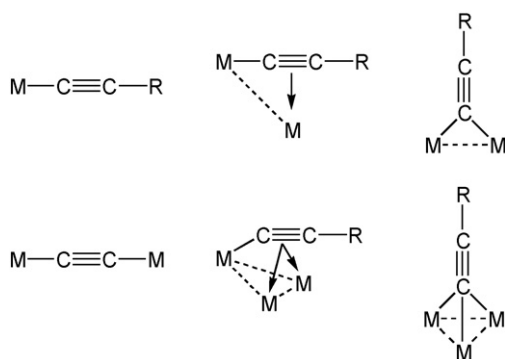
**Scheme 1.** A selection of bonding modes commonly observed in metal-alkynide complexes.

organic group) should show similar ligating behavior to the isoelectronic cyanide, $[N\equiv C]^-$ [5–7]. This was confirmed by the isolation of complexes of general formula $[M(C\equiv CR)_m]^{(m-n)-}$ (M = d-metal atom, $m$ = number of alkynide ligands, $n$ = oxidation number of M) through the outstanding and pioneering work of Nast [5]. Alkynides are very strong σ-donating ligands with minimal steric hindrance around the donor carbon atom. However, the substituent R can provide a degree of steric bulk to kinetically stabilize the resulting complexes. This is important because, in contrast to metal cyanide complexes that are typically robust species, the corresponding metal alkynides are, depending on the nature of R and M, often thermally sensitive, and reactive towards moisture and air or protic solvents, which can be explained by the high basicity of the mono-valent acetylide $[RC\equiv C]^-$ anion.

Against this background, homoleptic alkynide complexes have been receiving considerable attention in recent years due to their rich structural diversity, intriguing physical properties (photophysical, photochemical and electrochemical behavior) and potential applications in materials science, for example, optoelectronics and luminescence signaling [8–14]. d-Block metal carbon bonds are of covalent nature both for alkynide and cyanide transition metal complexes, with the possibility of additional $d_\pi$–$p_\pi$ interactions in the case of the alkynides (Scheme 1). This makes these compounds attractive because alkynides can coordinate and bind to metals in a variety of ways [15,16]. Thus, homoleptic complexes of type $[M(C\equiv CR)_m]^{(m-n)-}$ constitute a class of metal alkynides well suited to use in the synthesis of related higher nuclear organometallic systems, i.e., clusters such as $[Ag_{14}(C\equiv C^tBu)_{12}Cl]$ [17] and $[(AuC\equiv C^tBu)_6]_2$ [18] which display intermolecular interactions between the metal-alkynide fragments.

This review is intended to cover major aspects of homoleptic neutral and ionic mono- and polynuclear transition metal alkynide complexes including cluster complexes and metallocarbohedrenes. The synthesis, characterization, reactivity, reaction chemistry and structure and bonding of these systems will be highlighted. Where appropriate, applications are mentioned and mechanisms of formation and reaction are discussed.

## 2. Metallocarbohedrenes

Following the first observations of a metallocarbohedrene (= met-car) ($Ti_8C_{12}$) by mass spectrometry in 1992 by Castleman and coworkers [19,20], this class of molecular clusters with "magic-number" stoichiometry $M_8C_{12}$ (M = mainly early transition metal, including Ti, Zr, Hf, V, Nb, Mo) rapidly developed (Table 1) [21,22]. The discovery, synthesis and ionization dynamics of met-cars was summarized in two excellent reviews written by Leskiw and Castleman [21], and Rohmer et al. [22]. Since then, much experimental and theoretical work has focused on met-cars and their reactivity toward other molecules which will be discussed within this Chapter.

The composition of the cage-like met-car systems, which are thought to be *iso* structural, isoelectronic and, with some consideration given to the role of d-orbitals in the met-car bonding, isolobal with the elusive $C_{20}$ pentagonal dodecahedron, can be selectively chosen through synthetic methodologies [21,22]. Facile preparative routes to mixed metal nanoscale met-cars are also known [22]. These well behaved metal–carbon clusters are of interest both as stable and *meta*-stable new materials, as building blocks for new nanostructured, cluster-assembled materials with tailored properties, and as model compounds in catalysis [22]. This unique family of molecular carbon–metal clusters exhibit free electron behavior resulting from changing electronic energy levels with the nature of the appropriate transition metal [21]. Thus met-cars possess unusual electronic properties by virtue of their size and structure, making them excellent candidates as semi-conductors, implants for quantum dot devices as well as for use in the production of solar cells, photovoltaic devices and optical switches [21]. Within this Chapter only "naked" metallocarbohedrenes will be discussed, while metal clusters with terminal organic and/or organometallic ligands will not be considered. For a detailed, comprehensive discussion of the latter type of molecules including the rational synthesis and specific reactions see reference [23].

The synthetic methodology for met-cars is based on the reaction of metals with low pressure unsaturated small hydrocarbon molecules such as methane in a laser-induced plasma [25]. The plasma consists of neutral metal atoms, negative and positively charged metal ions and electrons. Hydrocarbons originating from the pulsed valve (Fig. 1) flush into the high-energy plasma, whereby they become dehydrogenated, atomized, excited, and ionized [25]. Two different strategies are thereby pursued: either the metal clusters, $M_n$, undergo many collisions with both reactants and carrier gas at a pressure between 1 and 50 Torr (Fig. 1); or, they react under single collision conditions at low pressure (1 mTorr) [25]. The yield of met-cars in some samples was ca. 1% [71] but is usually much lower. In general, the clusters are extremely sensitive to air, and may undergo degradation within minutes [53]. Therefore, theoretical studies are important to investigate the topological, physical and chemical features of these molecular clusters (vide infra) and to learn more about their thermodynamic stability.

A number of symmetric structures for $Ti_8C_{12}$ have been proposed and discussed, the most stable one showing $T_d$ symmetry (Fig. 2) [23]. The arrangement of the titanium atoms in this stable met-car structure can best be considered as a tetrahedron of inner metal atoms ($^iM$) capped with four outer metals ($^oM$) with the acetylide units ($[C\equiv C]^{2-}$) aligned with the long diagonals of the six $^iM_2{}^oM_2$ rhombi over the surface of the $^iM_4{}^oM_4$ tetracapped tetrahedron [23].

**Table 1**
Met-cars known to date.

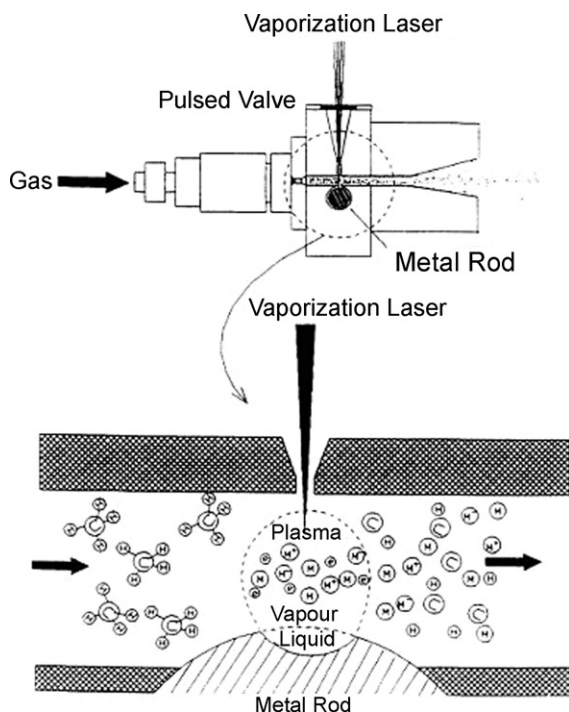| Met-car | References | |
|---|---|---|
| | Calculations | Experimental |
| $Sc_8C_{12}$ | [24] | [25] |
| $Ti_8C_{12}$ | [23,24,26–41] | [19,20,42–54] |
| $Zr_8C_{12}$ | [23,31,34,35,38,41,55] | [42,45,50,54,56,57] |
| $Hf_8C_{12}$ | | [42] |
| $V_8C_{12}$ | [47,54,58] | [47,54,58] |
| $Nb_8C_{12}$ | [23,55,34,35,59] | [46,50,54,60–62] |
| $Ta_8C_{12}$ | | [62] |
| $Cr_8C_{12}$ | [23] | [54,63] |
| $Mo_8C_{12}$ | [23,29,30] | [63,64] |
| $Fe_8C_{12}$ | [23,38,65] | [63] |
| $Ti_xM_yC_{12}$ | | [46,49,50,66–70] |

**Fig. 1.** Schematic view of the laser-induced plasma synthesis of met-cars [25].

Mechanistic studies have shown that the formation of met-car clusters takes place by assembly of eight $MC_2$ units followed by the *meta*-stable loss of $C_3$ and C fragments [21]. However, to denote the acetylenic character of the $C_2$ building blocks this class of clusters should better be named metallocarbohedrynes ($M_8(C_2)_6$) instead of metallocarbohedrenes ($M_8C_{12}$) [28]. The structure and bonding of the $T_d$ clusters include six acetylene-like $[C≡C]^{2-}$ units which are σ-bonded to the four outer capping metal atoms ($^oM$) and π-coordinated by the inner tetrahedral metals $^iM$ (Fig. 3) [22]. In the variety of met-car compositions, it is also worth noting that three main types have been identified: (i) carbon-poor clusters with a (nearly) 1:1 metal–carbon ratio, for example, $Nb_2C_2$ and $Ti_{14}C_{13}$; (ii) carbon-rich clusters (metal carbon ratio close to 1:1.5) including $M_8C_{12}$ or $M_8C_{13}$; and (iii) carbon-rich clusters with specific stoichiometries ($M_{13}C_{22}$, $M_{18}C_{27}$) [22]. The discussion that follows will be concerned largely with the most common of these structural types, $M_8C_{12}$.



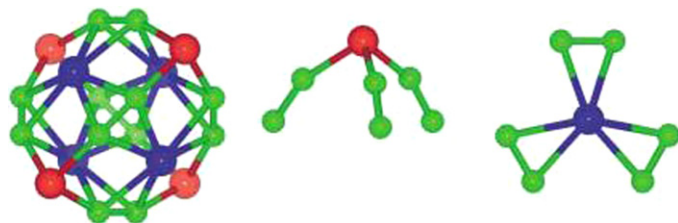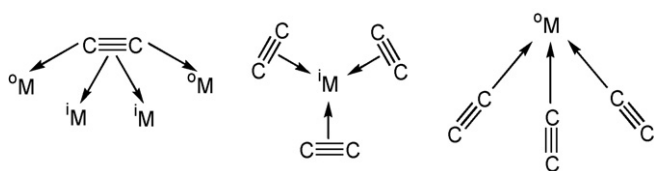**Fig. 2.** Structures and structural components of metallocarbohedrenes ($^iM$ = blue, $^oM$ = red, C = green) [23].



**Fig. 3.** Coordination sphere of iM belonging to the inner tetrahedron and of $^oM$ belonging to the outer capping tetrahedron in the $T_d$ symmetric $Ti_8C_{12}$ structure [22].



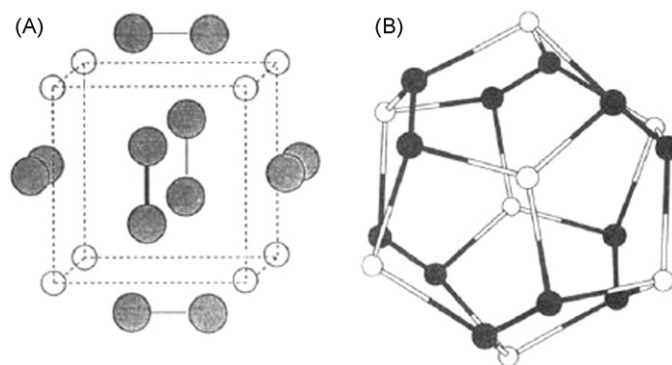**Fig. 4.** Two views of the $Ti_8C_{12}$ cluster in the cage structure of pentagonal dodecahedron ($T_h$ symmetry) [22].

Many computational studies of the geometry and properties of $M_8C_{12}$ clusters have been reported and demonstrate a variety of bonding motifs supporting a $T_d$ symmetry cluster (Fig. 4), rather than the originally proposed $T_h$ symmetry structure (Fig. 5) [22]. Other calculations showed that the $C_{3v}$ structure has the lowest energy among the variants considered [28]. The properties of metallocarbohedrenes, for instance ionization potentials and electron affinities [31,38,72,73], effect of metal substitution (mixed metal met-cars) [74], the formation of educts with polar or *non*-polar π-bonding molecules [75], and the prediction of optical, magnetic and collective electronic characteristics [28,76], were calculated by *ab initio* and *DFT* methods, respectively.

J.A. Rodriguez and coworkers have used DFT calculations to explore the chemical activity of met-cars $M_8C_{12}$ (M = Ti, V, Mo). The computational results indicate that these nano-particles exhibit a unique behavior, more complex than metal (M(0 0 1)) and metal carbide surfaces ($M_2C(0 0 1)$, MC(0 0 1)), which was attributed to the interplay of shifts in the metal d-bands and distortions in the geometry of the appropriate clusters [29,30]. However, the special geometry of met-cars diminishes the ligand effect of C on metal atoms. The met-cars can interact with adsorbates, for example, $H_2O$, CO, $SO_2$, S, and Cl [29,30]. The interaction of $H_2O$ and Cl with both the inner and outer titanium sites in $Ti_8C_{12}$ following a Lewis acid–base interaction mechanism is very exothermic, while with CO only the outer titanium atoms react because the addition to the inner Ti sites was calculated to be highly endothermic [29,30]. However, when changing to larger adsorbates, including thiophene, it is important to consider the *non*-metal positions in the cluster because steric repulsion can overcome the intrinsic reactivity of the metal atoms in corner or edge sites [30]. Based on higher level computational studies (MP2, MP4, QCISD) for $M_8C_{12}$ (M = Ti, Mo) a first-order Jahn-Teller distortion of $T_d$ symmetry was found for the appropriate titanium met-car, to which $Mo_8C_{12}$ is not subjected [29]. Nevertheless, the conclusion of these calculations was that $Mo_8C_{12}$ should have qualitatively similar reactivity patterns to those of $Ti_8C_{12}$. This result is interesting especially when one considers that the met-car $Ti_8C_{12}$ has been studied as a model catalyst for hydrodesulfurization (= HDS) of thiophene [27]. Elementary reaction steps and barriers were calculated using DFT methods. In comparison to industrial used catalysts (*i.e.*, NiMoS) the titanium met-car cluster facilitates carbon–sulfur bond cleavage and hydrogen dissociation, with sulfur removal energetically similar in both systems [27]. To the best of our knowledge, similar applications of the $Mo_8C_{12}$ met-car have not been investigated.

The electronic properties of a new type of hybrid nano-composites consisting of two stable systems of molecular dimensions (nanotubes and metallocarbohedrenes) were described by Ivanovskii and coworkers [24,26]. The 1D-crystals consisting of regular chains of met-cars $M_8C_{12}$ (M = Sc, Ti, Zr, V, Nb, Cr, Fe, Cu) located inside single-walled carbon, silicon, boron–nitrogen,
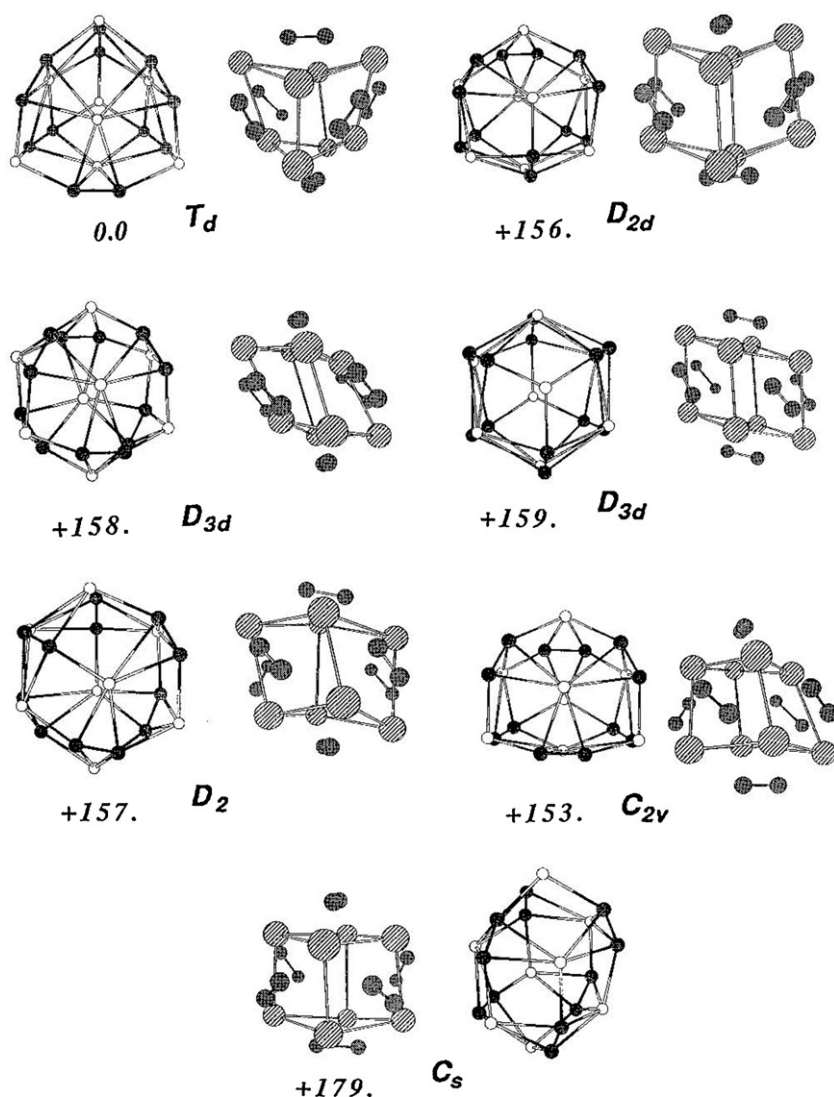
**Fig. 5.** The seven optimized geometric structures for $Ti_8C_{12}$ and their relative energies (kcal·mol$^{-1}$) compared to $T_h$ [22].

boron–carbon–nitrogen, and gallium–nitrogen nanotubes were studied by the tight-binding method within the Hückel approximation [24,26]. The electronic properties and relative stability of these hybrid materials can be considered as a function of the composition and atomic structure of the appropriate nanotubes as well as the chemical composition of the respective met-cars [24].

Evidence of met-cars ($Zr_8C_{12}$) assembled into nanoscopic features by mass-gated deposition of large zirconium–carbon clusters onto carbon-covered grids under hard- and soft-landing conditions, respectively, were reported by Gao et al. [56]. High resolution tunneling electron microscopy (= HRTEM) studies showed that only under soft-landing conditions zirconium met-cars were formed, while under hard-landing conditions bulk zirconium carbide was produced. Furthermore, calculations suggest the substitution of titanium in $Ti_8C_{12}$ by, for example, zirconium afford binary metal clusters such as $Ti_{8-n}Zr_nC_{12}$ with $n = 1$–5, whereby substitution can occur on both metal sites with nearly identical probability [56]. In addition, the fusion of two or even more dodecahedral clusters can produce $M_{13}C_{22}$ and $M_{18}C_{27}$ cages, respectively, their properties most probably explicable by extension of the met-car cluster topological characteristics [56].
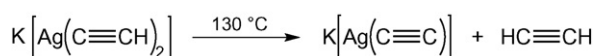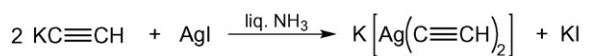
Neutral metal clusters $M_n$ (M = Nb, Ta; $n < 12$) are available by laser ablation of the metal and supersonic expansion into a vacuum, where reaction with unsaturated hydrocarbons (acetylene,

$\alpha$-olefins, 1,3-butadiene, benzene, toluene) under nearly single collision conditions in a pickup cell give neutral metal carbide clusters *via* the formation of *meta*-stable [$M_nC_xH_y$] species [62]. Time of flight mass spectrometry revealed that, at lower pressure, preferentially dehydrogenated products of type [$M_nC_x$] are formed, while at higher pressure [$M_nC_xH_y$] and [$M_nC_x$] compounds are produced with comparable intensities. In presence of aromatic hydrocarbons (benzene, toluene) met-car clusters $M_8C_{12}$ are mainly generated possessing $T_d$ symmetry [62].

In addition to the experimental work for the preparation of [$Fe_nC_{12}$] clusters ($n = 2$, 3, 4, 6, 8, 10, 12) by laser vaporization of iron atoms in an acetylene-containing plasma carried out by Pilgrim and Duncan [63], Harris and Dance reported DFT investigations of geometric structures and interconversions on these iron–carbon systems [65]. For $n \sim x$ ($Fe_nC_x$) the iron–carbon clusters contain isolated carbon atoms, as for $Fe_8C_{12}$, as expected, carbon is present only in [$C{\equiv}C$]$^{2-}$ units that are terminal- and side-on-bonded to iron. In this report, possible mechanisms for the photo-dissociation of iron atoms from [$Fe_{12}C_{12}$]$^+$ and [$Fe_8C_{12}$]$^+$ are also given [65].

In conclusion, the new field dealing with met-cars (based on transition metals (vide supra) and carbides of main group elements [21,22]) rapidly developed during the last two decades through experimental work and interpretative computational studies that help to understand their "supermagic" composition, their specific

$$2\ KC\!\equiv\!CH\ +\ AgI\ \xrightarrow{\text{liq. NH}_3}\ K\Big[Ag\big(C\!\equiv\!CH\big)_2\Big]\ +\ KI$$

$$K\Big[Ag\big(C\!\equiv\!CH\big)_2\Big]\ \xrightarrow{\ 130\,^\circ C\ }\ K\Big[Ag\big(C\!\equiv\!C\big)\Big]\ +\ HC\!\equiv\!CH$$

**Scheme 2.** Synthesis of K[Ag(C$_2$)] [77].

properties, their stability and their potential applications. The most abundant isomer of met-cars has $T_d$ symmetry as agreed by theoreticians and experimentalists.

## 3. Ternary metal carbides, [MC$_2$]$^{2-}$

Ternary metal carbides of general type M′[MC$_2$] (M = Cu, Ag, Au; M′ = Li, Na, K, Rb, Cs) [77–80], M$_2$′[MC$_2$] (M = Pd, Pt; M′ = Na, K, Rb, Cs) [77,81], and M$_4$′[M$_3$C$_5$] (M = Ni; M′ = Ca) [82] contain an electropositive alkali or alkaline earth metal (M′), which usually forms anionic carbides, and a d-block metal atom (M) forming a metallic carbide. The properties of these compounds can be found along the transition from ionic to metallic materials. The general synthetic

methodology for these carbides is based on a high temperature combination of the elements, or reactions of metal oxides with carbon [81].

The first ternary alkali metal carbide, K[AgC$_2$], was synthesized by Nast in 1963 by treatment of KC≡CH with the highly explosive silver acetylide salt [Ag$_2$C$_2$] in liquid ammonia [83]. The structure of this carbide in the solid state was published in 1999 by Ruschewitz and coworkers, who obtained K[AgC$_2$] by the reaction shown in Scheme 2 [77].

Using the strategy shown in Scheme 2, further ternary group 11 transition metal carbides M′[MC$_2$] (M = Cu [77], Ag [77], Au [80]; M′ = Li, Na, K, Rb, Cs) were prepared and characterized. In the synthesis of Na[CuC$_2$] from [CuI] and NaC≡CH an orange intermediate of composition Na[Cu$_5$(C$_2$)$_3$] consisting of a complicated three-dimensional framework comprised of Cu(I) ions and [C$_2$]$^{2-}$ units with small channels running parallel to [1 0 0] and [0 0 1] was formed [84]. On heating Na[Cu$_5$(C$_2$)$_3$] to 270 °C decomposition to Na[CuC$_2$], elemental copper and carbon occurred.

The solid state structures of the M′[MC$_2$] compounds (M = Cu, Ag, Au; M′ = Li, Na, K, Rb, Cs) have been determined, and the structures can be divided in three categories based on the size of the
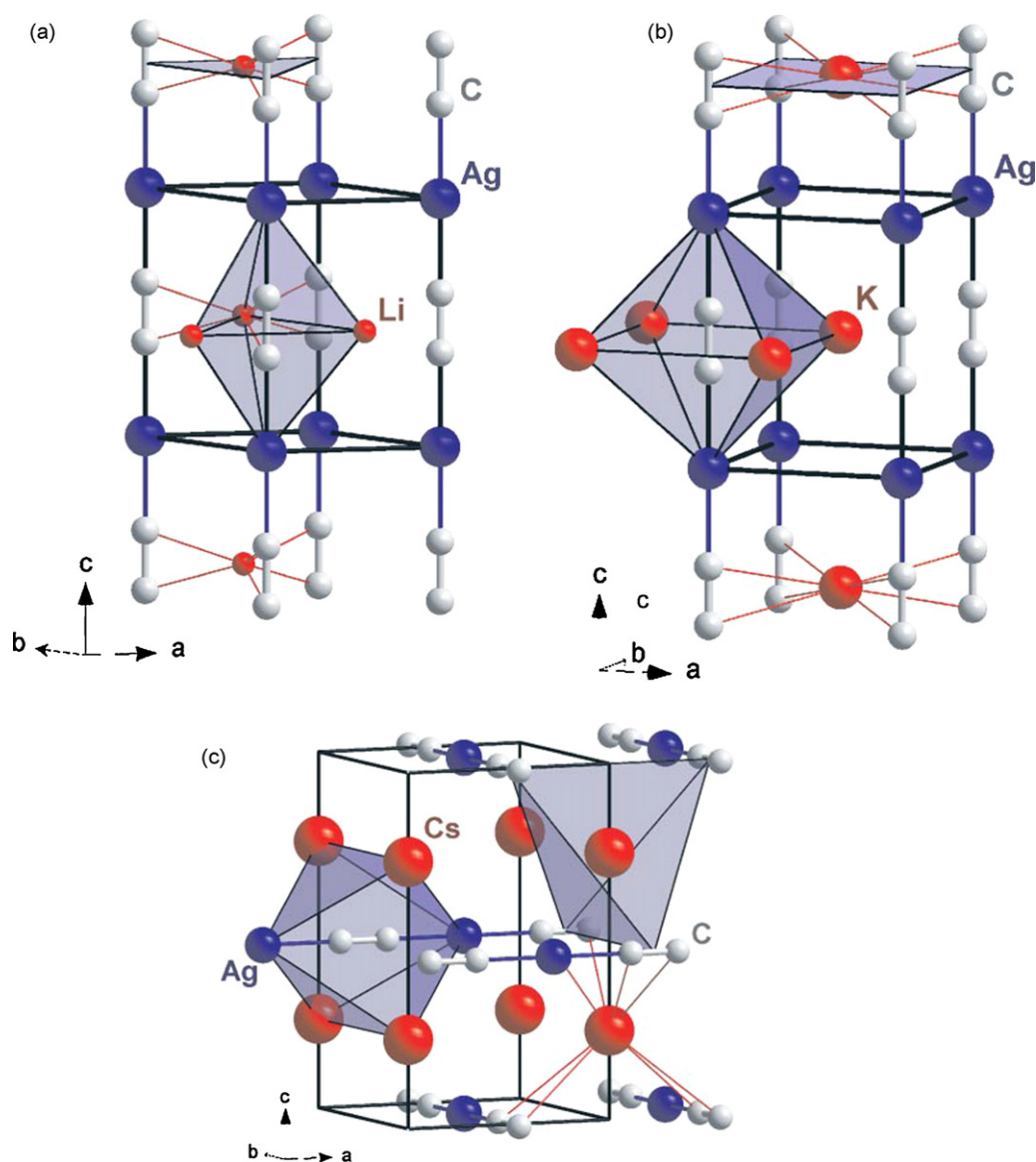


**Fig. 6.** Solid state structures of Li[AgC$_2$] (left), K[AgC$_2$] (right), and Cs[AgC$_2$] (bottom) [81].

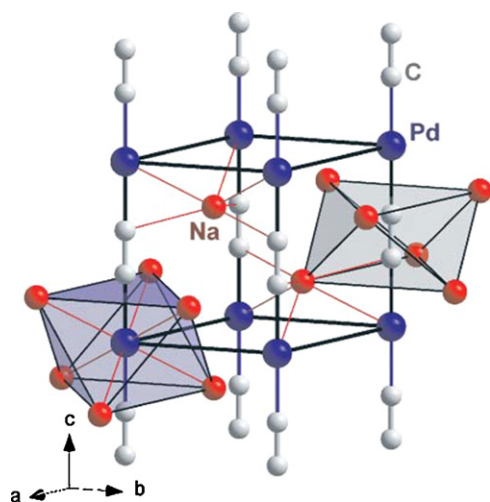**Fig. 7.** Structure of $Na_2[PdC_2]$ in the solid state [81].

appropriate alkali metal ion. These are represented by $Li[AgC_2]$, $K[AgC_2]$, and $Cs[AgC_2]$. The structure type $Li[AgC_2]$ ($Li[AgC_2]$, $Li[AuC_2]$) (Fig. 6, left) is characterized by $[Ag(C_2)_{2/2}]_n^-$ chains (hexagonal unit cell), whereby the lithium ions are $\pi$-bonded to three $C_2$ handles [79]. The metal carbide $K[AgC_2]$ (as well as $Na[CuC_2]$, $Na[AgC_2]$, $Na[AuC_2]$, $K[AgC_2]$, $K[AuC_2]$, $Rb[CuC_2]$, $Rb[AgC_2]$, $Rb[AuC_2]$, $Cs[AgC_2]$, $Cs[AuC_2]$) exhibits a polymeric structure with $[Ag(C_2)_{2/2}]_n^-$ chains (tetragonal $c$ axis) separated by potassium cations with side-on coordination to four $C_2$ units (Fig. 6, right) [77,81]. The $Cs[AgC_2]$ ($K[CuC_2]$, $Rb[CuC_2]$, $Cs[CuC_2]$, $Cs[AgC_2]$) structure is represented by $[Ag(C_2)_{2/2}]_n^-$ chains which are arranged in layers perpendicular oriented to the $c$ axis and rotated by 90° to each other (Fig. 6, bottom) [77,81]. The cesium ions are thereby pseudo-tetrahedrally coordinated by four $C_2$ units. The three different $M[AgC_2]$ structure types (M = Li, K, Cs) match the simple model of close packed rods ($[Ag(C_2)_{2/2}]_n^-$) and spheres (alkali metal ions) [77,81].

The ternary alkali group 11 metal carbides $M'[MC_2]$ are colorless to slightly grey (M = Cu, Ag) or yellow (M = Au) *non*-explosive,

but air and moisture sensitive materials. The color darkens from the lithium to the cesium derivatives. Conductivity measurements revealed an insulating behavior which was confirmed by DFT calculations (direct band gap = 2.3 eV) [81].

For the synthesis of the ternary acetylides $M_2'[MC_2]$ (M' = Na, K, Rb, Cs; M = Pd, Pt) the solid state reaction of $[M_2'C_2]$ with palladium or platinum metals was carried out at temperatures >140 °C in inert gas atmosphere [77,81,85–87]. All of these systems crystallize to give the same structure type, consisting of $[M(C_2)_{2/2}]_n^{2-}$ chains, separated by M' ions (Fig. 7) [77,81]. The M' ions are tri-coordinated by one carbon atom of three $C_2$ units and three palladium/platinum ions.

Conductivity measurements and band structure calculations were also carried out. They show that these materials are semiconductors with a small indirect band gap (ca. 0.1–0.2 eV) [81]. This is in agreement with the black color of these metal carbides. The kinetics of the formation of $Na_2[PdC_2]$ were investigated by using time-resolved synchrotron powder diffraction between 240 and 260 °C [88]. The activation barrier was calculated to 480(120) kJ mol$^{-1}$ and a diffusion mechanism has been proposed.

## 4. Homoleptic alkynide complexes of groups 3–5

Homoleptic early transition metal alkynides have been rarely investigated to date, although alkynides $[RC\equiv C]^-$ played an important role in the synthesis of heteroleptic organometallic d- and f-orbital element compounds [15,89]. The fewer number of publications concerning these complexes is based on their high reactivity toward air and moisture arising from kinetic and thermodynamic effects.

Homoleptic lanthanide alkynides with lanthanide metals (Ln = Er, Sm, and Lu) of general composition $[Ln(C\equiv CR)_4Li(thf)]$ (R = $^tBu$, Ph) were synthesized by Evans and coworkers in 1980 by reacting $[Ln(^tBu)_4Li(thf)_4]$ with $HC\equiv CR$ (R = $^tBu$, Ph), the phenyl derivative being less stable than the bulkier $^tBu$ system [90]. These lanthanide complexes were characterized by elemental analysis, IR, and UV–vis spectroscopy, and the magnetic moments were determined. Complexometric analysis reveals that only one thf molecule is present due to coordination of the alkynyl ligands to $Li^+$ [90]. Hydrolytic decomposition of the $^tBu$ substituted homolep-



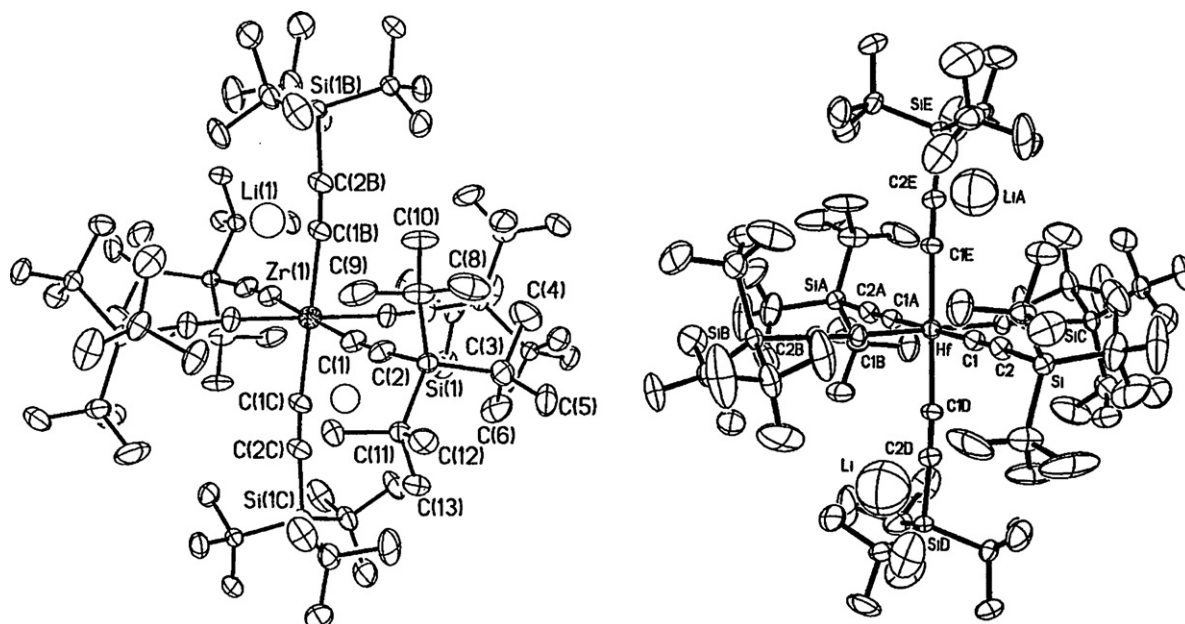**Fig. 8.** Molecular views of $[M(C\equiv CSi^tBu_3)_6]^{2-}$ (M = Zr (left), Hf (right)) illustrating the octahedral geometry in the solid state [93].
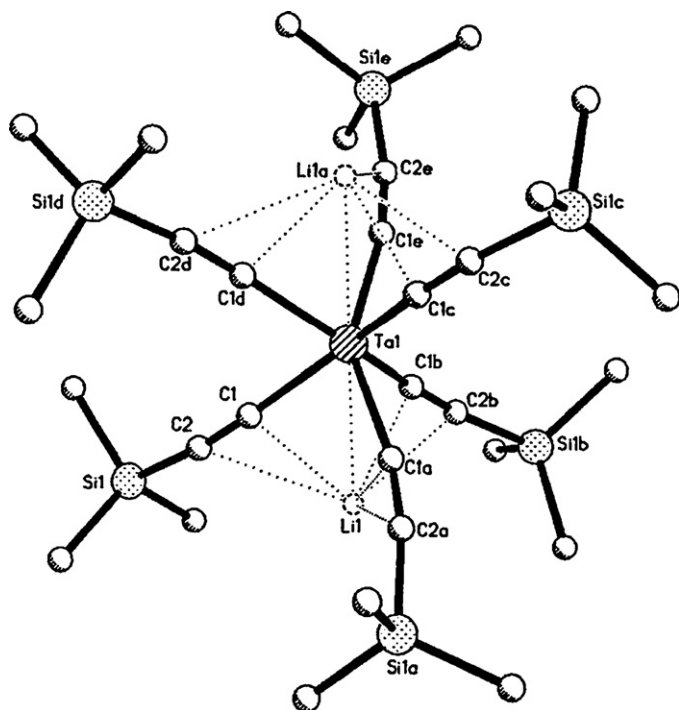
**Fig. 9.** Molecular view of $\{[Li(^tBu_3SiC\equiv C)_3]Ta(C\equiv CSi^tBu_3)_3\}$ showing a 2-fold lithium disorder [93].

tic complexes afforded 3,3-dimethylbut-1-yne. An yttrium analog and its reaction chemistry was published in 1989 by the same corresponding author. Treatment of $[Y(^tBu)_4Li(thf)_4]$ with $HC\equiv C^tBu$ gave $[Y(C\equiv C^tBu)_4Li(thf)]$ quantitatively [91]. Reacting the latter molecule with $K[C_5Me_5]$ resulted in the replacement of two alkynide ligands to form $[(\eta^5-C_5Me_5)Y(\mu-C\equiv C^tBu)_2Li(thf)]$ similar to the lanthanide complexes described above [91]. An unexpected reaction behavior for $[Me_2Si(N^tBu)(O^tBu)]_2Y(CH(SiMe_3)_2)]$ was observed when this molecule was reacted with $HC\equiv CR$ (R = $^tBu$, $SiMe_3$) [92]. Instead of the expected catalytic dimerization of the 1-alkynes a white precipitate was formed and identified as homoleptic $[Y(\mu-C\equiv CR)_3]_n$.

Six-coordinated $d^0$ complexes of type $[M(C\equiv CSi^tBu_3)_6]^{2-}$ (M = Zr, Hf) were synthesized by Wolczanski and coworkers [93]. Treatment of $MCl_4$ with six equivalents of $LiC\equiv CSi^tBu_3$ produced the colorless homoleptic complexes in low yield. The structure of both complexes in the solid state showed an octahedral ($O_h$) configuration, while theoretical investigations (DFT) suggest a trigonal prismatic ($D_{3h}$) or $C_{3v}$ arrangement (Fig. 8).

When only five equivalents of the lithium alkynide are used in the reaction with $MCl_4$ (M = Zr, Hf) then complexes $\{[(thf)_2Li(^tBu_3SiC\equiv C)_2]Zr(C\equiv CSi^tBu_3)_3(thf)\}$ and $\{[(Et_2O)Li(^tBu_3SiC\equiv C)_2]Hf(C\equiv CSi^tBu_3)_3(OEt_2)\}$ could be isolated [93]. The single crystal X-ray structure of the zirconium species revealed a distorted octahedral arrangement of five alkynyls and one solvent ligand around the Zr centre. The similar tantalum coordination complex $\{[M'(^tBu_3SiC\equiv C)_3]Ta(C\equiv CSi^tBu_3)_3\}$ (M' = Li, K, K(crypt 2.2.2)) could also be synthesized [93]. The single crystal X-ray structure determination of $\{[Li(^tBu_3SiC\equiv C)_3]Ta(C\equiv CSi^tBu_3)_3\}$ revealed a twisted trigonal prismatic structure illustrated in Fig. 9 indicating that the $Li^+$ ion is disordered between the two trigonal faces.

Comparing the structures of the homoleptic Ta, Zr and Hf transition metal complexes (Figs. 8 and 9) reveals that the trigonal prismatic structure is more favored by the Ta compound over the analogous Zr and Hf molecules [93]. Density functional (ADF) and effective core potential (GAMESS) calculations showed that the

structural difference results from a lessening electronic preference from the trigonal prism (primarily a greater HOMO–LUMO gap) upon moving from Ta to Zr, minor steric perturbation, and increased interligand repulsions in the dianion (VSEPR).

Homoleptic alkynide vanadium complexes are, to our knowledge, not known. To isolate vanadium(II) alkynides of type $[V(C\equiv CPh)_4]^{2-}$ and $[V(C\equiv CPh)_2]$, it is necessary to add a stabilizing chelating ligand, for example, TMEDA resulting in the formation of the appropriate adducts $[V(C\equiv CPh)_4(TMEDA)]^{2-}$ or $[V(C\equiv CPh)_2$ $(TMEDA)_2]$, respectively [94].

## 5. Homoleptic alkynide complexes of groups 6–9

Homoleptic alkynide complexes of group 6–9 elements are rare, perhaps surprisingly so given the predominance of homoleptic cyanide complexes and the intense interest in heteroleptic alkynide complexes of these metals. As is often the case, the earliest examples occur in the work of Nast [7]. In many of the earliest studies, potassium or sodium alkynide salts were employed as the source of the alkynide ligand, although more recent studies have employed lithium derivatives to excellent effect [13]. In one of the earliest studies, the chromium complex $K_3[Cr(C\equiv CH)_6]$ was isolated from the reaction of $[Cr(NH_3)_6][NO_3]_3$ with an almost 10-fold excess of $KC\equiv CH$ [95]. A magnetic moment of $\mu_{eff} = 3.86 \pm 0.19$ B.M., consistent with the three unpaired electrons expected for a Cr(III) complex, was determined for this compound. The alkynide ligands were readily displaced by water/hydroxide or cyanide [95].

Salts containing the dianion $[Mn(C\equiv CR)_4]^{2-}$ are thought to be formed from $Mn(SCN)_2$ and alkali metal (Na, K, Ba) salts of acetylene, propyne or phenylacetylene [96]. While these salts were not explosive, they did prove to be pyrophoric, and liberated the free alkyne upon protonation. Magnetic measurements were consistent with a high-spin Mn(II) centre ($\mu_{eff} = 5.9$ B.M.), and while crystallographic data are not available, networked structures seem likely. IR studies carried out some 20 years after the initial report revealed low $\nu_{(C\equiv C)}$ frequencies (ca. 1915 cm$^{-1}$), and are certainly consistent with acetylide bridged structures [97]. Closely related compounds have also been isolated from o-diethynylbenzene [98]. Further reaction of $K_2[Mn(C\equiv CH)_4]$ with oxygen was thought to give the very unstable hexa-alkynyl Mn(III) salt $K_3[Mn(C\equiv CH)_6]$ [96].

The first homoleptic iron complexes $M_4[Fe(C\equiv CR)_6]$ (M = Na, K; R = H, Me, Ph) [99] were prepared from $Fe(NCS)_2\cdot4NH_3$, while the diamagnetic, air-sensitive cyclohexyl derivative $K_4[Fe(C\equiv CCy)_6]$ ($\nu_{C\equiv C}$ 2048 cm$^{-1}$) was isolated from $Fe(NCS)_2\cdot2NH_3$ and $KC\equiv CCy$ in liquid ammonia [100]. The more stable alkynide-rich derivatives of composition $[Fe(C\equiv CCy)_2(PPh_3)_2]$ and $K_4[Fe(CN)_4(C\equiv CCy)_2]$ are formed from $KC\equiv CCy$ with $Fe(NCS)_2(PPh_3)_2$ or $K_3[Fe(CN)_4(NH_3)]$, respectively [100]. The low-spin nature of the Fe(II) derivatives was taken as evidence of the strong-field character of the alkynide ligand [100]. Oxidation ($O_2$) of $K_4[Fe(C\equiv CH)_6]$ was thought to afford $K_3[Fe(C\equiv CH)_6]$ as a dark purple solid, although the tendency of this material to detonate precluded magnetic measurements [99].

The six-coordinate Co(II) complexes $M_4[Co(C\equiv CR)_6]$ (M = Na, K; R = H, Me) are also pyrophoric and prone to explosive decomposition [101]. More stable compositions are found with bulkier cations, illustrated by the isolation of the mixed salts $[EPh_4]A[Co(C\equiv CR)_6]$ (A = Na, K; R = H, Me, Ph; E = P, As) after methathesis [102]. Kinetic stability of the $K_4[M(C\equiv CR)_6]$ salts can also be engineered through the use of a bulkier cyclohexylalkynide ligand, although the compounds are still pyrophoric in air, and decompose with the release of cyclohexylacetylene on reaction with water [100]. The magnetic moment $\mu_{eff}$ of $K_4[Co(C\equiv CCy)_6]$ varies from 3.32 B.M. (296 K) to 2.81 B.M. (77 K) as a function of temperature ($\Theta = -22$). Since these values fall between the values expected for low-spin and high-spin octahedral Co(II), it was thought likely that the compound

**Table 2**
Selected bond lengths (Å) and angles (°) for the homoleptic alkynide anions in $[M(C\equiv CSiMe_3)_6]^{n-}$ [13].
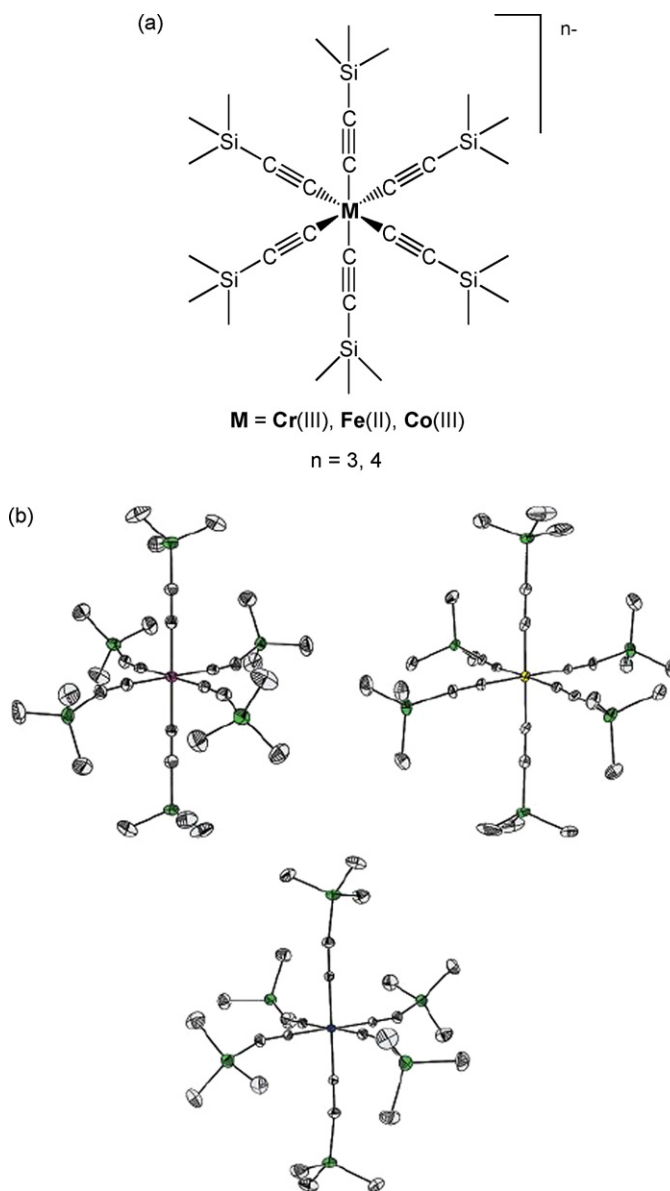
|  | $[Cr(C\equiv CSiMe_3)_6]^{3-}$ | $[Fe(C\equiv CSiMe_3)_6]^{4-}$ | $[Co(C\equiv CSiMe_3)_6]^{3-}$ |
|---|---|---|---|
| M—C | 2.077(3) | 1.917(7)–1.935(7) | 1.908(3) |
| C≡C | 1.215(4) | 1.233(8)–1.251(8) | 1.212(5) |
| C—M—C | 87.76(9)–92.24(9) | 86.7(2)–92.1(2) | 87.9(2)–92.1(2) |
| M—C≡C | 175.2(2) | 173.9(5)–176.3(6) | 178.7(3) |
| C≡C—Si | 162.9(2) | 169.2(5)–175.3(5) | 159.4(4) |

exists with a tetragonal pyramidal distortion in the solid state, with the population of high- and low-spin states giving rise to potential applications of similar compounds as spin cross-over materials [100].

More recently, Berben and Long have developed routes to homoleptic alkynide complexes containing $[M(C\equiv CSiMe_3)_6]^{n-}$ (M = Cr(III), Fe(II), Co(III)) from the reaction of $LiC\equiv CSiMe_3$ with anhydrous $CrCl_2$, $Fe(OTf)_2 \cdot NCMe$ or $Co(OTf)_2$ (OTf = $CF_3SO_3$) [13]. The preparations and product compositions are, however, sensitive to the reaction conditions and nature of the metal ion. For example, while $LiC\equiv CSiMe_3$ and $CrCl_2$ react in tetrahydrofuran from −25 °C to room temperature to give $Li_3[Cr(C\equiv CSiMe_3)_6] \cdot 6thf$ in 44% yield from a gram scale reaction, in glyme the reaction produces multiple products with only small amounts of $Li_8[Cr_2O_4(C\equiv CSiMe_3)_6] \cdot 6LiC\equiv CSiMe_3 \cdot 4glyme$ successfully crystallized from the reaction solution. The iron complex could only be isolated (45%) from diethyl ether solution as the adduct $Li_4[Fe(C\equiv CSiMe_3)_6] \cdot 4LiC\equiv CSiMe_3 \cdot 4Et_2O$, which is pyrophoric and said to occasionally detonate on exposure to air. The low solubility of $Co(OTf)_2$ in tetrahydrofuran reduced the yield of $Li_3[Co(C\equiv CSiMe_3)_6] \cdot 6thf$ to ca. 13%, with unreacted $Co(OTf)_2$ apparent in the reaction mixture. Use of an excess of $Co(OTf)_2$ under the same reaction conditions gave heteroleptic $Li_3[Co(C\equiv CSiMe_3)_5(C\equiv CH)] \cdot LiOTf \cdot 8thf$ [13]. The authors speculate that the desilylation and oxidation of the cobalt ion are linked, with the excess $LiC\equiv CSiMe_3$ reagent necessary to give the homoleptic compound by substitution [13].

Importantly, the solid state structures of each of the salts containing anionic homoleptic alkynide complexes were determined by crystallographic methods, revealing few deviations from idealized octahedral geometries (Fig. 10 and Table 2). The lithium counter ions are coordinated by π-interactions from the alkynide ligands, in addition to the solvent, and also $Me_3SiC\equiv C^-$ anions in the case of the iron complex. In keeping with the octahedral nature of the compounds, and the relatively strong ligand field of the acetylide ligand, the Cr(III) compound has an effective magnetic moment $\mu_{eff} = 3.85 \mu_B$ at 295 K consistent with S = 3/2, while the Co(III) complex is diamagnetic [13]. Given the rather inconsistent behavior of the iron complex it is understandable that magnetic data for this compound was not recorded.

DFT calculations indicate that the HOMOs of the model systems $[Cr(C\equiv CH)_6]^{3-}$, $[Fe(C\equiv CH)_6]^{4-}$ and $[Co(C\equiv CH)_6]^{3-}$ are comprised of the antibonding combinations of the $t_{2g}$ set of metal d-orbitals and the alkynide π-systems [13]. This general picture is supported by UV–vis spectroscopic data and TD-DFT calculations. In the case of the Cr(III) species, intense transitions at 43,900, 32,900 and 24,800 cm$^{-1}$ were assigned to LMCT and two MLCT bands, respectively. Weaker transitions were assigned to d–d bands, and allowed estimation of the ligand field splitting parameter $\Delta_o = 20,200$ cm$^{-1}$ and a Racah parameter B = 530 cm$^{-1}$. The d–d bands in $[Fe(C\equiv CSiMe_3)_6]^{4-}$ and $[Co(C\equiv CSiMe_3)_6]^{3-}$ were masked by the charge-transfer bands, and these transitions and hence, $\Delta_o$ and B, were estimated from TD-DFT calculations (iron complex: $\Delta_o = 32,450$ cm$^{-1}$, B = 457 cm$^{-1}$; cobalt complex: $\Delta_o = 32,500$ cm$^{-1}$, B = 516 cm$^{-1}$). Critically, the $\Delta_o$ data suggest that the alkynide ligand is a modestly weaker field ligand than cyanide but stronger

M = **Cr**(III), **Fe**(II), **Co**(III)

n = 3, 4

**Fig. 10.** Structures of the octahedral complexes $[Cr(C\equiv CSiMe_3)_6]^{3-}$ (left), $[Fe(C\equiv CSiMe_3)_6]^{4-}$ (right), and $[Co(C\equiv CSiMe_3)_6]^{3-}$ (below) in the solid state [13].
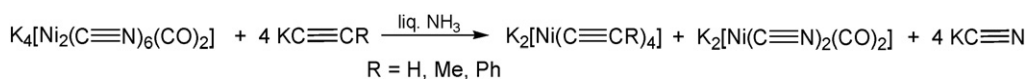
than chloride or methyl, while comparison of B with that of the free metal ions indicates a significant π-overlap of the metal orbitals with the ligands [13].

Despite the significant interest in alkynide complexes of the other metals in groups 6–9, and the large number of compounds that might be termed "acetylide rich", there are, to the best of our knowledge, no further examples of genuine homoleptic acetylide complexes of these metals.

## 6. Homoleptic alkynide complexes of group 10

In recent years, a large variety of heteroleptic group 10 transition metal alkynides have been prepared, while somewhat less is known about corresponding homoleptic complexes. The majority of this family of homoleptic organometallic compounds consisting of the anionic group 10 metal alkynides $[M(C\equiv CR)_4]^{2-}$ (M = Ni, Pd, Pt; R = H, single bonded organic group) was first synthesized by Nast and coworkers [103–105]. Neutral $[M(C\equiv CR)_2]$ compounds are also known, although they are extremely reactive and highly explosive

$$K_4[Ni_2(C\equiv N)_6(CO)_2] + 4 KC\equiv CR \xrightarrow{\text{liq. NH}_3} K_2[Ni(C\equiv CR)_4] + K_2[Ni(C\equiv N)_2(CO)_2] + 4 KC\equiv N$$

$$R = H, Me, Ph$$

**Scheme 3.** Synthesis of $K_4[Ni(C\equiv CR)_4]$ starting from a nickel(II) complex [118].

[6,106]. In addition, Nast described zero-valent diamagnetic $d^{10}$ alkynide coordination complexes of composition $K_2[M(C\equiv CR)_2]$ and $K_4[M(C\equiv CR)_4]$, respectively [105,107,108].

The nickel alkynides $[Ni(C\equiv CR)_4]^{2-}$ are pyrophoric, only stable at low temperatures, and rapidly decompose on addition of acid and basic reagents and hence, their characterization is limited. From the nickel triad, the respective palladium(II) species are least described. Platinum(II) alkynides are by far the most studied members of this group and are thermally more stable than the corresponding nickel systems, which accounts for the number of studies on these systems, particularly by Chandler et al. [109], Chen and coworkers [110,111], Forniés, Lalinde, Moreno [8–11,112], and Yam et al. [12]. Mononuclear, $[Pt(C\equiv CR)_4]^{2-}$, and multinuclear complexes thereof, are important research objects due to their potential applications as optoelectronic materials including sensors, light-emitting diodes, and as chromophores in artificial photo-synthetic models [8,11,12,113–116]. These compounds also received growing attention since they are attractive as non-linear optical, low-dimensional, conducting, and liquid-crystalline materials. Beyond that, they are of interest because the alkynyl groups allow coordination to further metal centers in a variety of different bridging modes to give higher nuclearity transition metal complexes containing metal–metal interactions [113].

The following chapter is divided into three sections based on the structural and electronic features of the corresponding group 10 transition metal alkynides.

### 6.1. Metal(0) alkynides of type $K_2[M(C\equiv CR)_2]$ (M = Pd, Pt) and $K_4[Ni(C\equiv CH)_4]$

Low oxidation states of d-block transition metal alkynides can be supported by alkynide ligands, $RC\equiv C^-$, which provide similar stability to cyanide ligands [7]. Following from the preparation of homoleptic zero-valent nickel alkynides, palladium and platinum analogues were also prepared: $K_2[M(C\equiv CR)_2]$ (M = Pd, Pt; R = H, Me, Ph) [104,105,107] and $K_4[Ni(C\equiv CH)_4]$ [108]. The diamagnetic nickel complex was synthesized by the reduction of the anionic Ni(II) acetylide $K_2[Ni(C\equiv CH)_4]$ (vide infra) on addition of an excess of potassium in anhydrous liquid ammonia [108]. Surprisingly, this complex is more stable than the corresponding nickel(II) species $K_2[Ni(C\equiv CH)_4]$, *non*-explosive but still highly pyrophoric and reactive toward protic solvents. In contrast to the dimeric nickel(I) cyanide complex $K_4[Ni_2(C\equiv N)_6]$, accessible by the reduction of $K_2[Ni(C\equiv N)_4]$ with potassium [117], the appropriate nickel(I) acetylide could not be isolated, when similar reaction conditions were applied [108]. Even using nickel(I) starting materials did not result in the formation of Ni(I) alkynides, rather these complexes disproportionate to give Ni(II) acetylides together with Ni(0) compounds as it could be demonstrated by Nast and Moerler (Scheme 3) [118].

Due to the diamagnetic character of $K_4[Ni(C\equiv CH)_4]$ a tetrahedral coordination geometry is proposed with the acetylides $HC\equiv C^-$ datively bonded to Ni(0) setting up $Ni\equiv C\equiv CH^-$ units. The bonding situation of $[Ni(C\equiv CH)_4]^{4-}$ is similar to $Ni(CO)_4$ and $[Ni(C\equiv N)_4]^{4-}$, respectively, which explains their relatively high stability [108].
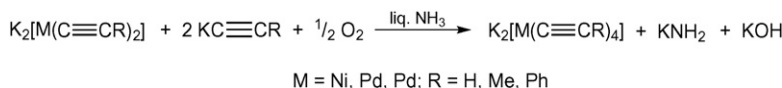
**Table 3**
Complexes of type $M_2[Ni(C\equiv CR)_4]$.

| R | M | Refs. |
|---|---|---|
| H | K | [103] |
| Me | K | [103] |
| Ph | K, Li(thf)$_4$ | [103,122] |
| CH$_2$CMe$_2$C$\equiv$N | K | [120] |
| CH$_2$CPh$_2$C$\equiv$N | K | [120] |
| C$\equiv$N | NEt$_4$ | [121] |

The syntheses of yellow crystalline palladium(0) and platinum(0) alkynides of type $K_2[M(C\equiv CR)_2]$ (M = Pd, Pt; R = H, Me, Ph) proceed by the reduction of $K_2[M(C\equiv N)_2(C\equiv CR)_2]$ [105,107] or *cis*-$[Pd(C\equiv CR)_2(dppe)]$ (dppe = 1,2-bis(diphenylphosphino)ethane) [104] with potassium in liquid ammonia. A further possibility to prepare these complexes is illustrated by the reduction of, for example, $K_2[Pd(C\equiv CPh)_4]$ with an excess of potassium in presence of dppe [104]. These complexes are diamagnetic, somewhat sensitive to light, pyrophoric, and decompose rapidly on addition of protic solvents. Treatment of $K_2[M(C\equiv CR)_2]$ with oxygen in liquid ammonia results in the well known oxidized complex $K_2[M(C\equiv CR)_4]$, the R = H derivatives being highly explosive (Scheme 4) [105].

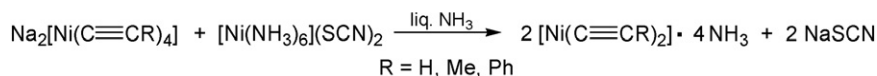The good solubility of $K_2[M(C\equiv CR)_4]$ in comparison to polymeric bis(*iso*-nitrile) palladium(0) complexes indicates these compounds to be less aggregated. IR spectroscopic studies showed a splitting of the $\nu_{C\equiv C}$ vibration indicating a low symmetry confirming multinuclear structures [105,107]. Using a similar approach, Ballester, Cano and Santos reported in 1982 the synthesis of zero-valent homoleptic $K_2[M(C\equiv C-C_6H_4-4-C\equiv CK)_2]$ (M = Ni, Pd) by reduction of the M(II) complex $[M(C\equiv C-C_6H_4-4-C\equiv CK)_2]$ with potassium [119]. These polymeric orange materials are, as expected, diamagnetic and very unstable to oxidation and hydrolysis.

### 6.2. Anionic metal(II) alkynides of type $K_2[M(C\equiv CR)_4]$

The tetra-alkynide transition metal complexes $[M(C\equiv CR)_4]^{2-}$ containing a metal(II) ion of the nickel triade are *iso*-structural with the corresponding cyanides, both featuring a square-planar environment at the metal centre [7]. As expected, within this series of compounds the metal–carbon bond strength increases from nickel to palladium and platinum which was experimentally confirmed by IR spectroscopy [120,121]. This trend in M–C bond strength finds expression in the reactivity and reaction behavior of these complexes, which will be discussed below.

#### 6.2.1. Nickel

General synthetic procedures for anionic nickel tetra-alkynides $M'_2[Ni(C\equiv CR)_4]$ (M' = Na, K; R = H, Me, Ph) (Table 3) are (i) treatment of nickel salts such as $K_2[Ni(C\equiv N)_4]$, $[NiX_2]$ (X = I, SCN, CN, dpi; dpi = anion of 1,3-bis-(2-pyridyl imino)*iso*-indoline) or $[NiX_2(PPh_3)_2]$ (X = Cl, Br, I) with alkali alkynides $RC\equiv C^-$ in liquid ammonia [103,120,122]; and (ii) the reaction of $(NEt_4)_2[NiCl_4]$ with $Me_3SnC\equiv C-C\equiv N$ in *N,N*-dimethylformamide [121]. These square-planar complexes are typically yellow, diamagnetic solids and

$$K_2[M(C\equiv CR)_2] + 2 KC\equiv CR + \tfrac{1}{2} O_2 \xrightarrow{\text{liq. NH}_3} K_2[M(C\equiv CR)_4] + KNH_2 + KOH$$

$$M = Ni, Pd, Pd; R = H, Me, Ph$$

**Scheme 4.** Synthesis of $K_4[M(C\equiv CR)_4]$ starting from a metal(0) complex [105].

$$Na_2[Ni(C\equiv CR)_4] + [Ni(NH_3)_6](SCN)_2 \xrightarrow{\text{liq. } NH_3} 2 [Ni(C\equiv CR)_2] \cdot 4 NH_3 + 2 NaSCN$$

$$R = H, Me, Ph$$

**Scheme 5.** Synthesis of nickel(II) alkynide ammoniates [123].
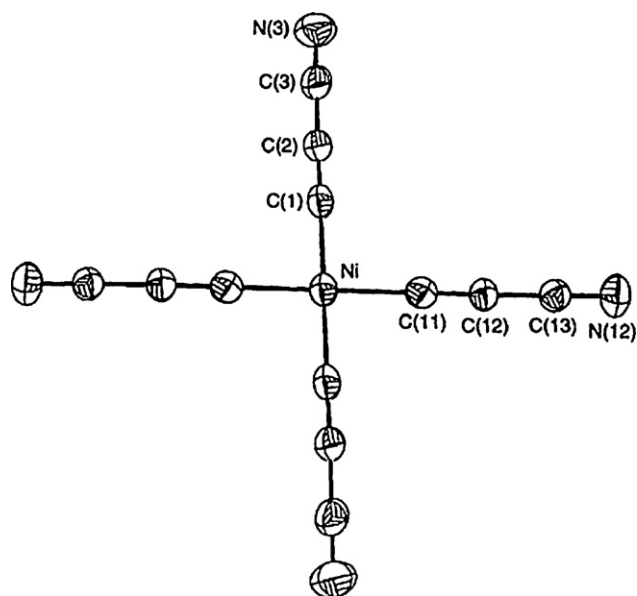


**Fig. 11.** ORTEP diagram with the atom-labeling scheme of homoleptic $[Ni(C\equiv C-C\equiv N)_4]^{2-}$ [121].

**Table 4**
Complexes of type $M_2[Pd(C\equiv CR)_4]$.

| R | M | Refs. |
|---|---|---|
| H | K | [104] |
| Ph | K | [104] |
| $CH_2CMe_2C\equiv N$ | K | [120] |
| $CH_2CPh_2C\equiv N$ | K | [120] |
| $C\equiv N$ | NEt$_4$ | [121] |
| $^t$Bu | Li | [124] |

are more or less explosive. More stable are the $CH_2CMe_2C\equiv N$ and $CH_2CPh_2C\equiv N$ derivatives (Table 3), which start to decompose at 80 or 55 °C, respectively, as revealed by DTA measurements [120]. Addition of dilute mineral acids to $[Ni(C\equiv CR)_4]^{2-}$ led to decomposition, while reaction with aqueous cyanide solutions gave *iso*-structural $[Ni(C\equiv N)_4]^{2-}$ along with $HC\equiv CR$ [123]. From this series of complexes the propynyl nickel(II) compound was the most reactive, giving propyne and $Ni(OH)_2$ on hydrolysis [123].

The structure of the homoleptic anion $[Ni(C\equiv C-C\equiv N)_4]^{2-}$ in the solid state is depicted in Fig. 11 and is determined to have a square-planar geometry. The nickel–carbon distances (1.856 Å) are consistent with the Ni–C separations in $[Ni(C\equiv N)_4]^{2-}$ (1.86 Å) [121].

A further type of nickel(II) alkynides are ammoniates with 2–4 molecules of $NH_3$ accessible by the reaction shown in Scheme 5 [123]. However, these complexes eliminate the coordinated ammo-

nia in vacuo to yield the polymeric black nickel(II) acetylides $[Ni(C\equiv CR)_2]$ (R = H, Me, Ph) (vide infra) [123]. These compounds, especially the nickel acetylide complex, are extremely explosive and could not be isolated. Magnetic measurements with the more stable phenylacetylide derivative, point to the formation of polymeric $Ni[Ni(C\equiv CPh)_4]$ in which both a paramagnetic and a diamagnetic $Ni^{2+}$ ion is present.

### 6.2.2. Palladium and platinum

Attempts to synthesize homoleptic $[Pd(C\equiv CR)_4]^{2-}$ and $[Pt(C\equiv CR)_4]^{2-}$ complexes (Table 4) from $[M(C\equiv N)_4]^{2-}$ salts and potassium alkynides under similar reaction conditions as described for the nickel alkynide derivatives (vide supra) led to the formation of heteroleptic mixed alkynide–cyanide compounds of structural type $K_2[M(C\equiv N)_2(C\equiv CR)_2]$ (R = H, Me, Ph) even when an excess of the alkynide is used [105,107]. Oxidation of $K_2[Pd(C\equiv CPh)_2]$ (Section 6.1) resulted most probably in the formation of impure $K_2[Pd(C\equiv CR)_4]$ [107]. A step-wise synthetic methodology starting from *cis*-$[PdCl_2(dppe)]$ (dppe = 1,2-bis(diphenyl)phosphino ethane) which finally leads to the title complexes in good yield is given in Scheme 6 [104].

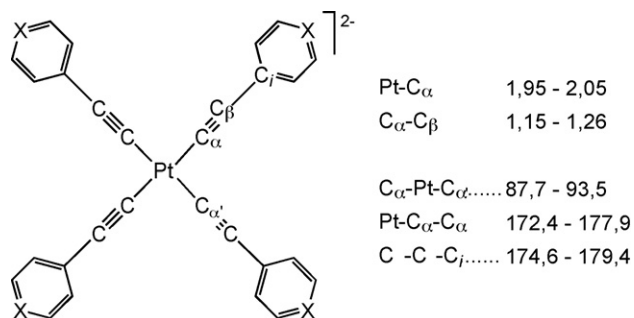Diorgano palladium compounds of type $[L_2PdR_2]$ (L = 2-electron donor ligand, R = organic group) generally release $R_2$ by reductive elimination. However, this reaction is inhibited in the case of $[(Ph_3P)_2Pd(C\equiv C^tBu)_2]$, when an excess of $LiC\equiv C^tBu$ is present. Instead of reductive elimination, the homoleptic palladium(II) complex $Li_2[Pd(C\equiv C^tBu)_4]$ is formed in high yield [124]. The tetra-alkynide platinum species (Table 5) were successfully prepared either from the reaction of $K_2[Pt(SCN)_4]$ with four equivalents of $KC\equiv CR$ in liquid ammonia or by the oxidation of $K_2[Pt(C\equiv CR)_2]$ with
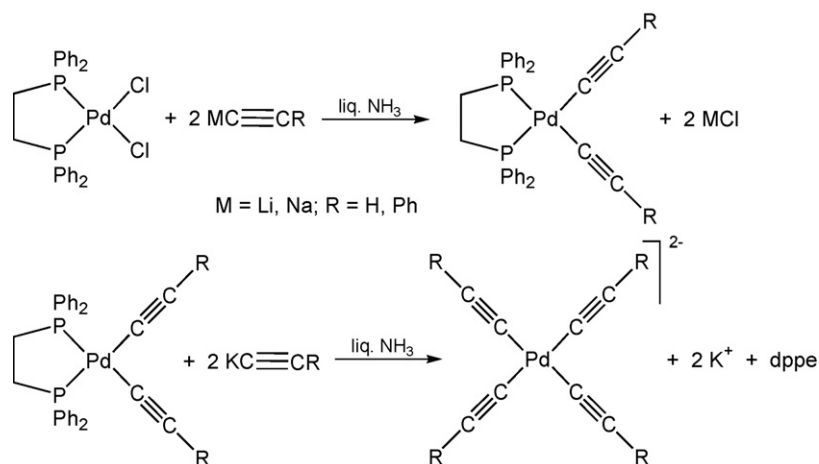


**Scheme 6.** Synthesis of palladiuml(II) alkynides [104].

**Table 5**
Complexes of type $M_2[Pt(C\equiv CR)_4]$.

| R | M | Refs. | R | M | Refs. |
|---|---|---|---|---|---|
| H | K | [105] | $C_6H_4$—4-$C_6H_5$ | $N^nBu_4$ | [127] |
| Me | K | [105] | $C_6H_4$—4-$CF_3$ | $N^nBu_4$ | [127] |
| $^tBu$ | $N^nBu_4$ | [125] | $C_6H_4$—4-OMe | $N^nBu_4$ | [127] |
| $SiMe_3$ | $N^nBu_4$ | [126] | $C_6H_4$—3-OMe | $N^nBu_4$ | [127] |
| $CH_2CMe_2C\equiv N$ | K | [120] | $C_6H_4$—4-CN | $N^nBu_4$ | [127] |
| $CH_2CPh_2C\equiv N$ | K | [120] | $C_6H_4$—4-$C\equiv CH$ | $N^nBu_4$ | [127] |
| Ph | K, $N^nBu_4$ | [105,125,127] | $C_6H_4$—4-$C\equiv C$—$C_6H_5$ | $N^nBu_4$ | [127] |
| 4-$C_5H_4N$ | $N^nBu_4$ | [12,127] | $(\eta^5$-$C_5H_4)(\eta^5$-$C_5H_5)$Fe | $N^nBu_4$ | [10] |
| 3-$C_5H_4N$ | $N^nBu_4$ | [12,127] | $C\equiv CPh$ | $N^nBu_4$ | [12] |
| 2-$C_5H_4N$ | $N^nBu_4$ | [127] | $C\equiv C$—$C_6H_4$—4-Me | $N^nBu_4$ | [12] |
| 5-$C_4H_3$-1,3-$N_2$ | $N^nBu_4$ | [12] | $C\equiv N$ | $NEt_4$ | [121] |



| | |
|---|---|
| $Pt$-$C_\alpha$ | 1,95 - 2,05 |
| $C_\alpha$-$C_\beta$ | 1,15 - 1,26 |
| $C_\alpha$-$Pt$-$C_{\alpha'}$...... | 87,7 - 93,5 |
| $Pt$-$C_\alpha$-$C_\alpha$ | 172,4 - 177,9 |
| $C$ -$C$ -$C_i$...... | 174,6 - 179,4 |

**Fig. 12.** Schematic view of $[Pt(C\equiv C$-$C_5H_4$—4-X$)_4]^{2-}$ complexes with ranges of bond distances (Å) and angles (°) for various groups X (X = C–$CF_3$, C–$C\equiv N$, N) [127].

oxygen in presence of $KC\equiv CR$ and ammonia [105]. Square-planar tetrakis(cyanoacetylide) palladium(II) and platinum(II) complexes were synthesized in a manner similar to that described for their nickel(II) analogues (Section 6.2.1) from $(Et_4N)_2[MCl_4]$ and $Me_3SnC\equiv C$—$C\equiv N$ [121]. The $K_2[M(C\equiv CCH_2CR_2C\equiv N)_4]$ complexes (M = Pd, Pt; R = Me, Ph) are thermally more stable than the nickel derivatives (vide supra) as shown by DTA studies (initial decomposition temperature: R = Ph: 150 °C (M = Pd), 185 °C (M = Pt); R = Me: 75 °C (M = Pd, Pt) [120].

In addition to the synthetic routes discussed above, Forniés and Lalinde reported in 1990 about the reaction of $[PtCl_2]$ or $[PtCl_2(tht)_2]$ (tht = tetrahydro-thiophene) with $[AgC\equiv CR]_n$ (R = Ph, $^tBu$) resulting in the formation of a new type of a homoleptic platinum complex of composition $[Pt_2Ag_4(C\equiv CR)_8]$ [125]. Based on these studies a fascinating family of polynuclear homo- and heterometallic transition metal alkynides developed [7,15,16]. A straightforward access to the structural unit $[Pt(C\equiv CR)_4]^{2-}$ in $[Pt_2Ag_4(C\equiv CR)_8]$ is given by treatment of $[PtCl_2]$ or $[PtCl_2(tht)_2]$ with $LiC\equiv CR$ and $[^nBu_4N]Br$ in diethyl ether or tetrahydrofuran as solvent [127]. This approach could be extended to many other alkynides featuring a high variety of different organic groups R which are of electron-donating, -withdrawing, or -delocalizing character (Table 5). The structures of such molecules in the solid state were determined by single X-ray structure analysis, showing that in general the platinum atom sits on an inversion centre with a planar geometric surrounding. The platinum alkynide entities are, as expected, in a linear arrangement with bond distances and angles typical for platinum-acetylide σ-bonding (Fig. 12) [127].

The electrochemical and photophysical properties of $[Pt(C\equiv CR)_4]^{2-}$ compounds have been studied. On the basis of theoretical calculations (TD-DFT) carried out for $[Pt(C\equiv C$—$C_6H_4$—4-$C\equiv N)_4]^{2-}$ the experimentally observed emissions were assigned to the $\pi$–$\pi^*$ (RC≡C) triplet intra-ligand and $d_\pi(Pt)$–$\pi^*(RC\equiv C)$
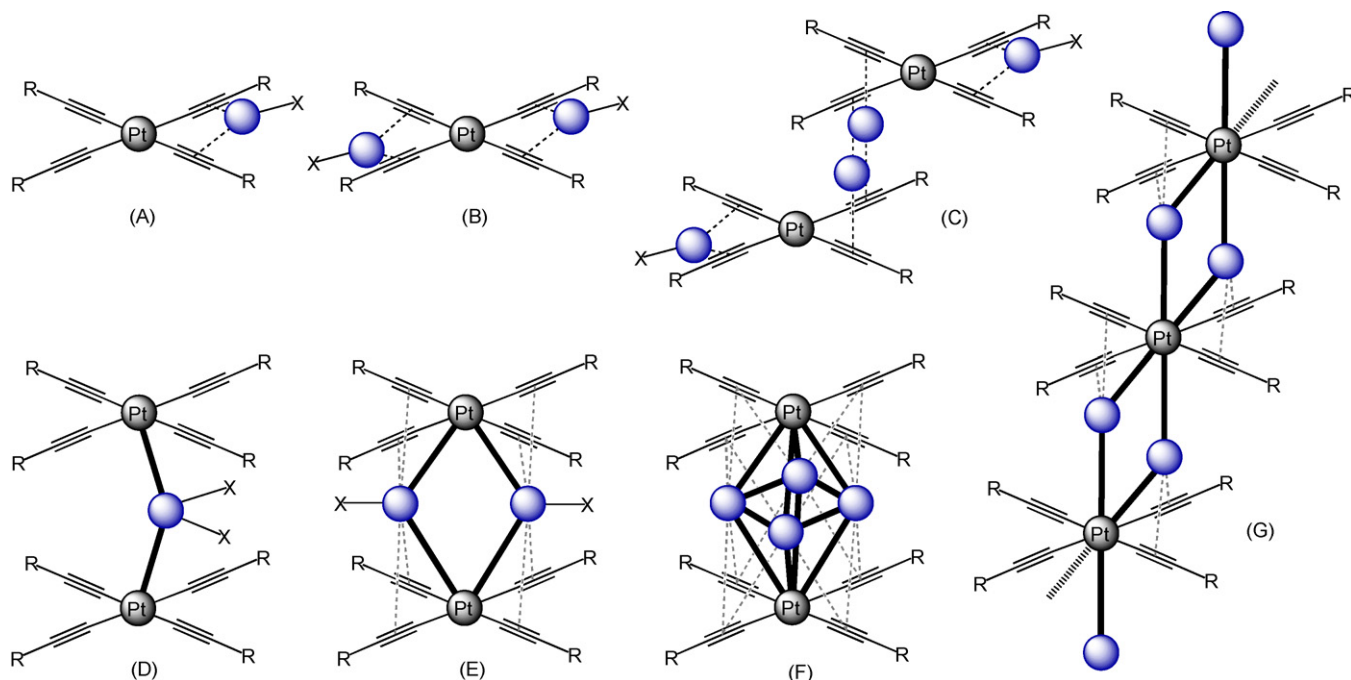


**Fig. 13.** Schematic drawing of multinuclear platinum alkynides of structural type A–G.
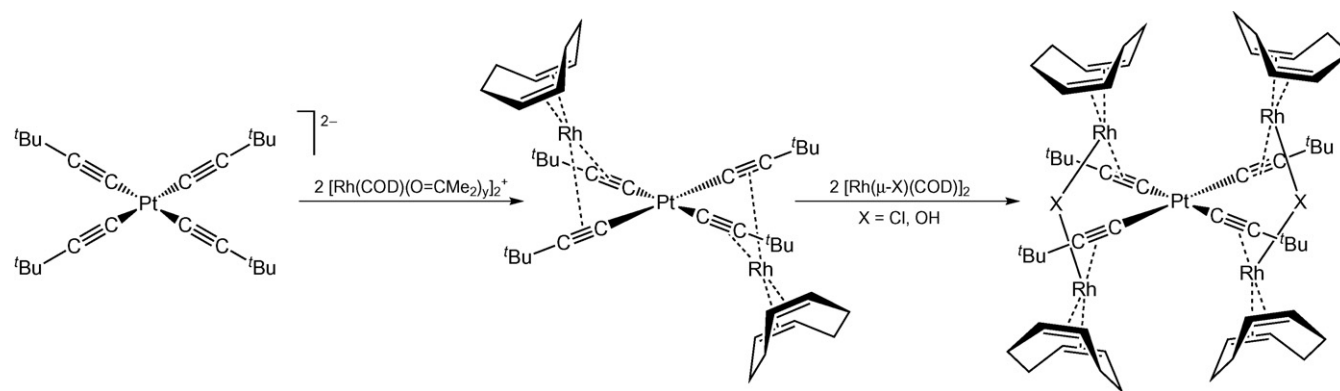
**Scheme 7.** Synthesis of [Pt(C≡C$^t$Bu)$_4$(Rh(COD))$_2$] and [Pt($\mu$-C≡C$^t$Bu)$_4$(Rh$_2$($\mu$-X)(COD)$_2$)$_2$] [131].

metal-to-ligand charge-transfer transitions [127]. According to the nature of R the emission maxima is tunable in the region of 446–608 nm. For the anionic homoleptic tetra-ferrocenylethynyl platinate [Pt(C≡CFc)$_4$]$^{2-}$ (Fc = ($\eta^5$-C$_5$H$_4$)($\eta^5$-C$_5$H$_5$)Fe) the electronic spectrum exhibits two typical low-energy bands at 326 and 344 nm, respectively, which can be assigned to $\pi$–$\pi^*$ and d–$\pi^*$ transitions, for comparison, [Pt(C≡CPh)$_4$]$^{2-}$ shows its absorptions at 335 and 347 nm [10]. Preliminary cyclic voltammetric measurements were also carried out [10].

A diverse range of unexpected heteroleptic platinum alkynide molecules are accessible from the tetra-alkynyl platinate species [Pt(C≡CR)$_4$]$^{2-}$ by either ligand exchange and/or hydrophosphination, when treated with Ph$_2$PH or Ph$_2$PH(O) [128]. Nevertheless, these reactions will not be reported in detail here, rather we concentrate on the preparation of multinuclear homoleptic metal alkynides containing heterobimetallic Pt-M subunits which are depicted in Fig. 13.

Platinum tetra-alkynides [Pt(C≡CR)$_4$]$^{2-}$ in which two platinum(II) $\pi$-tweezer [15,89] units are available can be used as starting materials for the successful preparation of a series of neutral or ionic homo- and heterobimetallic transition metal complexes, whereby two or all four alkynide ligands are simultaneously chelating low-valent transition metal building blocks in, for example, a $\mu$-$\sigma$,$\pi$ fashion (Fig. 13) [15,89,13,129].

Paramagnetic hetero-polynuclear homoleptic platinum–cobalt complexes of type **B**, ($^n$Bu$_4$N)$_2$[Pt(C≡CR)$_4$(CoCl$_2$)$_2$] (R = SiMe$_3$, $^t$Bu) have been synthesized by addition of two equivalents of CoCl$_2\cdot$6H$_2$O to ($^n$Bu$_4$N)$_2$[Pt(C≡CR)$_4$] [130]. These molecules decompose in solution, while in the solid state the blue materials are stable for months. The single solid state structure of the $^t$Bu derivative shows that each CoCl$_2$ fragment is embedded between two alkynyl ligands, whereby the cobalt ions are located above and below the planar Pt(C≡C$^t$Bu)$_4$ unit [130].

Neutral PtRh$_2$ and PtRh$_4$ tetra-alkynides of structural type [Pt(C≡CR)$_4$(Rh(COD))$_2$] and [Pt($\mu$-C≡C$^t$Bu)$_4$(Rh$_2$($\mu$-X)(COD)$_2$)$_2$] (X = Cl, OH; R = $^t$Bu, SiMe$_3$; COD = cyclo-octa-1,5-diene) were synthesized in moderate yields from homoleptic ($^n$Bu$_4$N)$_2$[Pt(C≡CR)$_4$] by sequential treatment with [Rh(COD)(Me$_2$C=O)$_2$](ClO$_4$) and

[Rh($\mu$-X)(COD)]$_2$ (Scheme 7) [131]. In these reactions the platinum ions remain $\sigma$-bonded to the alkynide ligands, no trans-alkynylation processes being observed. This contrasts from appropriate platinum and iridium compounds, see below. Nevertheless, a different reaction behavior is found, when the organometallic titanium $\pi$-tweezer [Ti](C≡CSiMe$_3$)$_2$ ([Ti] = ($\eta^5$-C$_5$H$_4$SiMe$_3$)$_2$Ti) was reacted with [Rh(Cl)(COD)]$_2$ [132]. Upon cleavage of the titanium–carbon bonds homotri-, [Rh($\mu$-$\sigma$,$\pi$-C≡CSiMe$_3$)$_3$($\mu$-Cl)], and -bimetallic complexes ([Rh(COD)($\mu$-$\sigma$,$\pi$-C≡CSiMe$_3$)]$_2$), were obtained along with [Ti]Cl$_2$ [132].

In these heterometallic PtRh molecules, the dianionic homoleptic tetra-alkynyl platinate moiety acts as a chelating metalloligand toward two cationic Rh(COD) units as confirmed by spectroscopic studies. In addition, the solid state structure of pentanuclear PtRh$_4$ ([Pt($\mu$-C≡C$^t$Bu)$_4$(Rh$_2$($\mu$-X)(COD)$_2$)$_2$] with X = Cl and HO) was established by single crystal X-ray structure analysis. The platinum and rhodium metals exhibit an essential square-planar environment with the expected structural features [131]. The alkynyl ligands are asymmetrically- and datively-bonded to the rhodium(I) centers which are located above and below the platinum coordination plane [131]. However, when instead of [Rh(Cl)(COD)]$_2$ or [Rh(COD)(Me$_2$C=O)$_2$](ClO$_4$) the corresponding iridium species are reacted with ($^n$Bu$_4$N)$_2$[Pt(C≡CSiMe$_3$)$_4$], an unsymmetrical heterobimetallic complex was obtained (Scheme 8) [133].

The PtIr complex shown in Scheme 8 exhibits in the solid state a bent $\sigma$,$\pi$ double-alkynyl bridging system formed by a $\sigma$-alkynyl migration of one Me$_3$SiC≡C$^-$ ligand from platinum to iridium. Compared with the rhodium compound in which each alkynide ligand is $\sigma$-bonded to the Pt center, the PtIr system comprises an unsymmetrical [Pt($\sigma$-C≡CR)$_3$($\pi$-C≡CR)]$^-$ bridging moiety [133]. The heterobimetallic PtIr complex [Pt($\sigma$-C≡CSiMe$_3$)$_2$($\mu$-2$\kappa$C$^\alpha$:$\eta^2$-C≡CSiMe$_3$)][Ir(COD)($\mu$-1$\kappa$C$^\alpha$:$\eta^2$-C≡CSiMe$_3$)]$^-$ is also suited to use in the synthesis of heterotrimetallic transition metal alkynide complexes through reaction with metal compounds including [cis-M(C$_6$F$_5$)$_2$(thf)$_2$] (M = Pd, Pt), [Rh(COD)(Me$_2$CO)$_x$]$^+$, [Pd($\eta^3$-C$_3$H$_5$)($\mu$-Cl)]$_2$, and [AgClO$_4$] in which the appropriate metal atoms are connected by $\sigma$- and $\pi$-bonded alkynide ligands [133]. A similar reaction behavior was observed during the synthe-
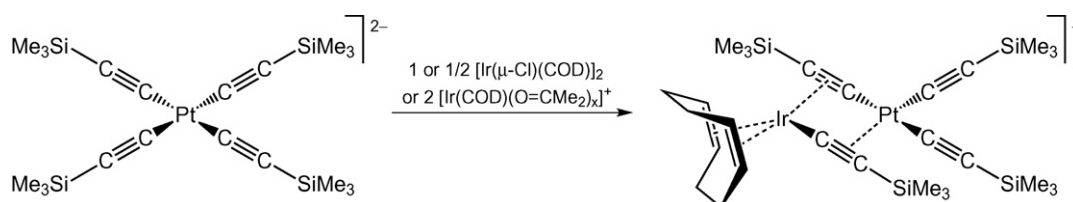


**Scheme 8.** Reaction behavior of [Pt(C≡CR)$_4$]$^{2-}$ toward iridium COD complexes [133].
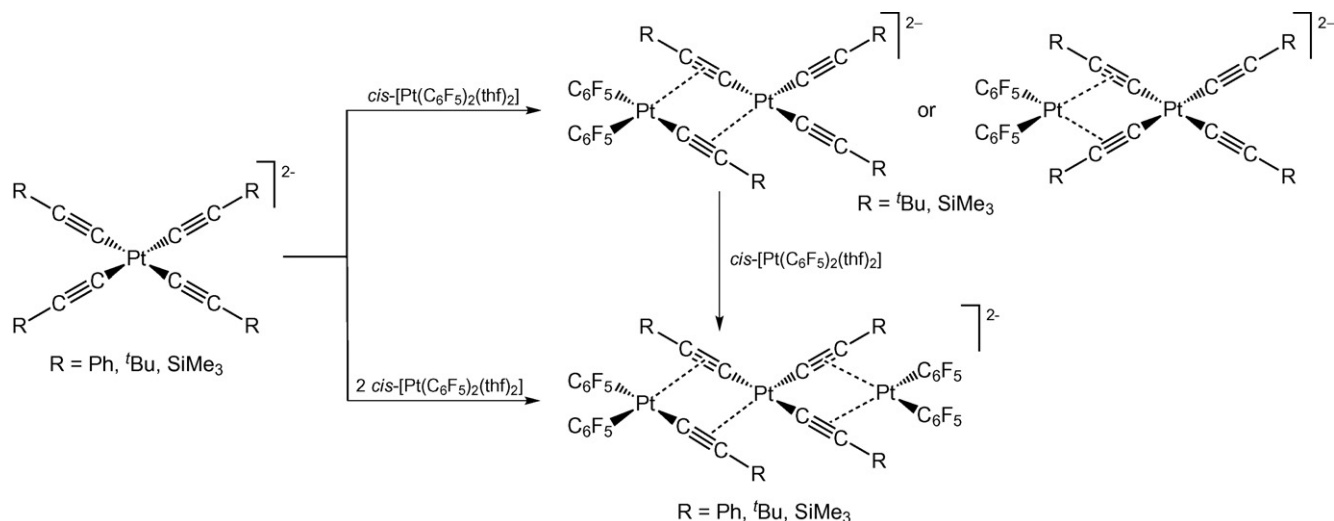
**Scheme 9.** Reaction behavior of $(^nBu_4N)_2[Pt(C\equiv CR)_4]$ with $[cis\text{-}Pt(C_6F_5)_2(thf)_2]$ in the ratio of 1:1 and 1:2, respectively [126].

sis of di- and tri-nuclear platinum complexes. Treatment of $(^nBu_4N)_2[Pt(C\equiv CR)_4]$ ($R = Ph$, $^tBu$, $SiMe_3$) with one equivalent of $[cis\text{-}Pt(C_6F_5)_2(thf)_2]$ gave dinuclear $[Pt(\sigma\text{-}C\equiv CR)_2(\mu\text{-}2\kappa C^\alpha{:}\eta^2\text{-}C\equiv CR)][Pt(C_6F_5)_2(\mu\text{-}1\kappa C^\alpha{:}\eta^2\text{-}C\equiv CR)]^{2-}$ and $[(RC\equiv C)_2Pt\{(\mu\text{-}\sigma,\pi\text{-}C\equiv CR)_2Pt(C_6F_5)_2\}]^{2-}$, respectively (Scheme 9) [126]. Addition of a further equivalent of $[cis\text{-}Pt(C_6F_5)_2(thf)_2]$ to the latter compound produced a homo-trimetallic $Pt_3$ complex as shown in Scheme 9.

All compounds depicted in Scheme 9 were fully characterized by IR and NMR spectroscopies as well as X-ray structure analysis. In the trimetallic platinum complex, all metal atoms have basically square-planar geometries, although the nature of the ligating groups varies due to the migration of a $RC\equiv C$ $\sigma$-bonded alkynyl ligand of the $[Pt(C\equiv CR)_4]^{2-}$ moiety to one of the two $Pt(C_6F_5)_2$ fragments [126]. The tetra-alkynyl platinate $[Pt(C\equiv CR)_4]^{2-}$ ($R = Ph$, $^tBu$, $SiMe_3$) can also act as a double alkynylation reagent toward $[(\eta^5\text{-}C_5Me_5)M(PEt_3)(Me_2C=O)_2](ClO_4)_2$ ($M = Rh$, Ir) yielding heterobimetallic bis($\mu$-alkynide)(MPt) and unsymmetrical trimetallic double bis($\mu$-alkynide) (MPtPt) transition metal complexes (Scheme 10) [134].

The palladium allyl chloride $[Pd(\eta^3\text{-}C_3H_5)(\mu\text{-}Cl)]_2$ also allows the synthesis of PtPd homoleptic complexes of structural type **A** and **B** (Fig. 13) depending on the stoichiometry with respect to the tetra-alkynyl platinate $[Pt(C\equiv CR)_4]^{2-}$ ($R = Ph$, $^tBu$, $SiMe_3$) [135]. In these molecules two alkynyl ligands of individual $Pt(C\equiv CR)_2$ building blocks are $\mu\text{-}\sigma,\pi$-bonded to a electrophilic cationic palladium allyl unit. A dynamic behavior is observed for the $Pd(\eta^3\text{-}C_3H_5)$ moiety in type **A** molecules by $^1H$ NMR studies suggesting an exchange process taking place between bridging and terminal alkynyl ligands [135]. This phenomenon is, however, not observed for type **B** molecules.

A structural type **B** molecule containing platinum and mercury metal atoms could be synthesized starting from $HgX_2$ ($X = Cl$, Br, I) and $[Pt(C\equiv CR)_4]^{2-}$ ($R = {}^tBu$, $SiMe_3$) [136]. The thus formed bis($\eta^2$-alkynyl)dihalogeno-mercury(II) compounds $[Pt\{(\mu\text{-}\sigma,\pi\text{-}C\equiv CR)_2HgX_2\}_2]^{2-}$ contain $\pi$-alkyne mercury moieties. In these compounds the dianionic platinum alkynyl fragment acts as an organometallic $\pi$-tweezer and chelates two neutral $HgX_2$ building blocks which was proven by IR and NMR spectroscopic data [136].

However, changing from mercury(II) salts to cadmium(II) perchlorate, $Cd(ClO_4)_2\cdot 6H_2O$, produced insoluble materials pointing to polymeric structures [137]. By addition of $^nBu_4NX$ ($X = Cl$, Br, CN) the polymeric structure is broken and smaller $Pt_2Cd_2$ molecules of structural type **E** (Fig. 13), $[\{Pt(\mu\text{-}\kappa C^\alpha C^\alpha\text{-}C\equiv CPh)_4CdX\}_2]^{2-}$ were formed. This molecule is also formed when $[Pt(C\equiv CPh)_4]^{2-}$ is reacted with $[CdCl_2\cdot 2.5H_2O]$ [138]. Within this reaction a type **E** molecule along with a type **B** system ($[\{Pt\{(\mu\text{-}\sigma,\pi\text{-}C\equiv CPh)_2CdX_2\}_2]^{2-}$) is formed. Complex $[\{Pt(\mu\text{-}\kappa C^\alpha C^\alpha\text{-}C\equiv CPh)_4CdCl\}_2]^{2-}$ crystallized as a centrosymmetric tetra-nuclear $Pt_2Cd_2$ organometallic anion in which two eclipsed $[Pt(C\equiv CPh)_4]^{2-}$ units are connected via two CdCl entities. In this tetra-nuclear cluster four platinum–cadmium interactions with a distance of 2.960(1) Å and a rather unusual $\mu\text{-}\kappa C^\alpha C^\alpha$ bonding mode for the alkynyl bridging ligands are found [137,138].

Slow diffusion of acetone solutions of $Cd(ClO_4)_2\cdot 6H_2O$ and $[Pt(C\equiv CPh)_4]^{2-}$ resulted in formation of the decanuclear $Pt_4Cd_6$ cluster $[Pt_4Cd_6(C\equiv CPh)_4(\mu\text{-}C\equiv CPh)_{12}(\mu_3\text{-}OH)_4]$ [137]. This cluster contains a hexanuclear $[Cd_6(\mu_3\text{-}OH)_4]^{8+}$ and four tetraphenylalkynyl platinate anions which are connected by PtCd and $\pi$-phenylacetylide–cadmium interactions (Fig. 14).

Recently, a variety of rhomboidal $Pt_2Cd_2$ systems (structural type **E** molecules, Fig. 13) of composition $[Pt(C\equiv CR)_4CdL]_2$ ($R = Tol$, $C_6H_4\text{-}4\text{-}OMe$, $C_6H_4\text{-}3\text{-}OMe$; $L = dmso$, acetone, py, $NC_5H_4\text{-}4\text{-}Me$, $NC_5H_4\text{-}4\text{-}CF3$, pzH) was synthesized by reacting $[Pt(C\equiv CPh)_4]^{2-}$ and $Cd^{2+}$ in different donor solvents [139]. The acetone and dmso stabilized complexes were prepared directly while the
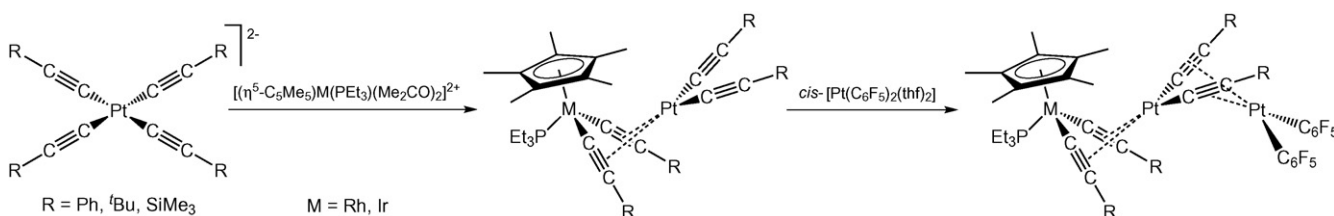


**Scheme 10.** Synthesis of heterobimetallic MPt and trimetallic MPtPt complexes (M = Rh, Ir) [134].
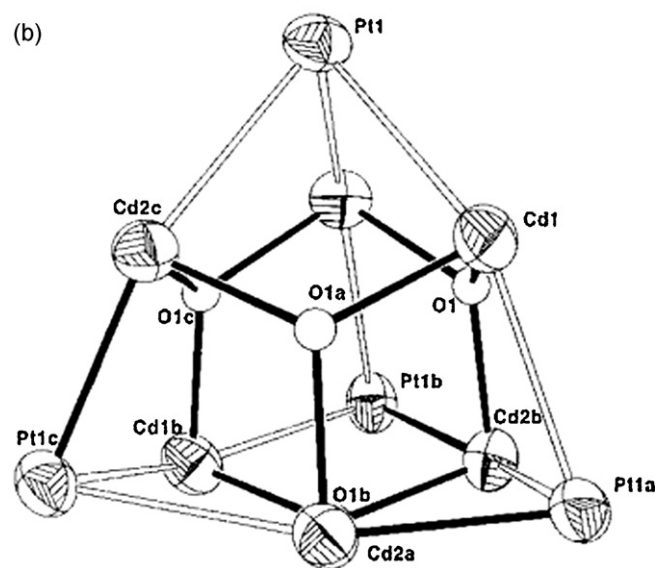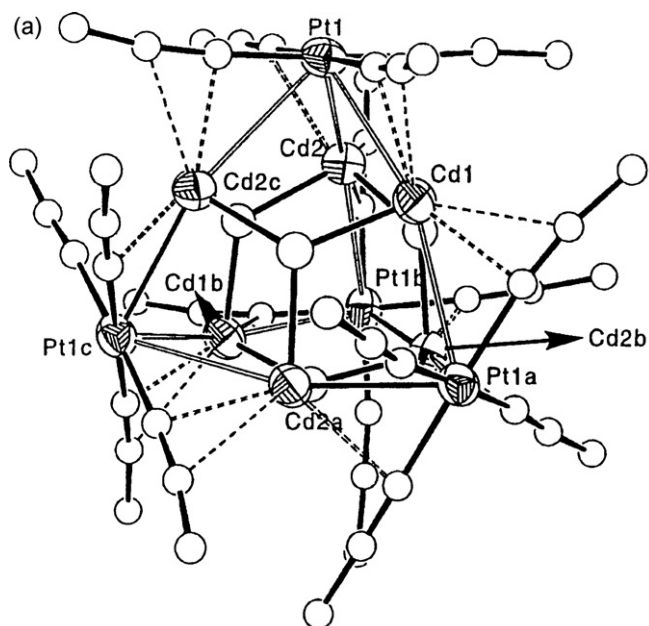
**Fig. 14.** Structure of $[Pt_4Cd_6(C\equiv CPh)_4(\mu\text{-}C\equiv CPh)_{12}(\mu_3\text{-}OH)_4]$ in the solid state (Please, notice that the phenyl groups have been omitted for clarity, left) and the central $Pt_4Cd_6(\mu_3\text{-}OH)_4$ cluster unit (right) [137].

N-donor molecules were introduced by ligand exchange of the acetone derivatives. The precipitation of white, insoluble polymers of composition $[Pt(C\equiv CR)_4Cd]_n$ was observed from $[Pt(C\equiv CR)_4Cd(acetone)]_2$ by dissociation of the weakly bonded solvent molecules. The $CdL^{2+}$ unit in $[Pt(C\equiv CR)_4CdL]_2$ was stabilized by a synergistic combination of $Pt\cdots Cd$ and $Cd\cdots$alkynyl bonding interactions. Depending on the organic group R symmetrical or unsymmetrical planar $Pt_2Pd_2$ frameworks are formed in the solid state [139].

The luminescence properties of each of the cadmium complexes described above have been investigated [137–139]. A contribution of the platinum–cadmium interaction to the orbitals involved was assumed. The emission was tentatively attributed to $\pi^*(C\equiv CPh) \rightarrow C\equiv C(Pt_2\text{-}Cd_2)$ (cluster centered-to-ligand charge transfer) mixed with a Pt–Cd-based charge transfer [138].

In copper, silver, and gold chemistry structural type **B**, **C**, and **F** molecules (Fig. 13) are most favored. Table 6 summarizes the
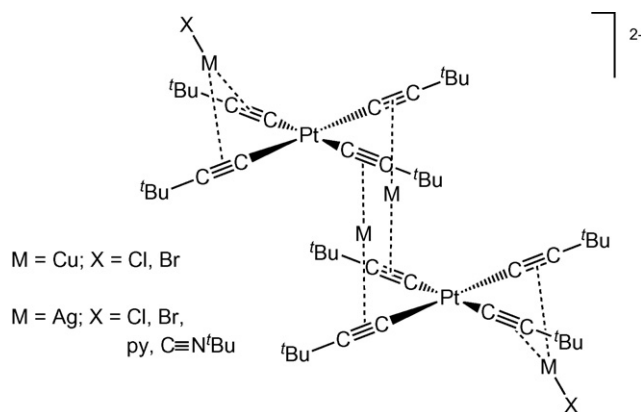


**Fig. 15.** Schematic representation of the complex anions $[Pt_2M_4(C\equiv C^tBu)_8X_2]^{2-}$ [140].

tri- (type **B**) and hexanuclear (types **C** and **F**) complexes in which platinum metal centers are linked with copper(I), silver(I) or gold(I) ions only by alkynyl groups synthesized to date.

Type **B** molecules (Fig. 13 and Table 6) are accessible either by reacting $[Pt(C\equiv CR)_4]^{2-}$ (R = Ph, $^tBu$) with two equivalents of [MX] (M = Cu, Ag; X = Cl, Br, C≡N$^tBu$, py) or treatment of the hexanuclear cluster $[Pt_2M_4(C\equiv CPh)_8]$ with Lewis-bases including halides (Cl$^-$, Br$^-$), iso-nitriles (C≡N$^tBu$) or pyridine in the ratio of 1:4 [140]. Complexes $[Pt\{(\mu\text{-}\sigma,\pi\text{-}C\equiv CPh)_2MX\}_2]^{n-}$ (M = Cu, Ag; $n$ = 2: X = Cl, Br; $n$ = 0: C≡N$^tBu$, py) (Table 6) are obtained in good yield by these methods. The structure of the appropriate complexes in the solid state are represented by the general example $[Pt\{(\mu\text{-}\sigma,\pi\text{-}C\equiv CPh)_2CdX_2\}_2]^{2-}$ (see above). The trinuclear $PtM_2$ organometallic anion shows a centrosymmetric structure, whereby the two MX units are chelated by the $Pt(C\equiv CR)_4$ alkynyl groups; no metal–metal interaction occurs [140]. Additional evidence for the $\pi$-coordination of the alkynyl ligands to group 11 metal ions was obtained from IR and NMR spectroscopies. However, when $[Pt_2M_4(C\equiv CPh)_8]$ is replaced by the analogues $^tBu$-functionalized hexanuclear clusters, and chloride, bromide or pyridine as a co-reactand, type **C** complexes of composition $[Pt_2Ag_4(C\equiv C^tBu)_8X_2]^{2-}$ could be isolated [140]. Another entry to these clusters is given by the addition of [AgX] (X = Cl, Br) or [CuCl] to $(^nBu_4N)_2[Pt(C\equiv C^tBu)_4]\cdot 2H_2O$ in the molar ratio of 2:1 [140]. In $[Pt_2M_4(C\equiv C^tBu)_8X_2]^{2-}$ two individual $[Pt\{(\mu\text{-}\sigma,\pi\text{-}C\equiv C^tBu)_2MX\}(C\equiv C^tBu)_2]$ building blocks are connected to each other by $\eta^2$-coordination of the free $^tBuC\equiv C$ ligands to copper(I) or silver(I) ions (Fig. 15). Evidence for the composition of the latter molecules comes from FAB mass-spectrometry as well as IR and NMR spectroscopies [140].

Hexanuclear type **F** clusters (Fig. 13 and Table 6) of composition $[Pt_2M_4(C\equiv CR)_8]$ (M = Cu, Ag, Au; R = Ph, $^tBu$) have been prepared by Forniés [8,10,11,112,125] and Yam [12,113] using the methodologies shown in Scheme 11.

These clusters contain six transition metal atoms which are arranged in a somewhat irregular octahedron with the square-planar surrounded platinum atoms mutually *trans* (apical positions) and the group 11 metals in the equatorial plane showing Pt–Pt distances larger than 4.4 Å [11,12]. The Pt–M bond distances are comparable with those ones found in related complexes, for example, [1,1-ferrocenediyl-$Pt_2Cu_3(C\equiv CPh)_6$], suggesting the presence of weak metal–metal interactions [141]. The Cu–Cu separations are ca. 3.03 and 3.30 Å, larger than the distances in metallic copper (2.56 Å) or the sum of the van der Waals radii of two copper atoms (2.8 Å) ruling out any bonding interactions between the metals. For the appropriate silver clusters silver–silver distances of ca. 3.19 and 3.22 Å are observed which are larger than the dis-

**Table 6**
Structural type **B**, **C**, and **F** molecules of M = Cu, Ag, and Au.

| Type | M | X | R | Refs. |
|------|---|---|---|-------|
| **B** (PtM$_2$) | Cu | Cl, Br | Ph | [140] |
| | | | $^t$Bu | [140] |
| | Ag | Cl, Br, C≡N$^t$Bu, py | Ph | [140] |
| | | | $^t$Bu | [140] |
| **C** (Pt$_2$M$_4$) | Cu | Cl, Br | $^t$Bu | [140] |
| | Ag | Cl, Br, py | $^t$Bu | [140] |
| **F** (Pt$_2$M$_4$) | Cu | – | Ph | [125,113,114] |
| | | | $^t$Bu | [125,113,115,116] |
| | | | SiMe$_3$ | [113] |
| | | | C$_6$H$_4$—3-OMe | [11] |
| | | | C≡CC$_6$H$_4$—4-OMe | [113] |
| | Ag | – | Ph | [113,125] |
| | | | $^t$Bu | [125] |
| | | | C$_6$H$_4$—3-OMe | [11] |
| | | | C≡CC$_6$H$_4$—4-Me | [12] |
| | Au | – | $^t$Bu | [125] |

tances in metallic silver (2.89 Å) but shorter than the sum of the van der Waals radii of two silver atoms (3.4 Å) pointing to weak metal–metal interactions.

While clusters with $^t$BuC≡C ligands exist both in solution and in the solid state as discrete monomers, the corresponding pheny-lacetylide derivatives possess, depending on the crystallization conditions, a mono-, di-, tri- or even polymeric structure (Fig. 13) with unsupported intermolecular platinum–platinum distances of 3.0–3.5 Å [113,114]. This becomes noticeable by the color of the obtained solid materials supporting the formation of inter-cluster metal–metal separations. In general, the higher the aggregation grade the deeper the color, i.e., monomers are pale-yellow (Ag) or red (Cu). Dark violet-green materials are obtained when the initial solutions are completely vacuum dried and then treated with pre-cipitating solvents [114]. The electronic interactions between the clusters were studied by UV–vis spectroscopy. A more detailed dis-cussion is given below, i.e., for [Pt$_2$M$_4$(C≡C—C$_6$H$_4$—3-OMe)$_8$]$_n$ [11]. A remarkable feature of the oligomers/polymers is both the orienta-tion of the Pt$_2$M$_4$ building blocks with respect to each other and the eclipsed or staggered orientation of the square-planar tetra-alkynyl

platinate unit. The two platinate entities are in a staggered confor-mation (38°) in the trimeric system (Fig. 16, right) [114], while for dimeric [Pt$_2$Cu$_4$(C≡CPh)$_8$] (Fig. 16, left) [113] the angles of the indi-vidual platinate entities differ (upper octahedron: 7.8° (eclipsed), lower octahedron: 40.8° (staggered)). Within the oligomeric struc-tures the Pt$_2$M$_4$ cluster units are successively twisted between 40° and 44°.

Furthermore, studies were carried out to examine the influence of solvent and hydrogen-bonding interactions in the self-assembly of Pt$_2$M$_4$ clusters (M = Cu, Ag) (Fig. 17) [11]. Weak non-covalent metal–solvent interactions (Pt⋯HCCl$_3$, or Ag⋯O$_{thf}$) are observed with direct influence toward the axial Pt–Pt bonding result-ing in different aggregation numbers (vide supra) [11]. In the methoxy derivative [Pt$_2$Ag$_4$(C≡C—C$_6$H$_4$—3-OMe)$_8$]$_n$ the formation of C—H⋯O$_{OMe}$ hydrogen bonds between alternate Pt$_2$Ag$_4$ cluster units is observed contributing also to axial platinum–platinum interactions, resulting in a 1D arrangement leading to a smaller tor-sion angle of the square-planar tetra-alkynyl platinate units (19.6°) (vide supra) [11]. The formation of hydrogen bonds results in a deformation of the otherwise square-planar tetra-alkynyl platinate
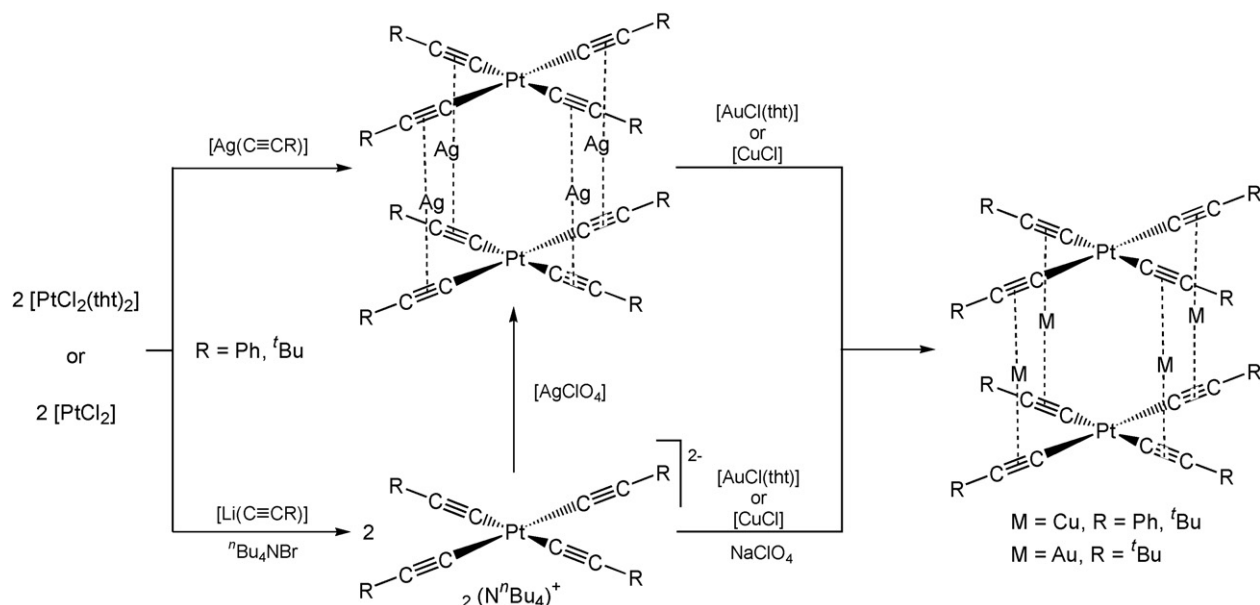


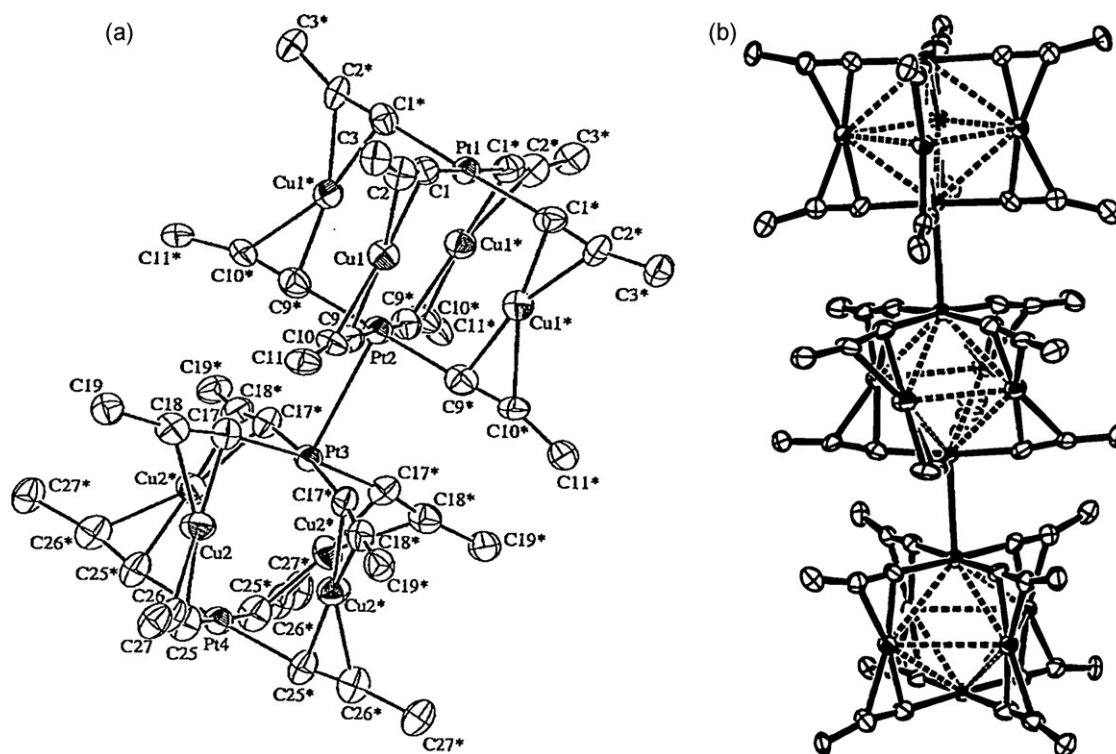**Scheme 11.** Preparation methods for hexanuclear Pt$_2$M$_4$ clusters [Pt$_2$M$_4$(C≡CR)$_8$] [125].

Fig. 16. Structures of dimeric (left) and trimeric (right) $[Pt_2Cu_4(C\equiv CPh)_8]$ in the solid state (phenyl rings are omitted for clarity) [113,114].

units leading to a more compact cluster fragment, and hence a better platinum–platinum interaction. This can be taken to explain the formation of polymeric chains.

A polymeric complex comprised of decanuclear platinum–silver $[Pt_2Ag_8(C\equiv C^tBu)_8(OClO_3)_2(Me_2CO)_2]^{2+}$ units was obtained from the reaction of $[Pt_2Ag_4(C\equiv C^tBu)_8]$ with $[AgClO_4]$ [115]. Each of the additional four silver ions is thereby chelated by two phenyl alkynyl platinate ligands (Scheme 12). The platinum–silver $Pt_2Ag_8$ cluster entities are linked by $\mu$-bridging perchlorate anions. Addition of 2,2′-bipyridine causes the polymeric structure to be broken, with formation of complexes of structural type C and F (depending on the molar ratio), with four additional Ag(bpy) moieties each $\pi$-coordinated by two alkynyl ligands [116]. Direct treatment of $[Pt_2Ag_4(C\equiv C^tBu)_8]$ with 2,2′-bipyridine leads to a polymeric structure in which bipyridine connects the monomeric clusters via Ag–N bonds.

The luminescence behavior of the polynuclear platinum–copper and platinum–silver acetylide clusters discussed above was studied showing that photoluminescence depends on the axial Pt⋯Pt interactions either in the solid state or in solution [11,12,113–116]. The photoluminescence spectra of $[Pt_2Ag_4(C\equiv C-C_6H_4-3-OMe)_8]$ in different aggregation states are depicted in Fig. 18 by way of example [11]. As it can be seen from this figure, the cluster is brightly emissive. The emissions of the monomeric, yellow cluster with or without coordinated tetrahydrofuran can be attributed to a $^3MLM'CT$ ($Pt(d)/\pi(C\equiv CR) \rightarrow Pt(p_z)/Ag(sp)/\pi^*(C\equiv CR)$) state which is affected by Pt⋯Pt and Ag⋯Ag interactions, and additionally Ag⋯O solvent contacts in the tetrahydrofuran coordinated derivatives. However, polymeric $[Pt_2Ag_4(C\equiv C-C_6H_4-3-OMe)_8]_n$ is less emissive and shows phosphorescence resulting from either a $^3MMLCT$ excited state or an admixture of Pt–Pt centered $^3(d\sigma^*p_z\sigma)$ and $^3MMLCT$ excited states [11].

Cyclic voltammetry measurements carried out with $[Pt_2M_4(C\equiv C-C\equiv C-C_6H_4-4-Me)_8(thf)_4]$ suggest that the group 11 metal ions M (M = Cu, Ag) are more readily oxidized and reduced than the platinum(II) ion [12].

By decomposing the molecular clusters $[Pt_2M_4(C\equiv C^tBu)_8]$ (M = Cu, Au) adsorbed on silica or titania, bimetallic catalysts could be prepared as demonstrated by Chandler et al. [109] and Bus and van Bokhoven [142]. The $SiO_2$-supported PtAu clusters are 1.5 nm in diameter and are of uniform composition, with the surfaces being enriched with gold. The respective titania-supported particles are larger (2–3 nm) and not so uniformly structured. Both the supported PtCu and PtAu clusters were used as catalysts for toluene hydrogenation, whereby it was observed that they show less activity as compared with traditionally prepared monometallic platinum catalysts [109].

Reactions between the tetra-alkynyl platinates $[Pt(C\equiv CR)_4]^{2-}$ (R = Ph, $C_6H_4-4-Me$, $C_6H_4-4-OMe$, $C_6H_4-4-^tBu$, $^tBu$, $SiMe_3$) and $[M_2(\mu-Ph_2PXPPh_2)_2(MeC\equiv N)_2]^{2+}$ (M = Cu, Ag, Au; X = NH, $CH_2$) yielded acetylide-linked heteroleptic PtM, $PtM_2$, $Pt_2M_3$, and $Pt_2M_4$ complexes, whereby two platinum–carbon$_{alkynyl}$ bonds were cleaved and replaced by $Ph_2PXPPh_2$ linking units [110,111]. A summary of complexes prepared in this manner is shown in Scheme 13. These complexes emit strongly, with lifetimes in the microsecond range in the solid state. A trend in the emission energy depending on the different electronic nature of R was observed and ascribed to alkynyl-to-cluster $[RC\equiv C \rightarrow PtM]$ LMMCT transitions [110,111].

Structural type F molecules (Fig. 13), $[Pt_2Tl_4(C\equiv CR)_8]$ (R = Ph, $C_6H_4-4-Me$, 1-naphthyl, $^tBu$, $SiMe_3$) featuring four thallium(I) ions sandwiched by two homoleptic tetra-alkynyl platinate building blocks are accessible from $(^nBu_4N)_2[Pt(C\equiv CR)_4]\cdot nH_2O$ (R = Ph, $^tBu$, $SiMe_3$) or $Li_2[Pt(C\equiv CR)_4]$ (R = Ph, $^tBu$, $C_6H_4-4-Me$, 1-naphthyl) and inorganic $[TlNO_3]$ or $[TlPF_6]$ [112,143]. The lithium salt gives much higher yields (ca. 80%) than the analogous tetra-n-butylammonium salt (ca. 55%). As typical for type F molecules, the two platinate fragments are eclipsed and are connected by four "naked" Tl(I) ions. Each of the thallium(I) ions is thereby asymmetrically coordinated by four alkynyl ligands of the platinate fragments (two associated with each Pt unit) forming a $A_4Tl$ square-pyramidal geometry with thallium at the apex and A = midpoint of the alkynyl ligand [143]. Noteworthy is that in the case of the 1-naphthyl deriva-
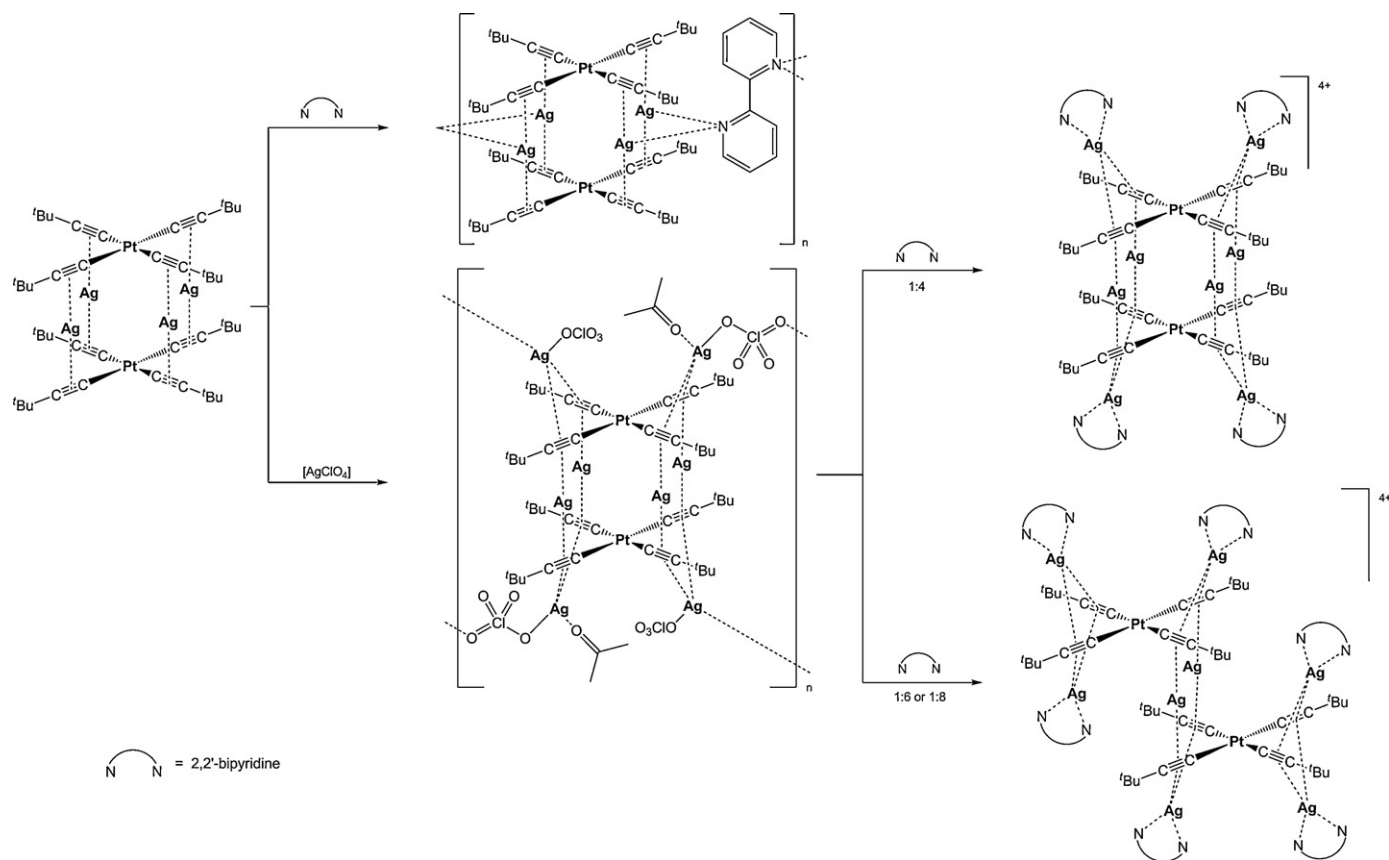
**Scheme 12.** Reaction behavior of $[Pt_2Ag_4(C{\equiv}C^tBu)_8]$ toward $[AgClO_4]$ and 2,2′-bipyridine [116].

tive additional Tl⋯acetone (solvent) and Tl⋯naphthyl secondary interactions are observed [112]. For the appropriate $C_6H_4$—4-$CF_3$ substituted compounds the platinum centers form two unsupported Pt–Tl bonds and hence, an extended columnar structure resulting from $PtTl_2(C{\equiv}C$—$C_6H_4$—4-$CF_3)_4$ moieties coordinated to each other through secondary Tl⋯$\eta^2$-acetylenic interactions are likely [112]. Most commonly, the chemistry of such molecules is characterized by attractive metal–thallium interactions as well as intermolecular Tl contacts and Tl-ligand bonds. The luminescent behavior of these heterometallic platinum–thallium containing molecules has been reported and discussed in detail [112,143], but not only the alkynide compounds show luminescence also the respective platinum cyanide complex [$trans$-$Tl_2Pt(C{\equiv}N)_4$] [144]. The luminescent properties of these systems measured in solution
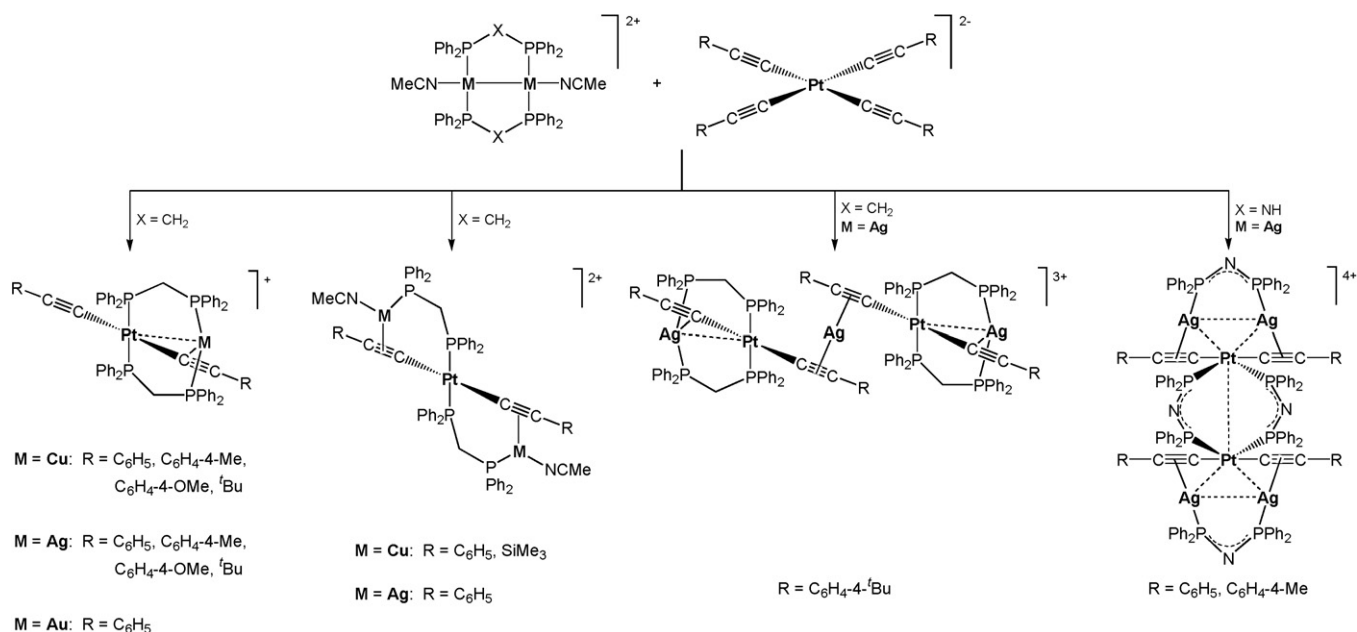


**Scheme 13.** Reaction chemistry of $[Pt(C{\equiv}CR)_4]^{2-}$ (R = Ph, $C_6H_4$-4-Me, $C_6H_4$-4-OMe, $C_6H_4$-4-$^tBu$, $^tBu$, $SiMe_3$) toward $[M_2(\mu$-$Ph_2PXPPh_2)_2(MeC{\equiv}N)_2]^{2+}$ (M = Cu, Ag, Au; X = NH, $CH_2$) [110,111].

(a)

(b)

(c)
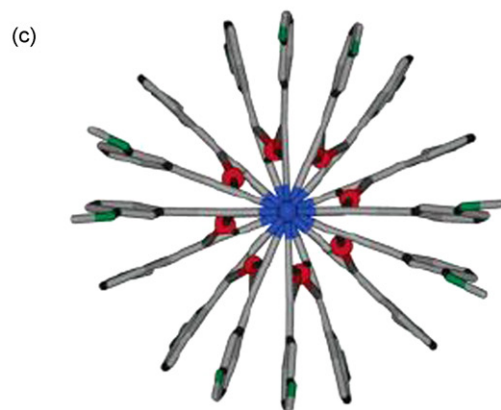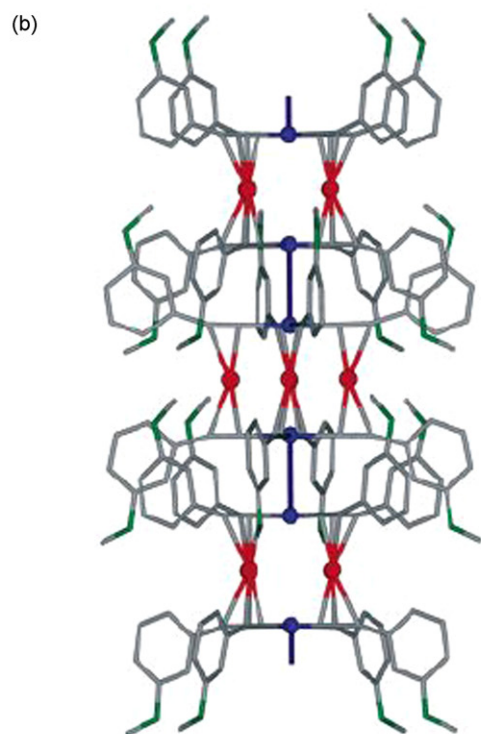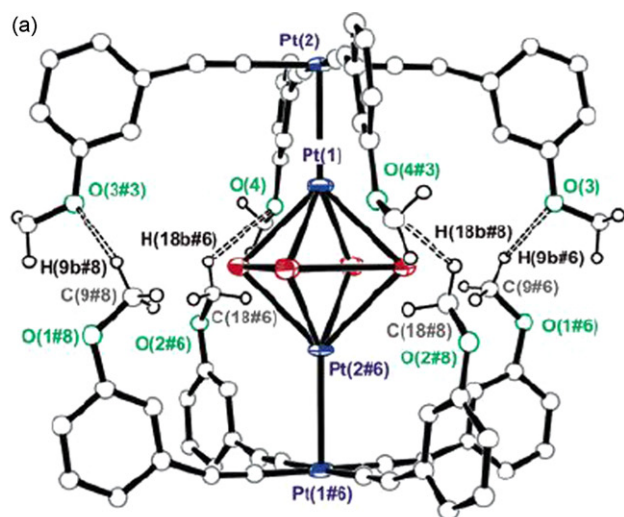
**Fig. 17.** Structure of $[Pt_2Ag_4(C≡C–C_6H_4–3-OMe)_8]_n$ in the solid state. Left: Hydrogen-bonding of one single unit. Middle: Schematic view of three units. Right: Perspective view of the chain along the $a$ axis [11].
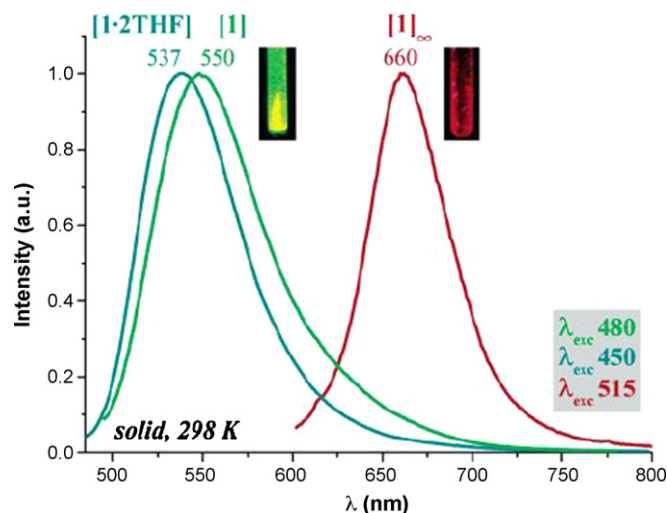


**Fig. 18.** Normalized solid state emission spectra of $[Pt_2Ag_4(C≡C–C_6H_4–3-OMe)_8]$ (green, 550 nm), $[Pt_2Ag_4(C≡C–C_6H_4–3-OMe)_8(thf)_2]$ (blue, 537 nm), and $[Pt_2Ag_4(C≡C–C_6H_4–3-OMe)_8]_∞$ (red, 660 nm) [11].

(blue) differ from those in the solid state (orange) [112,143]. In general, excitation of solid samples with visible light resulted in intense luminescence, whereby the emission spectra are dominated by a broad asymmetric orange luminescence. The phenyl–alkynyl derivatives are compared with the others somewhat blue-shifted [112,143]. In comparison with similar platinum–silver complexes the emissions are notably shifted to lower energies. The authors explain this by structural differences.

A trimetallic $Pt_2Pb$ complex (type **D** molecule, Fig. 13) was reported by Lalinde in 2008 [9]. The impact of the tetra-alkynyl platinate building block on the lead environment and photoluminescence properties was also studied. This homoleptic molecule could be prepared by treatment of $(^nBu_4N)_2[Pt(C≡C–C_6H_4–4-Me)_4]$ with 0.5 equivalents of $[Pb(ClO_4)_2)]·3H_2O$ [9]. Single X-ray diffraction studies reveal that two platinate fragments are connected by a dicationic $Pb(H_2O)_2$ unit in $[Pt_2Pb(C≡C–C_6H_4–4-Me)_8(H_2O)_2]$. A trigonal-bipyramidal coordination sphere around the lead(II) ion is set up by the platinum atoms in axial positions and the two aqua ligands in equatorial positions. The third position is defined by the sterochemically active $6s^2$ lone pair of electrons of the Pb(II) centre. Of interest are the Pt(II)–Pb(II) bond distances of 2.9109(5) and 2.8908(5) Å being only somewhat longer than the sum of the covalent radii (2.75 Å) [9]. The Pt(II)–Pb(II)–Pt(II) unit is bent (149.95(2)°). The stabilization of this complex by solely Pt–Pb bonds is remarkable, since in $[Pt_2Tl_4(C≡CR)_8]$ chemistry (vide supra) in which also a $6s^2$ lone pair of electrons at thallium is available Tl···$η^2$–acetylenic interactions are observed. The luminescent behavior of trimetallic $[Pt_2Pb(C≡C–C_6H_4–4-Me)_8(H_2O)_2]$ was studied showing that this complex exhibits metal-centered emissions at only low temperature (77 K) at 497 nm (solid) and 478 nm (glass), respectively, related to the bent Pt–Pb–Pt entity $(^3[Pt\,d_z^2 → Pb\,6p_z])$ [9].

For a detailed discussion of the chemistry, structures and luminescence properties of homo- and hetero-polynuclear platinum complexes containing the homoleptic structural subunit $[Pt(C≡CR)_4]^{2−}$ see reference [8].

Youngs and Tessier reported in 1997 the synthesis and reaction chemistry of the tetra-alkynyl platinum complex $(^nBu_4N)_2[Pt(OBET)_2]$ (OBET = 1,2-bis(2-ethynylphenyl)ethyne) in which two platinum(II) π-tweezer units [145] and two alkyne "pockets" are available for further coordination. Depending on the size and the coordination geometry preferences of the metal species to be coordinated either the organometallic π-
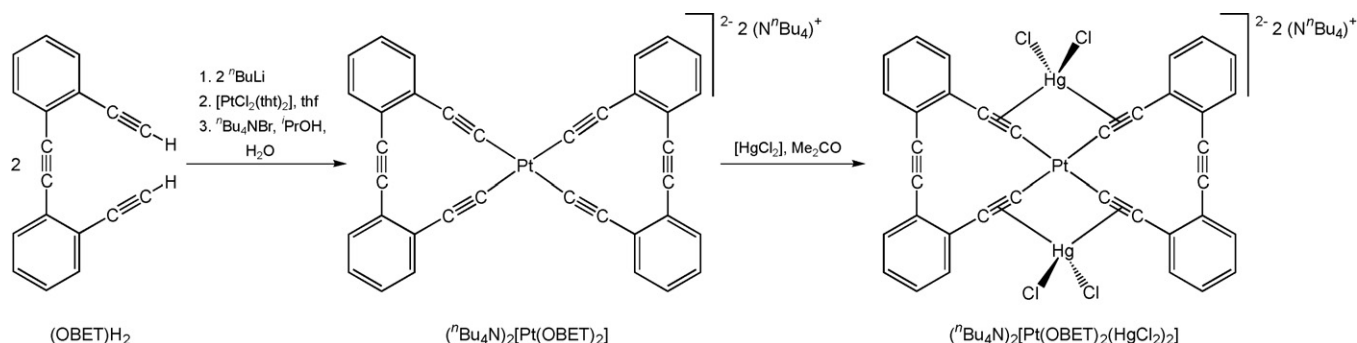
**Scheme 14.** Synthesis of ($^n$Bu$_4$N)$_2$[Pt(OBET)$_2$] and ($^n$Bu$_4$N)$_2$[Pt(OBET)$_2$(HgCl$_2$)$_2$], respectively [145].

tweezers or the alkyne "pockets" are occupied. The synthesis of ($^n$Bu$_4$N)$_2$[Pt(OBET)$_2$] and its reaction towards [HgCl$_2$] is shown in Scheme 14.

The benefit of the OBET ligand over other alkynides in [Pt(C≡CR)$_4$]$^{2-}$ complexes is that the OBET benzo ring in [Pt(OBET)$_2$]$^{2-}$ is in plane bonded within the platinum and carbon acetylide atoms with essentially linear Pt—C≡C—C units. In the solid state this molecule forms an integrated stack system with alternating layers of platinum alkynide anions and ammonium cations.

### 6.3. Neutral metal(II) alkynides, [M(C≡CR)$_2$]

The majority of homoleptic transition metal complexes are anionic with only a few neutral species known at present. The first neutral organometallic alkynide metal compound was synthesized by Nast and coworkers in 1960 by vacuum treatment of [Ni(C≡CR)$_2$]·4NH$_3$ (R = H, Me, Ph), which was in turn obtained by the reaction of Na$_2$[Ni(C≡CR)$_4$] with [Ni(NH$_3$)$_6$](SCN)$_2$ in liquid ammonia [6]. While Ni(C≡CH)$_2$ is extremely explosive and could not be isolated, for [Ni(C≡CPh)$_2$] a complex structure of type {Ni[Ni(C≡CPh)$_4$]}$_n$ was postulated based on magnetic measurements. The structure of this species premises on the diamagnetic and paramagnetic behavior which was assigned to the [Ni(C≡CPh)$_4$]$^{2-}$ building block and the Ni$^{2+}$ cation [6].

In 1982 Ballester *et al.* reported about the successful synthesis of structural type [M(C≡C—C$_6$H$_4$-4-C≡CK)$_2$]·$n$NH$_3$ complexes (M = Ni, Pd) by reacting [Ni(NCS)$_2$(NH$_3$)$_4$] or [Pd(C≡N)$_2$(en)] with the dipotassium salt of *para*-diethynylbenzene in liquid ammonia (vide supra) [119]. These diamagnetic complexes contain a variable amount of NH$_3$ which can partly be removed under high vacuum. The corresponding nickel derivative could also be prepared from [NiX$_2$(PPh$_3$)$_2$] (X = Cl, Br, I) and K$_2$[C≡C—C$_6$H$_4$-4-C≡C], respectively [119]. IR spectroscopy was used to determine the structure of these neutral metal alkynides. All of these materials are diamagnetic, implying a planar geometry around M [119].

A straightforward one-step synthesis method for neutral nickel phenylacetylide [Ni(C≡CPh)$_2$] is given by the electrochemical reaction of phenyl acetylene and nickel in acetonitrile in presence of the electrolyte Et$_4$NBr using a electrolysis cell [106]. The Ni(C≡CPh)$_2$ precipitates during electrolysis; the isolated yield is 66%. The alkynyl carbon–hydrogen bond is thereby cleaved (cathode) by electrical means rather than by alkali (vide supra) by evolution of dihydrogen. The nickel metal is dissolved at the anode giving nickel(II) ions. The superior advantage of this electrochemical method compared to the processes described above are simple reaction conditions, easy work-up, excellent purity, and crystallinity. In a similar way following homoleptic neutral transition metal alkynides could be prepared: M(C≡CPh)$_n$ ($n$ = 3: M = Fe, Co; $n$ = 2: M = Zn; $n$ = 1: M = Cu, Ag, Au) [106]. For a detailed discussion see corresponding Sections.

## 7. Homoleptic alkynide complexes of group 11

In contrast to the other groups, there is a vast array of homoleptic alkynide complexes of the metals of group 11, ranging from simple linear [M(C≡CR)$_2$]$^-$ and trigonal planar [M(C≡CR)$_3$]$^{2-}$ anionic species to polymeric compounds {M(C≡CR)}$_n$ and clusters in which ethynide fragments [C$_2$]$^{2-}$ are encapsulated within a metallic framework. In addition, there are a growing number of mixed-metal cluster species representing a family of diverse structures. Much of the early chemistry of homoleptic Group 11 alkynide complexes has been reviewed in various contexts [146–151].

Homoleptic alkynide complexes of group 11 have numerous applications from use as synthetic intermediates [152], which has origins in the early Cu(I) mediated cross-coupling reactions of aryl halides with cuprous acetylides [153–155]. Copper alkynide complexes have long been recognized as intermediates in the oxidative dimerization of alkynes to diynes [156], and more recently, copper alkynides have been used to prepare diynes through nucleophilic displacement reactions with alkynyl iodonium salts [157]. Indeed, polymeric [{Cu(C≡CR)}$_n$] and [Cu(C≡CR)$_2$]$^-$ act as relatively soft nucleophiles in numerous contexts [158–162] and copper–alkynyl clusters are widely implicated in copper catalyzed reactions, including the alkyne-azide coupling ("click") reaction [163,164]. The luminescent properties of many homoleptic alkynide complexes of coinage metals has prompted wide-spread interest [11,165–171], while the range of structural types leads to a significant body of work concerning the structural chemistry of these systems in the solid state. The gas-phase chemistry of group 11 metals and carbon fragments with acetylenic character is also well developed [172,173].

Homoleptic alkynide complexes of group 11 have been known for well over a century, with the formation of insoluble silver and copper carbides ([M$_2$C$_2$]) being used as an early test for acetylene, although the tendency for these compounds to explode violently when dry suggests that alternative methods of detection are more appropriate in the modern context! In a colorful article from 1900, Mathews and Watters described both the history of formulation of these metal carbides, and the extension of the classical tests for acetylene to the preparation of the even more sensitive auric carbide ([Au$_2$C$_2$]) [4]. Nast and coworkers have explored reactions of the gold carbide [Au$_2$C$_2$] with alkynide anions, which are thought to give species of general form [RC≡CAuC≡CAuC≡CR]$^{2-}$ (R = Ph, Me, H), although structural data were not forthcoming [174,175]. In more recent times, Mak et al. have explored the stabilization of [Ag$_2$C$_2$] in the form of double, triple and quadruple salts through reactions of the carbide with other Ag(I) salts and Ag[BF$_4$]. These compounds and their structures have been comprehensively reviewed [176–178] and as such only the most recent results will be presented here (see below).

The preparation of polymeric [{M(C≡CR)}$_n$] complexes is now well established. For example, the reaction of [AuCl(SMe$_2$)]
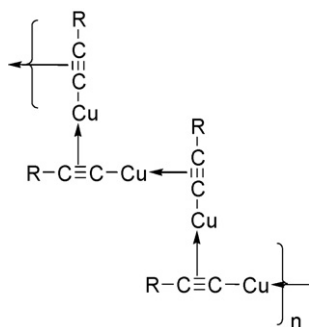
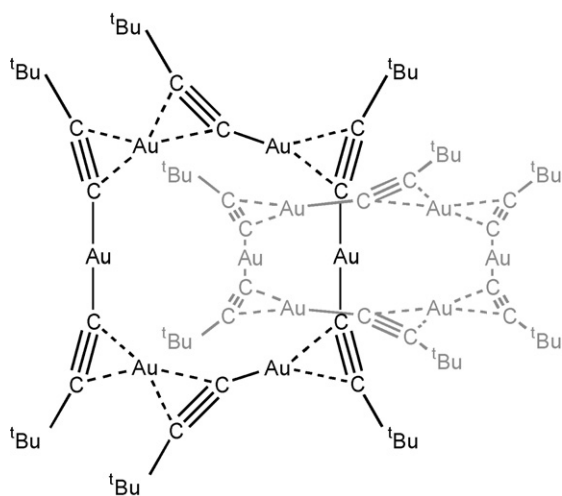Fig. 19. One of the earliest proposals for the polymeric nature of copper(I) alkynides [183].



Fig. 20. A schematic representation of [2]catenane-[{Au(C≡C$^t$Bu)}$_6$]$_2$ [18].
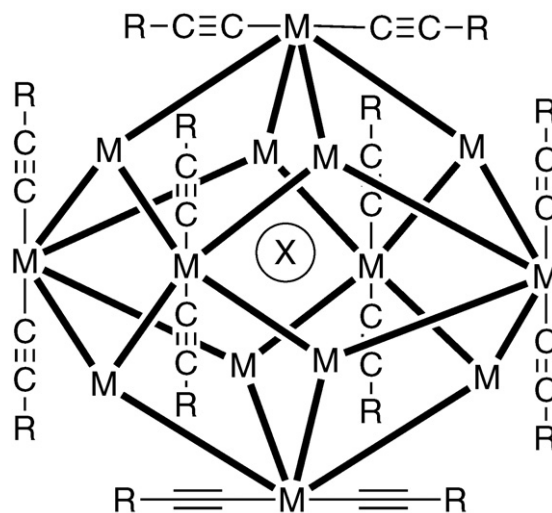


Fig. 22. The cage structure [M$_{14}$(C≡CR)$_{12}$X]$^n$ (X = Cl, Br, n = +1; X = vacancy, n = 0). $\pi$-interactions between the alkynyide fragments and the metal centres are not shown for clarity. Lines of connection between the metal centres are shown to help define the molecular shape [190].

phosphines or amines, and preliminary orbital considerations [183], later confirmed by single crystal [18,184] and powder X-ray diffraction studies [165].

The simplest homoleptic alkynide compounds {M(C≡CR)}$_n$ exist in a range of networked, polymeric and cluster structures, with MC≡CR units linked through $\pi$-bonding and metallophilic interactions [15,185,186]. However, although the polymeric or cluster structures of Cu(I), Ag(I) and Au(I) alkynides has long been recognized [182,183], the precise structures are a complicated, and as yet unresolved, function of metal and alkynide substituents [17,18,165,187]. For example, while treatment of [Au(NH$_3$)$_2$]BF$_4$ with one equivalent of HC≡CPh affords the heteroleptic complex [Au(C≡CPh)NH$_3$], in the case of the reaction between [Au(NH$_3$)$_2$]BF$_4$ and HC≡C$^t$Bu the [2]catenane-[{Au(C≡C$^t$Bu)}$_6$]$_2$ is obtained [18]. Each ring of the [2]catenane features an approximately hexagonal arrangement of six gold atoms (Au···Au 3.215(2)–3.352(2) Å), and three distinct gold-alkynide moieties: [Au($\eta^1$-C≡C$^t$Bu)$_2$]$^-$, [Au($\eta^1$-C≡C$^t$Bu)($\eta^2$-AuC$_2$$^t$Bu)], and [Au($\eta^2$-AuC$_2$$^t$Bu)$_2$]$^+$ (Fig. 20). The observation of three $\nu_{C≡C}$ bands in both solid and solution state suggests that the ring structure is maintained in solution, while the observation of two $^t$Bu resonance signals in the NMR spectrum is consistent with the $C_2$ symmetry of the individual rings.
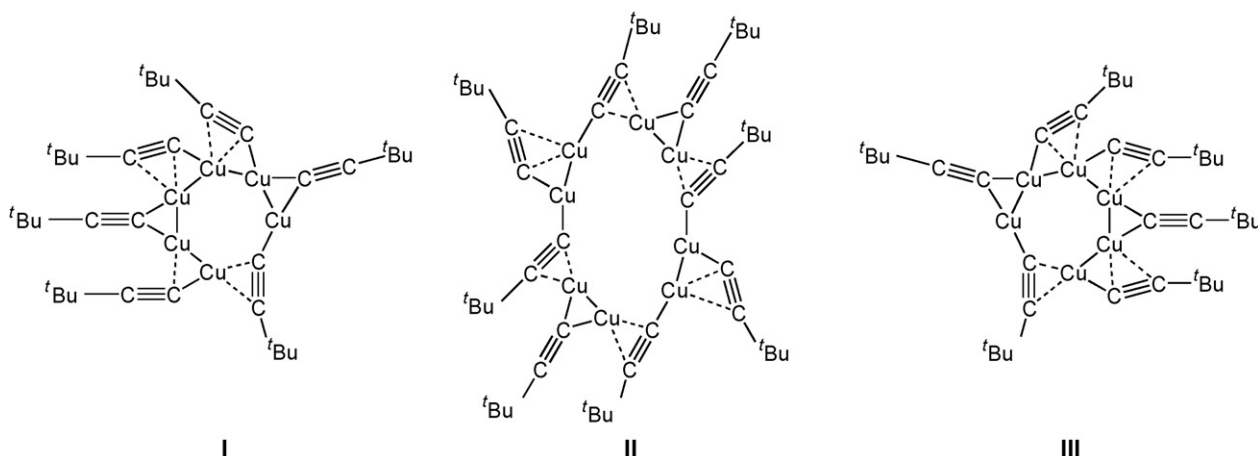
with terminal alkynes in the presence of NEt$_3$ or directly from [PPN][Au(acac)$_2$] and the alkyne have been shown to be an efficient route to polymeric [Au(C≡CR)}$_n$] [179]. The copper and silver alkynide complexes {M(C≡CR)}$_n$ were long thought to be polymeric on grounds of their generally low solubility, in all but a few cases where more soluble derivatives and molecular weight determinations suggested formation of smaller aggregates or clusters (Fig. 19) [180–182]. Early suggestions of defined structures containing $\mu$-$\eta^1$,$\eta^2$-C≡CR were based on the formation of defined molecular species [M(C≡CR)L] from reactions of the polymer and



Fig. 21. A schematic drawing showing the three {Cu(C≡CBu$^t$)}$_n$ rings that interlock to form the double catenane [{Cu(C≡CBu$^t$)}$_{20}$]. Rings I and III each form a catenane around the central ring II [165].

A double catenane [{Cu(C≡C$^t$Bu)}$_{20}$]·C$_6$H$_6$ has also been structurally characterized with a distorted [{Cu(C≡CBu$^t$)}$_8$] ring supporting two [{Cu(C≡C$^t$Bu)}$_6$] cycles (Fig. 21) [165].

However, attempts to form silver containing catenanes gave a structurally ill-defined polymer [Ag(C≡C$^t$Bu)}$_n$], which upon recrystallization in the presence of chloride ions gave the cage compound [Ag$_{14}$(C≡C$^t$Bu)$_{12}$Cl]$^+$, the counter-ion presumed to be OH$^-$ (Fig. 22). The same cage, and its bromide and fluoride analogues, were formed in "one-pot" synthesis from HC≡C$^t$Bu, AgBF$_4$, NEt$_3$ and NBu$_4$X (X = Cl, Br) [17,188]. In the cage the

silver atoms are arranged as a rhombic dodecahedron with Ag···Ag distances in the range of 2.953(2)–2.986(2) Å, consistent with a degree of argentophilic interaction. In an interesting variation, depolymerization of [Ag(C≡CFc)}$_n$] by reaction with [M$_2$(N≡CMe)$_2$(μ-Ph$_2$PNHPPh$_2$)$_2$][BF$_4$]$_2$ (M = Cu, Ag, Au) afforded both the adduct [Fc{C=CH(Ph$_2$NHPPh$_2$)}]BF$_4$ and the rhombic dodecahedral clusters [Ag$_8$M$_6$(C≡CFc)$_{12}$Cl]BF$_4$, in which the Ag$_8$ cube is face capped by the metal centres of essentially linear [M(C≡CFc)$_2$]$^-$ fragments. The source of the encapsulated chloride was not identified [189]. It was presumed that the spherical halide
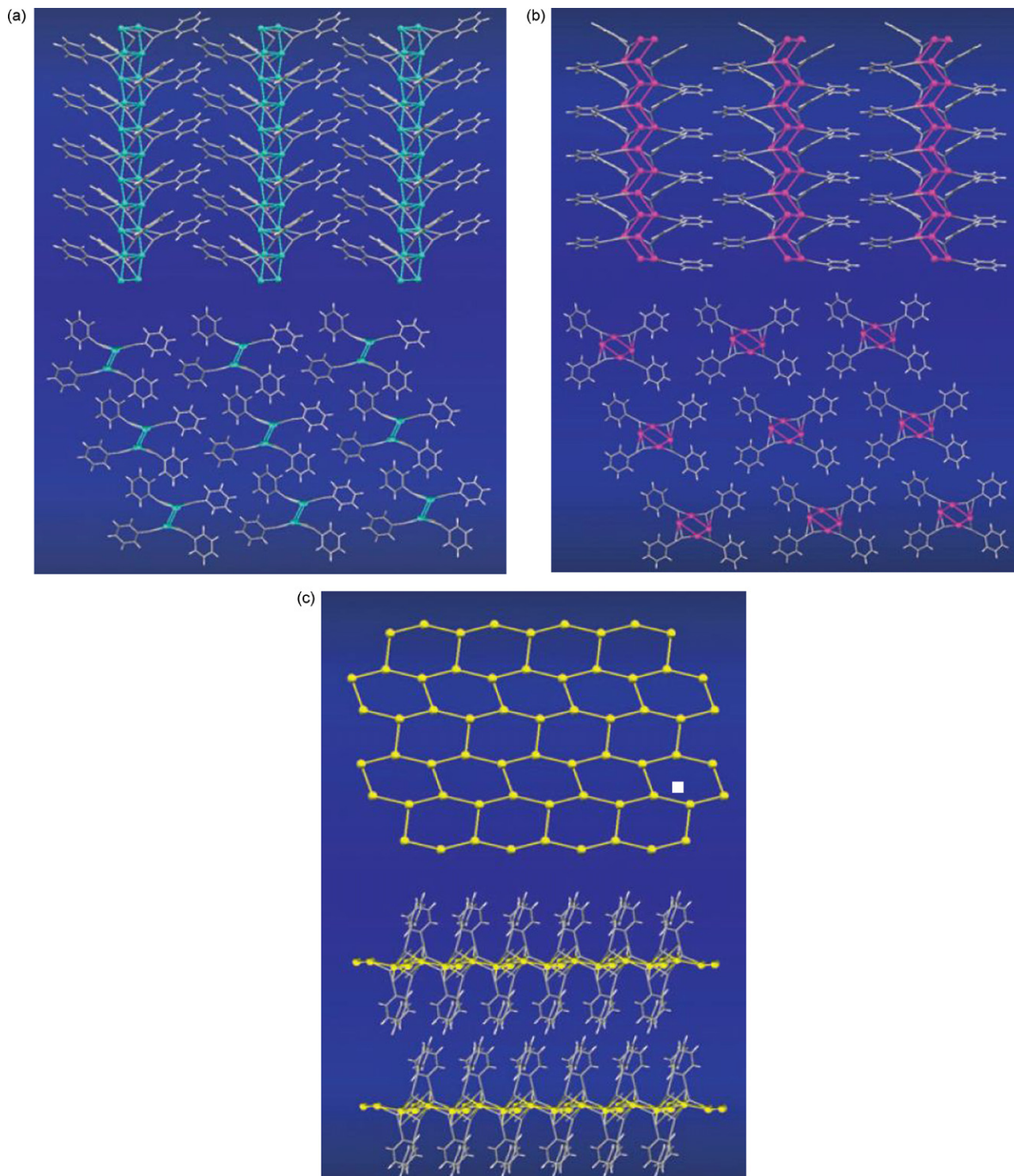


**Fig. 23.** Polymeric structures of group 11 metal(I) phenylacetylides found by Che et al. [165] (a) copper, (b) silver, (c) gold.
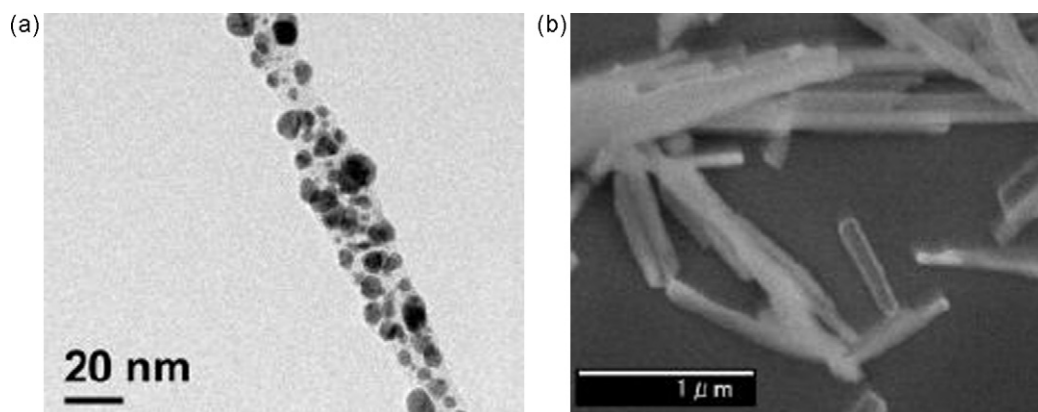
**Fig. 24.** SEM image of [Ag(C≡CPh)] wire bundles (left) and TEM image of an UV-irradiated silver phenylacetylide nanowire (right) [191].

anion acts as a template for the cage formation, although later studies have prepared "template free" examples of the same cage structure [190].

The much larger copper cluster [{Cu(C≡C$^t$Bu)}$_{24}$], obtained from [CuBr(SMe$_2$)] and LiC≡C$^t$Bu, consists of a raft-like array of Cu(C≡C$^t$Bu) moieties around a central distorted octahedral Cu$_6$ core. The alkynide ligands interact with the copper atoms in a variety of coordination modes, from $\mu_2$-$\eta^1$, $\mu_2$-$\eta^2$, $\mu_3$-$\eta^1$, $\mu_3$-$\eta^2$ to $\mu_2$-$\eta^2$:$\mu_2$-$\eta^2$ in which a single copper atom is sandwiched by two alkynide ligands and $\mu_4$-$\eta^2$ with four copper atoms coordinated to a single alkynide C$_\alpha$ carbon atom, one of which further interacts with C$_\beta$ [187]. The $n$-propyl derivative [{Cu(C≡CPr)}$_n$] has been obtained as a polymeric sheet with a zig-zag arrangement of copper atoms linked by $\mu$-$\eta^1$,$\eta^2$ and $\mu_3$-$\eta^1$,$\eta^1$,$\eta^2$ coordination modes of the alkynide ligands. A chain polymer is found for [{Cu(C≡CPh)}$_n$] and [{Ag(C≡CPh)}$_n$], the former with some evidence for cuprophilic interactions (Fig. 23). The gold analogue, [{Au(C≡CPh)}$_n$], consists of a honeycomb-like layer of gold atoms with extensive Au···Au interactions (2.98–3.27(1) Å) and with the gold layers being pillared by the phenylacetylide ligands (Fig. 23) [165].

The polymeric nature of [{M(C≡CR)}$_n$] systems generally causes great difficulty in obtaining single crystals for X-ray diffraction. In a clever twist, slow ligand dissociation from [Ag(C≡CPh)(PMe$_3$)] has been used to grow "wire-like" crystalline samples of [{Ag(C≡CPh)}$_n$] [191]. The dimensions of the wire-like arrays (Fig. 24) could be controlled by choice of solvent, with thinner wires being formed in higher polarity solvents that favour PMe$_3$ dissociation and thicker wires being isolated from solvents of lower polarity. Shorter wires were also obtained from stirred solutions. All told, aspect ratios from 30 to >100 were obtained, with wires as long as 100 μm being observed. UV irradiation of these wire-like assemblies resulted in photoreduction to silver nanoparticle arrays (2.3 ± 0.6 and 5.8 ± 2.1 nm for 15 min and 3 h irradiation, respectively) embedded in poly(phenylacetylene) matrices (Fig. 24). The organic matrix serves to maintain the rod-like characteristics of the nano-objects. Related procedures can be used to form wire-like arrays of copper from [Cu$_2$C$_2$] [192,193], which has led to significant interest in the structures and transformations of compounds derived from silver and copper polyynides [194–196].

The use of bis(alkyne)s as ligand precursors has also been explored, with early work in the area again being initiated by Nast et al. [197]. Both linear anionc species such as [PPN][Au(C≡CC$_6$H$_4$C≡CH)$_2$] and polymeric compounds of general form [{Au$_2$($\mu$-C$_6$H$_4$(C≡C))$_2$}] being formed from the bis(alkyne), [PPN][Au(acac)$_2$] or [AuCl(SMe$_2$)], and NEt$_3$, respectively [198]. Treatment of either species with donor ligands resulted in the formation of well defined, crystalline adducts. In the case of 2,5- and 2,6-diethynyl pyridine, reactions with excess of [AgX] (X = NO$_3$,

CF$_3$CO$_2$) afforded 2D networks of Ag clusters, linked into 3D arrays by bridging anions (Fig. 25) [199].

The linear anionic complexes [M(C≡CR)$_2$]$^-$ and polymers [{M(C≡CR)}$_n$] (M = Cu, Ag) act as ethynyl transfer agents to a wide variety of other metals and similar species are doubtless involved in many Cu(I) catalyzed transmetallation reactions of alkynes [200,201]. The formation and precipitation of the copper polymer [{Cu(C≡CR)}$_n$] and the relative instability of the silver analogue can be used to dictate the direction of alkynide transfer between the metals of group 11. For example, treatment of [PPN][Cu(C≡CPh)$_2$], which is rather more stable than the alkali metal salts first prepared by Nast [202] with gold complexes including [Au(C≡CPh)(PPh$_3$)], [AuCl(PPh$_3$)], [AuCl(C≡CPh)]$^-$ or [{Au(C≡CPh)}$_n$] results in the transfer of the alkynide ligands from Cu to Au, giving [Au(C≡CPh)$_2$]$^-$ [203]. While [Au(C≡CPh)$_2$]$^-$ does not react with [{Cu(C≡CPh)}$_n$], the copper polymer reacts with the tris(alkynide) [Au$_2$(C≡CPh)$_3$]$^-$ to give [Au$_2$Cu(C≡CPh)$_4$]$^-$, thought to proceed by alkynide transfer from copper to gold [204]. Ligand exchange between gold and silver in the reaction of [AuCl(PPh$_3$)] and [{Ag(C≡CPh)}$_n$] gives [{AuAg(C≡CPh)$_2$}$_n$] and [AgCl(PPh$_3$)]$_4$, *via* the formation of [Au(C≡CPh)(PPh$_3$)] and [AgCl].

The mixed polymers [{AuM(C≡CPh)$_2$}$_n$] are also conveniently prepared by ligand exchange reactions of [Au(C≡CPh)(L)] with [{M(C≡CPh)}$_n$] [M = Cu, Ag; L = AsPh$_3$, P(OPh)$_3$] [205]. The silver bis(alkynide) anion [Ag(C≡CPh)$_2$]$^-$ can be conveniently isolated
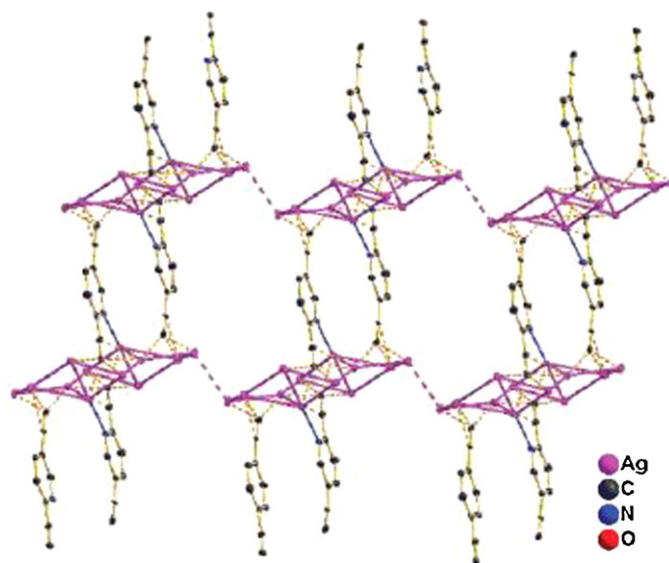


**Fig. 25.** 2D organometallic network formed by [Ag$_2$(2,5-C≡CpyC≡C)·4CF$_3$CO$_2$Ag] units [199].
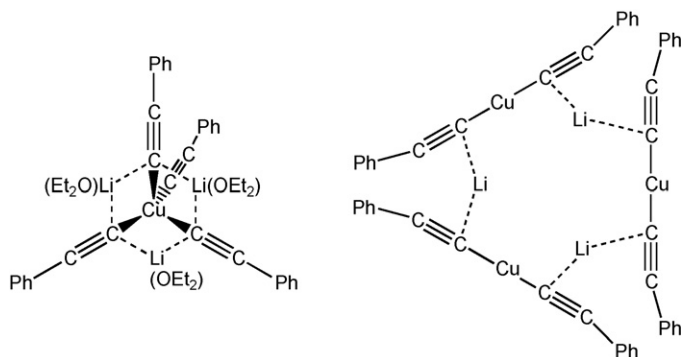
**Fig. 26.** The two sub-units that comprise the structure of [Li$_6$(Et$_2$O)Cu$_4$(C≡CPh)$_{10}$] [207].



**Fig. 28.** Schematic representation of the homoleptic core in the polymeric cluster [Ag$_3$(C≡C$^t$Bu)$_2$$^+$]$_n$ [213].

as the [PPN]$^+$ salt from the 1:2:3 reaction of [PPN]Cl with [{Ag(C≡CPh)}$_n$] and PPh$_3$, with AgCl(PPh$_3$)$_3$ being formed as a by-product. The anion can be used as an alkynide ligand source in reactions with [AuCl(PPh$_3$)], to give [Au(C≡CPh)$_2$]$^-$, or Pt(II) dihalides [206].

The stability of the rod-like [M(C≡CR)$_2$]$^-$ moiety, coupled with the predominance of metallophilic and π-C≡C···M interactions allows the conceptual use of this sub-unit as a supramolecular synthon, illustrated by the structure of the aryl-alkynyl cuprate [Cu$_2$Li$_2$(C≡CR)$_2$Ar$_2$] (Ar = C$_6$H$_4$-2-{CH$_2$N(Me)CH$_2$CH$_2$NMe$_2$}, R = C$_6$H$_4$-4-Me, C$_6$H$_4$-4-SiMe$_3$) [207]. In the case of the reaction of [CuBr(SMe$_2$)] with LiC≡CPh in diethyl ether gives [Li$_6$(Et$_2$O)Cu$_4$(C≡CPh)$_{10}$] which is comprised of two structural subunits: a tetrahedral [Cu(C≡CPh)$_4$]$^{3-}$ moiety with three Li(OEt$_2$) units coordinated by a Cu(C≡CPh)$_2$ "tweezer", and a trimer of linear [Cu(C≡CPh)$_2$]$^-$ moieties linked through Li$^+$ ions coordinated by π-interactions with the alkynide ligands which resides like a crown on the first sub-unit (Fig. 26). Greater excess of LiC≡CPh and reaction at elevated temperatures produced a compound formulated as [Li$_6$(Et$_2$O)$_3$Cu$_3$(C≡CPh)$_9$] [187]. Remarkably, even in the absence of modern spectroscopic and crystallographic methods much earlier studies recognized the significance of structured aggregates arising from the reactions of [{M(C≡CR)}$_n$] and alkynyl anions, even if the proposals for the nature of the products was rather simplistic [208].

The pentanuclear cluster [Ag$_5$(C≡CPh)$_6$]$^-$, which is prepared from depolymerization of [{Ag(C≡CPh)}$_n$] with [PPN][Ag(C≡CPh)$_2$], is thought to feature a trigonal bipyramidal arrangement of silver atoms (Fig. 27), with similar metal geometries found in the anions [Au$_3$M$_2$(C≡CPh)$_6$]$^-$ (M = Cu, Ag) (see below) [209].
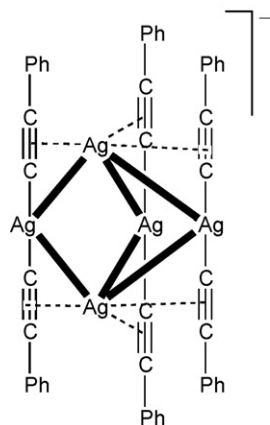


**Fig. 27.** Schematic representation of the pentanuclear cluster anion [Ag$_5$(C≡CPh)$_6$]$^-$ [209].
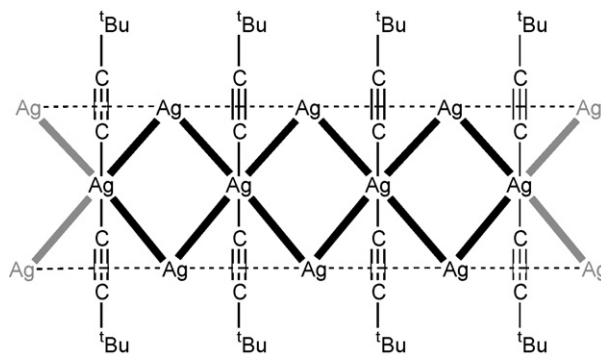
The reaction of three equivalents of [MC≡CH] (M = Na, Rb, Cs) with [CuI] in liquid ammonia afforded M$_2$[Cu(C≡CH)$_3$]·$x$NH$_3$ containing the trigonal planar [Cu(C≡CH)$_3$]$^{2-}$ dianion, with cation metathesis giving the analogous [Ca(NH$_3$)$_6$]$^{2+}$ salt [210]. Schuster and Schmidbaur have explored the chemistry of poly(alkynide) derivatives of Au(III), drawing analogies with cyanide analogues [211]. The compound Au(C≡CPh)$_3$ could only be isolated as the PMe$_3$ adduct from sequential reaction of AuCl$_3$ with LiC≡CPh and PMe$_3$; the use of the larger phosphine PPh$_3$ leads to reductive elimination of PhC≡CC≡CPh and formation of [Au(C≡CPh)(PPh$_3$)]. Sequential reaction of [AuCl(PMe$_3$)] with Br$_2$ and LiC≡CPh also gives [Au(C≡CPh)$_3$(PMe$_3$)], as does the reaction of [Au(C≡CPh)(PMe$_3$)] with Tl(C≡CPh)$_2$Cl. However, addition of LiC≡CPh to [Au(C≡CPh)$_3$(PMe$_3$)] gives the tetra(ynyl) square planar complex [Au(C≡CPh)$_4$]$^-$ which could not be isolated as a pure sample, but converts readily to [Au(C≡CPh)$_2$]$^-$ following reductive elimination of PhC≡CC≡CPh.

Cationic homoleptic alkynide coinage metal clusters are also known, and mass spectrometry has been shown to be a useful tool through which to follow the formation and further reactions of small to medium nuclearity cationic alkynide clusters, which allows a degree of structure–reactivity relationship to be established [212]. The trinuclear cluster polymer {[Ag$_3$(C≡C$^t$Bu)$_2$][BF$_4$]·0.6H$_2$O}$_n$ is formed from a 1:2 reaction of [AgBF$_4$] with [{Ag(C≡C$^t$Bu)}$_n$]. In this system [{Ag(C≡C$^t$Bu)$_2$}]$^-$ moieties are bonded to Ag$^+$ ions via Ag–Ag bonding contacts (Ag···Ag ca. 3 Å) and π-interactions with the alkynide ligands (Fig. 28) [213].

Similar structures are also formed from [AgNO$_3$] or [AgOTs], HC≡C$^t$Bu and NEt$_3$ [188]. If the reaction stoichiometry is adjusted to 1:6 ([AgBF$_4$]:[{Ag(C≡C$^t$Bu)}$_n$]) then dicationic [Ag$_{14}$(C≡C$^t$Bu)$_{12}$]$^{2+}$ is obtained without a templating anion [17,188]; other routes to this "template free" species also being possible [190]. The usual [Ag(C≡C$^t$Bu)$_2$]$^-$ building block ions cap the faces of a cube of Ag$^+$ ions supported by Ag–Ag (mean Ag–Ag bond length 2.9727(7) Å) and μ$_3$, η$^1$-C≡C$^t$Bu interactions. In an interesting variation of the templating theme (Fig. 29), the clusters [Ag$_{17}$(C≡C$^t$Bu)$_{14}$(CO$_3$)]OTf and [Ag$_{19}$(C≡C$^t$Bu)$_{16}$(CO$_3$)]BF$_4$ were obtained from [Ag(C≡C$^t$Bu)]$_n$ and [AgOTf] or [AgBF$_4$], respectively, in "wet" solvents, the presence of atmospheric CO$_2$ and TMEDA. Higher yields (ca. 80% vs. ca. 18%) were obtained following the addition of K$_2$CO$_3$ to the reaction mixtures [214].

The predominance of π-C···M and M···M metallophilic interactions in the alkynide complexes of group 11 metals leads to remarkable possibilities for the "self-assembly" of larger clusters, including mixed-metal systems. Metal-atom substitution and transmetallation reactions can also be used in the synthesis of multi-metallic coinage metal clusters, with final product composition driven by thermodynamic factors. For example, com-
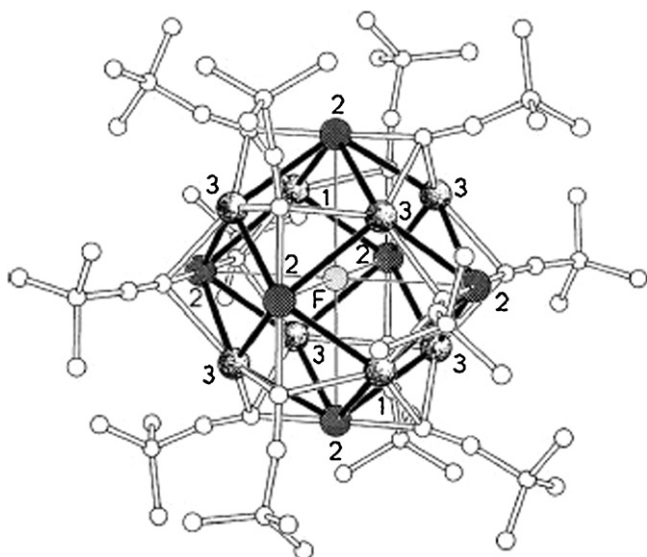
Fig. 29. The rhombohedral cage complex $[Ag_{14}(C\equiv C^tBu)_{12}F]BF_4$ showing the interpenetrating octahedral and cubic arrangements of Ag atoms with the fluoride in the centre [188].

bination of [AuCl(tht)] (tht = tetrahydro-thiophene, $SC_4H_8$) with $[Cu(N\equiv CMe)_4]PF_6$ in the presence of $HC\equiv CPh$ and $NEt_3$ gives the bright orange, light sensitive cluster $[Au_6Cu_6(C\equiv CPh)_{12}]$ [166]. The cluster can be considered as a trigonal planar array of six $[Au(C\equiv CPh)_2]^-$ rods with three Cu atoms lying above and below each face forming three fused $Au_3Cu_2$ trigonal bipyramids, all supported by Cu–Au, Au–Au and $\pi$-$C\equiv C$–Cu interactions (Fig. 30).

Hexanuclear complexes $[Pt_2Ag_4(C\equiv CR)_8]$ (R = Ph, $^tBu$) were obtained from $[PtCl_2(tht)]$ and four equivalents of $[\{Ag(C\equiv CR)\}_n]$ [125]. The cluster core consists of an octahedral $Pt_2Ag_4$ core, with the apical Pt centres bearing four alkynide ligands. The silver atoms in the cluster core could be substituted by gold (upon reaction with [AuCl(tht)]) or copper (from [CuCl]). The same structures can also be assembled from $[NBu_4]_2[Pt(C\equiv CR)_4]$ and $[AgClO_4]$ (CARE!), [CuCl] or [AuCl(tht)] (Fig. 31) (see also Section 6.2.2) [125].
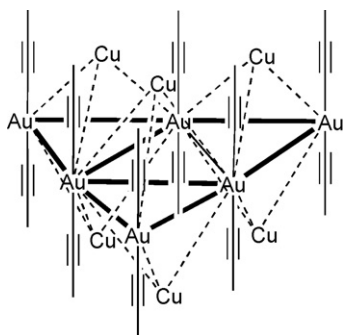


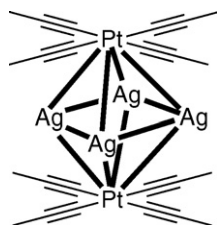Fig. 30. A schematic representation of the core structure of $[Au_6Cu_6(C\equiv CPh)_{12}]$ [166].



Fig. 31. A schematic representation of the molecular structure of $[Pt_2Ag_4(C\equiv CR)_8]$ [125].



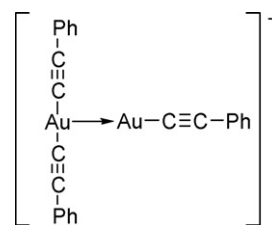Fig. 32. The structure of $[Au_2(C\equiv CPh)_3]^-$ proposed by Abu-Salah [215].

Depolymerization of $[\{Au(C\equiv CPh)\}_n]$ with two equivalents of $[Au(C\equiv CPh)_2]^-$ gives a bimetallic anion $[Au_2(C\equiv CPh)_3]^-$, thought to feature an Au → Au dative interaction (Fig. 32) [215]. The same complex anion could be obtained from a 1:1 reaction of $[\{Au(C\equiv CPh)\}_n]$ and $[Au(C\equiv CPh)_2]^-$ in the presence of pyridine. The pyridine is thought to depolymerize $[\{Au(C\equiv CPh)\}_n]$, giving $[Au(C\equiv CPh)(py)]$, with subsequent displacement of the labile pyridine ligand by the bis(alkynide) anion yielding $[Au_2(C\equiv CPh)_3]^-$, the structure of which was assigned based on the observation of a $\nu_{C\equiv C}$ band at $2110\,cm^{-1}$, elemental analytical data and molecular weight measurements [204,215].

Further reactions of $[Au_2(C\equiv CPh)_3]^-$ with $[\{Cu(C\equiv CPh)\}_n]$ gave the copper bridged species $[\{Au(C\equiv CPh)_2\}_2(\mu\text{-}Cu)]^-$, which upon treatment with both $[\{Au(C\equiv CPh)\}_n]$ and $[\{Cu(C\equiv CPh)_n]$ gave pentanuclear $[Au_3Cu_2(C\equiv CPh)_6]^-$, structurally similar to that shown in Fig. 33. The analogous gold–silver heterometallic cluster $[Au_3Ag_2(C\equiv CPh)_6]^-$ is obtained in similar fashion [204].

The anionic clusters $[Au_3M_2(C\equiv CR)_6]^-$ (M = Cu [216], Ag [204,209,217]) [167,204,218] also feature $[Au(C\equiv CR)_2]^-$ rods linked by $\pi$-, Au–Au, and M–Au interactions (Fig. 33). As with the homometallic analogues $[M_5(C\equiv CR)_6]^-$ the metallic core may be thought of as a trigonal bipyramid, with apical heterometal atoms [167]. DFT calculations indicate the HOMO to be largely metal d and ethynyl $\pi$ in character, with the LUMO being an in-phase combination of the metal sp orbitals. The composition of the clusters can be tuned with a degree of precision through control of the stoichiometry of reaction of the $[M(C\equiv CR)_2]^-$ rigid-rod building block with $[\{M'(C\equiv CR)\}_n]$, giving rise to species such as $[Ag_4Cu(C\equiv CPh)_6]^-$ [209,219,220].

Trimetallic systems can also be prepared using similar building block approaches, with reaction of $[PPN][Au(C\equiv CPh)_2]^-$, $[\{Ag(C\equiv CPh)\}_n]$ and $[\{Cu(C\equiv CPh)_n]$ affording $[PPN][AuAg_6Cu_6(C\equiv CPh)_{14}]$ [220]. This heterotrimetallic species is thought to offer a similar structure to that determined crystallographically for $[PPN][Ag_6Cu_7(C\equiv CPh)_{14}]$ [220] with a linear $[Au(C\equiv CPh)_2]^-$ moiety linked by metal–metal interactions to three tetra-nuclear $[Ag_2Cu_2(C\equiv CPh)_4]$ subunits (Fig. 34). In the subunits, the copper atoms are $\sigma$-bonded to two $C\equiv CPh$ ligands, with the silver atoms held by $\pi$-interactions with two alkynide fragments and metal–metal interactions [220].
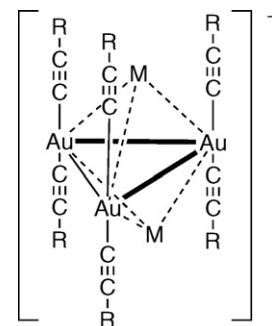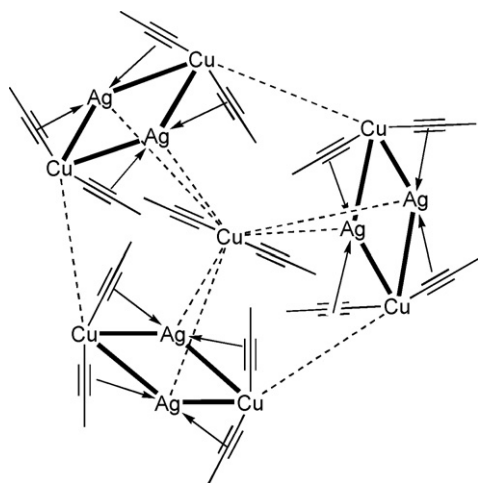


Fig. 33. A schematic representation of the core structure in the cluster anions $[Au_3M_2(C\equiv CR)_6]^-$ (M = Cu, Ag).

**Fig. 34.** A schematic representation showing the three almost square $Ag_2Cu_2(C\equiv CR)_4$ subunits linked to a $Cu(C\equiv CR)_2$ core in $[Ag_6Cu_7(C\equiv CPh)_{14}]^-$ [220].

The pentametallic cluster $[Au_3AgCu(C\equiv CPh)_6]^-$ is obtained from the reactions of $[Au_3Cu_2(C\equiv CPh)_6]^-$ with $[\{Au(C\equiv CPh)\}_n]$ and $[\{Ag(C\equiv CPh)\}_n]$ in the presence of pyridine, from $[Au_3Ag_2(C\equiv CPh)_6]^-$ with $[\{AuCu(C\equiv CPh)_2\}_n]$, or from $[Au_2Cu(C\equiv CPh)_4]^-$ and $[\{AuAg(C\equiv CPh)_2\}_n]$, respectively [221]. A mixture of salts containing the anions $[AuAg_6Cu_6(C\equiv CPh)_{14}]^-$, $[Au_3Ag_2(C\equiv CPh)_6]^-$ and $[Au(C\equiv CPh)_2]^-$ was obtained from $[Au_3Cu_2(C\equiv CPh)_6]^-$, $[\{Ag(C\equiv CPh)\}_n]$ and $[\{Cu(C\equiv CPh)_n\}]$. Closely related product mixtures containing $[AuAg_6Cu_6(C\equiv CPh)_{14}]^-$ and $[Au_3AgCu(C\equiv CPh)_6]^-$ were obtained from $[Au_3Ag_2(C\equiv CPh)_6]^-$, $[\{Ag(C\equiv CPh)\}_n]$ and $[\{Cu(C\equiv CPh)_n\}]$, while $[Ag_6Cu_7(C\equiv CPh)_{14}]^-$ was formed together with $[\{Ag(C\equiv CPh)\}_n]$ from cluster expansion of $[Ag_4Cu(C\equiv CPh)_6]^-$ with $[\{AgCu(C\equiv CPh)_2\}_n]$ [221]. Cluster expansion is also achieved by redistribution reactions arising from addition of $[CuCl]$ to $[Au_2Cu(C\equiv CPh)_4]^-$. The trinuclear complex $[Au_2CuCl(C\equiv CPh)_4]^{2-}$ and $[CuCl]$ or $[\{AuCu(C\equiv CPh)_2\}_n]$ gave $[Au_3Cu_2(C\equiv CPh)_6]^-$, while $[Au_2CuCl(C\equiv CPh)_4]^{2-}$ with a mixture of $[\{Ag(C\equiv CPh)\}_n]$ and $[\{Cu(C\equiv CPh)_n\}]$ gave $[AuAg_6Cu_6(C\equiv CPh)_{14}]^-$ [221]. Higher nuclearity clusters including $[Ag_6Cu_7(C\equiv Ph)_{14}]^-$ can also be obtained from ligand exchange and condensation processes in mixtures of $[\{Ag(C\equiv CPh)\}_n$, $[\{Cu(C\equiv CPh)\}_n$ and $[Ag(C\equiv CPh)_2]^-$. The metal core geometry can be visualized as three almost square $Ag_2Cu_2$ clusters encapsulating the seventh copper atom [222,223].

An interesting variation on a trigonal $Cu_3(C\equiv CH)_3$ motif has been prepared from decarboxylation of the organometallic carboxylic acid $Co_2(\mu\text{-}HC_2CO_2H)(CO)_6$ upon reaction with $Cu(OMe)_2$ (Fig. 35). The reduction of Cu(II) to Cu(I) is thought to be promoted by oxidation of the cobalt cluster prior to decarboxylation [224].

In condensation of $[Ag_2C_2]$ with silver salts, a common feature is the encapsulation of the $[C_2]^{2-}$ moiety within $Ag_n$ ($n \geq 6$) cages [177]. These $Ag_nC_2$ clusters serve as supramolecular synthons that can be used to construct larger polymeric layered structures of three-dimensional systems through vertex sharing or anion bridging [178]. Recently, Mak has extended these concepts and identified a range of new supramolecular synthons formed from double silver(I) salts of phenylethynide [225,226] and various isomers of phenylene diethynide [227]. In the case of compounds formed from reactions of $[AgNO_3]$ and polymeric species $[Ag_2(C\equiv CRC\equiv C)]_n$ ($R = 1,3\text{-}C_6H_4$, $2,3\text{-}C_4H_2S$) or $[Ag(C\equiv CR)]_n$ ($R = 3$-pyridyl, 2-pyrazinyl) the nitrate anion serves to both stabilize the silver-ethynide aggregate, and also permit additional $\pi$–$\pi$ interactions by virtue of its limited steric bulk [228]. These $\pi$-stacking motifs dominate the long-range order in the solid state, with structures from ribbons to three-dimensional cross-linked structures. When larger ligands with more flexible structures are employed, such
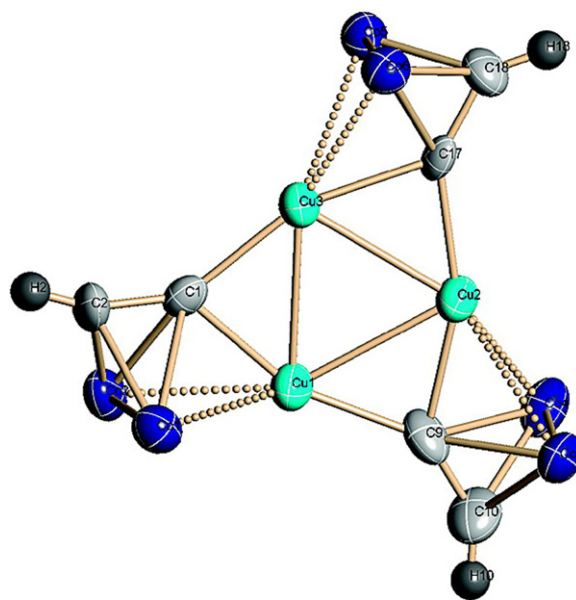


**Fig. 35.** The solid state structure of cluster $Cu_3\{\mu\text{-}C_2HCo_2(CO)_6\}_3$ formed from reaction of $Co_2(\mu\text{-}HC_2CO_2H)(CO)_6$ with $Cu(OMe)_2$ (carbonyl ligands are omitted for clarity) [224].

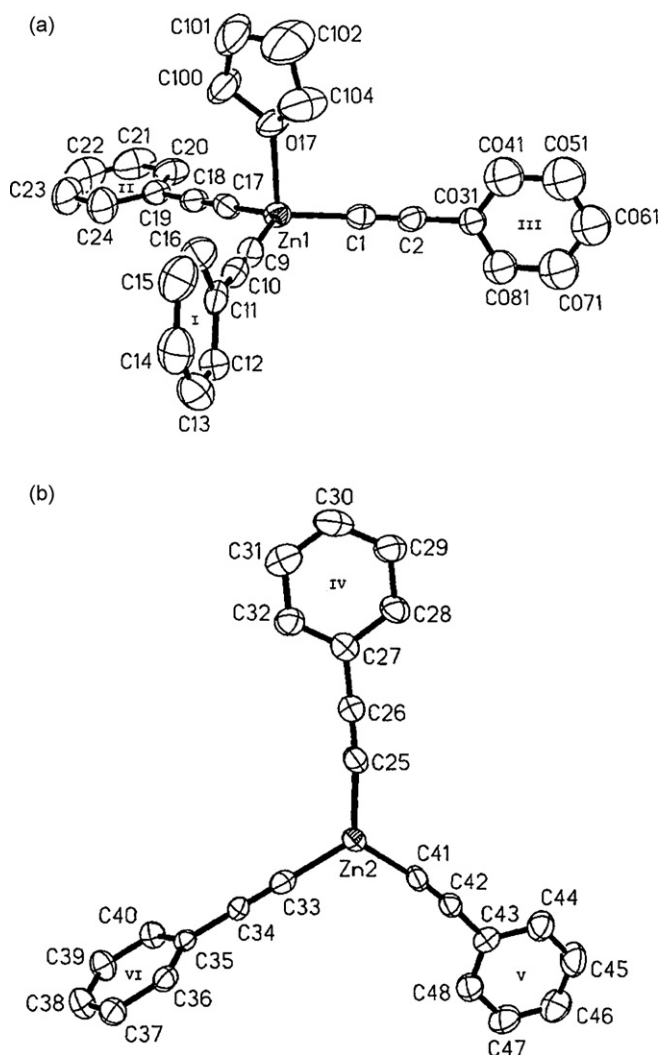as bis-prop-2-ynyloxy-naphthalenes, the situation become more complex with the $\mu_4$- and $\mu_5$-coordination modes of the $Ag_n\subset C\equiv CR$ and $Ag_n\subset C\equiv CRC\equiv C\supset Ag_n$ fragments augmented by weaker Ag-$\pi$, CH$\cdots\pi$ and Ag$\cdots$Ag interactions [229]. Similar supramolecular design concepts can be employed with mono- and diethynide ligands bearing additional donor functionalities [230–233].

## 8. Homoleptic alkynide complexes of group 12

This Chapter describes the synthesis, structure, bonding, and reactivity of group 12 homoleptic transition metal alkynides. The group 12 complexes can be used, for example, in carbon–carbon bond forming reactions by treatment with electrophiles [234]. However, the limited availability and difficulties associated with handling alkynyl group 12 metal reagents has restricted their applications in organic synthesis. The group 12 transition metals display weak Lewis acidity, such that in reactions with nucleophilic complexes these species can serve as electrophilic alkynyl equivalents [235]. Particularly, the cadmium and mercury species are very toxic and hence, their use as organyl transfer reagents is confined. In general, homoleptic group 12 metal alkynides are of structural type $[M(C\equiv CR)_2]$ (M = Zn, Cd, Hg; R = H, single bonded organic group) with a linear acetylide–metal–acetylide arrangement. A further favored structure is $[M(C\equiv CR)_4]^{2-}$ in which the metal ion M possesses a tetrahedral coordination geometry. The pioneer in this field of chemistry is Nast, who firstly synthesized group 12 metal alkynides of zinc and cadmium in the late 1950 s, while di(alkynyl) mercurates were already described much earlier [3,236].

### 8.1. Zinc

The first zinc alkynide, $K_2[Zn(C\equiv CH)_4]$, was prepared by Nast and Müller in 1958 by reacting divalent $[Zn(SCN)_2]\cdot 2NH_3$ or $K_2[Zn(C\equiv N)_4]$ with $KC\equiv CH$ in liquid ammonia [237]. The thus formed diammoniate $K_2[Zn(C\equiv CH)_4]\cdot 2NH_3$ releases $NH_3$ by heating to 60–70 °C in high-vacuum. Zincate $K_2[Zn(C\equiv CH)_4]$ is diamagnetic, *non*-explosive, *non*-pyrophoric, but easily eliminates acetylene when treated with protic solvents. In 1968 the structure of $K_2[M(C\equiv CH)_4]$ (M = Zn, Cd) in the solid state was determined from X-ray powder data [238]. Both complexes are iso-type and

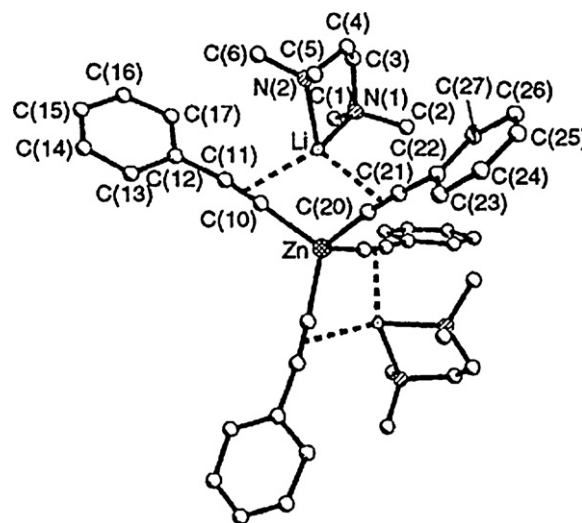**Fig. 37.** Molecular structure of [Li(tmeda)]$_2$[Zn(C≡CPh)$_4$] in the solid state [244].



**Fig. 36.** Crystal structures of the two anions [Zn(C≡CPh)$_3$(thf)]$^-$ (left) and [Zn(C≡CPh)$_3$]$^-$ (right) forming [Na(12-crown-4)$_2$]$_2$[Zn(C≡CPh)$_3$(thf)][Zn(C≡CPh)$_3$] in the solid state [243].

contain isolated [M(C≡CH)$_4$]$^{2-}$ tetrahedra, which are surrounded by six potassium ions arranged in a distorted octahedron. Following Nastĭs preparation of K$_2$[Zn(C≡CH)$_4$] (vide supra), Ruschewitz and coworkers reported the synthesis of diverse alkali and alkaline earth metal tetra-ethynylo zincates and cadmates of type M′$_2$[M(C≡CH)$_4$] (M = Zn, Cd; M′ = Na, K, Rb, Cs) and M′[M(C≡CH)$_4$] (M′ = Mg, Ca, Sr, Ba), respectively [84,239]. Raman spectroscopic studies indicated that these molecules are setup by tetrahedral fragments [M(C≡CH)$_4$]$^{2-}$ with carbon–carbon triple bonds.

Polymeric [Zn(C≡CPh)$_2$] was prepared either by the reaction of dimethyl [240] or diethyl [241,242] zinc with phenylacetylene or electrochemically from elemental zinc and phenylacetylene in acetonitrile in presence of tetra-ethyl ammonium bromide as electrolyte [106]. Its characterization was based on elemental analysis, IR and NMR spectroscopy [241].

Zincate [Na(12-crown-4)$_2$][Zn(C≡CPh)$_3$] was recently synthesized by Dehnicke and coworkers from the homoleptic amido complex [Na(12-crown-4)$_2$][Zn{N(SiMe$_3$)$_2$}$_3$] and HC≡CPh [243]. Crystallization of this compound from tetrahydrofuran solutions gave solvent containing single crystals of composition [Na(12-crown-4)$_2$]$_2$[Zn(C≡CPh)$_3$(thf)][Zn(C≡CPh)$_3$] (Fig. 36).

The metal atom of the [Zn(C≡CPh)$_3$]$^-$ group is in a trigonal-planar arrangement, while the [Zn(C≡CPh)$_3$(thf)]$^-$ moiety forms a flat trigonal pyramid with the oxygen atom in apical position (bond angle (O–Zn–C) = 96.6°) [243]. Both building blocks differ in their Zn–C bond distances which are ca. 2.003 Å (thf adduct) or 1.967 Å, respectively.

The tetrahedral coordinated homoleptic tetra-phenylethynyl zincate [Li(tmeda)]$_2$[Zn(C≡CPh)$_4$] is accessible by nucleophilic substitution of the bis(trimethylsilyl)amido ligands in [Zn(N(SiMe$_3$)$_2$)$_2$] by LiC≡CPh [244]. The structure of [Li(tmeda)]$_2$[Zn(C≡CPh)$_4$] in the solid state comprises a pseudo-tetrahedral [Zn(C≡CPh)$_4$]$^{2-}$ organometallic anion with two [Li(tmeda)]$^+$ cations bonded via alkynyl-lithium π-interactions (Fig. 37) [244].

Homoleptic zinc alkynyls [Zn(C≡CR)$_2$] (R = Ph, CMe$_2$OH, SiMe$_3$, C$_5$H$_{11}$, CH$_2$NMe$_2$) can be used as cross-coupling reagents in presence of catalytic amounts of [Pd(PPh$_3$)$_4$/CuI] for the formation of new sp–sp$^2$ carbon–carbon bonds including the synthesis of diverse enynes and enediynes, respectively [245]. The appropriate bis(alkynyl) zinc derivatives were prepared by the reaction of ZnCl$_2$ with two equivalents of LiC≡CR. Mixed [Zn(C≡CSiMe$_3$)$_2$]/[Zn(CH$_2$SiMe$_3$)$_2$] zinc reagents can successfully be applied for enantioselective synthesis of propargyl amines through Zr-catalyzed addition to aryl amines [246]. The corresponding chiral propargyl amines are thereby obtained in up to 90% ee. The addition of the zinc alkyl species improves significantly the conversion rate (without addition of [Zn(CH$_2$SiMe$_3$)$_2$]: 5–10% conversion; with addition of [Zn(CH$_2$SiMe$_3$)$_2$]: >98%) [246].

## 8.2. Cadmium

The synthesis of homoleptic cadmium acetylides was firstly reported by Nast and Richers [247]. In a typical experiment they reacted [Cd(SCN)$_2$] with four equivalents of KC≡CR (R = H, Ph) in presence of [Ba(SCN)$_2$] in liquid ammonia to obtain poorly soluble Ba[Cd(C≡CH)$_4$] [247]. A synthetic methodology appropriate for the formation of [Cd(C≡CPh)$_2$] is based upon the reaction of cadmium diphenyl with phenyl acetylene at low temperature in diethyl ether solutions. The colorless crystals are only soluble in liquid ammonia by formation of [Cd(C≡CPh)$_2$]·xNH$_3$. The removal of the ammonia being achieved, as for the zinc compounds described above, at elevated temperatures [247]. The appropriate bis(acetylide) cadmium complex [Cd(C≡CH)$_2$]·xNH$_3$ was prepared by the same authors from [Cd(NH$_2$)$_2$] and gaseous acetylene in liquid ammonia. In contrast to [Cd(C≡CPh)$_2$], this compound decomposes readily at 0 °C to give cadmium carbide
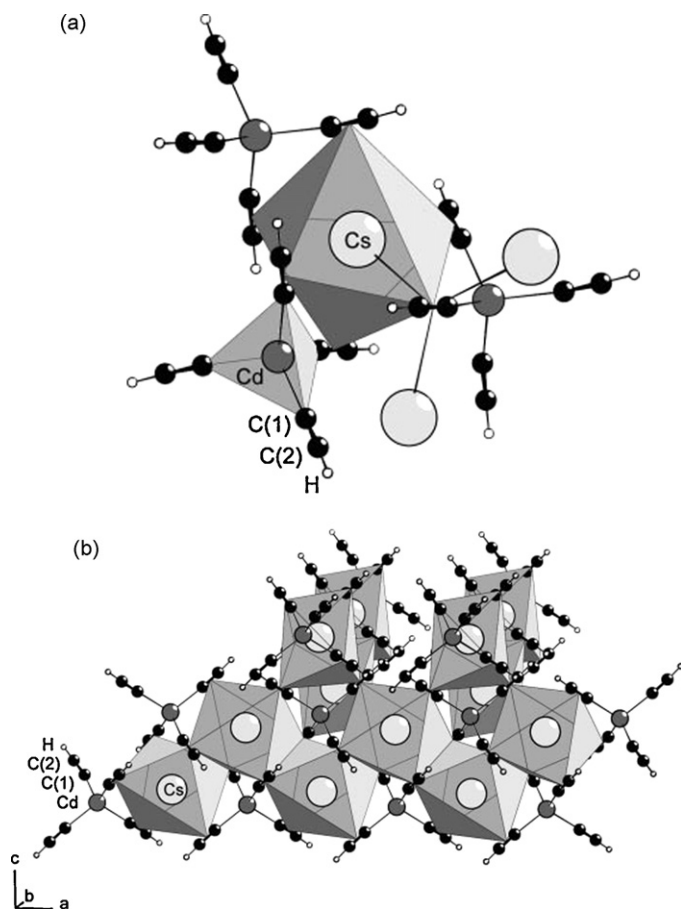
**Fig. 38.** The structure of $Cs_2[Cd(C\equiv CH)_4]$ in the solid state [248].

$[CdC_2]\cdot 0.5NH_3$, which upon protolysis produces acetylene [247]. As discussed earlier for homoleptic alkynyl zincates, a series of cadmates of structural type $M'_2[Cd(C\equiv CH)_4]$ ($M'$ = Na, K, Rb, Cs) and $M'[Cd(C\equiv CH)_4]$ ($M'$ = Mg, Ca, Sr, Ba) were synthesized and structurally characterized [239,248]. While $Na_2[Cd(C\equiv CH)_4]$ is, as the appropriate zinc species, amorphous to X-rays, all other systems are iso-typic to the respective potassium complexes [248]. As outlined above these molecules crystallize in the tetragonal space group $I4_1/a$ containing $[Cd(C\equiv CH)_4]^{2-}$ tetrahedra (Fig. 38). The alkali cations are octahedrally surrounded by six side-on coordinated ethynyl ligands of the $[Cd(C\equiv CH)_4]^{2-}$ units, whereby each of the four acetylide groups is trigonally coordinated by three Cs atoms resulting in a polymeric framework (Fig. 38). These molecules show structural relationships to Scheelit and Anatas [248].

Reaction of $CdMe_2$ with phenylacetylene or 1-octyne in the ratio of 1:2 resulted in the formation of linear $[Cd(C\equiv CR)_2]$ (R = Ph, $C_6H_{13}$) [240]. These compounds were characterized by elemental analysis, IR and NMR spectroscopy as well as titration against EDTA.

The ferrocene ethynyl-functionalized homoleptic cadmium complex $[Cd(C\equiv CFc)_2]$ was synthesized by treatment of $CdBr_2$ with two equivalents of $LiC\equiv CFc$ (Fc = $(\eta^5-C_5H_4)(\eta^5-C_5H_5)Fe$) [249]. This compound decomposes even at low temperature via

carbon–carbon bond formation to give the all-carbon butadiyne $FcC\equiv CC\equiv CFc$ (Scheme 15).
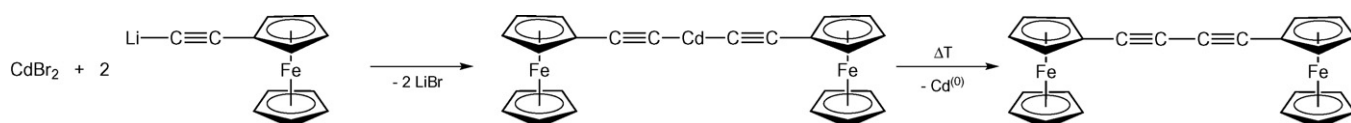
### 8.3. Mercury

The first homoleptic mercury(II) compound was $[Hg(C\equiv CMe)_2]$ which was prepared in different ways by Kutscheroff as early as 1884 [3], following an effort to synthesize $C_3H_4HgO$ via direct reaction of HgO with propyne in water. After several days crystals with a strong smell of garlic were extracted. Elemental analysis of the obtained compound lead to the composition $[Hg(C\equiv CMe)_2]$. Other attempts using alkaline solutions of $HgI_2/KI$ or $[HgCl_2]$/acetone and propyne resulted in the formation of the same compound. In 1899 Nef described the synthesis of $[Hg(C\equiv CPh)_2]$ from an alkaline solution of KI and $HgCl_2$ by adding $HC\equiv CPh$ [236], while based on these studies in 1926 Johnson and McEwen [250] obtained a series of bis(alkynyl) mercury(II) compounds $[Hg(C\equiv CR)_2]$ (R = Cl, Br, Me, Et, $^tBu$, $^nC_5H_{11}$, $^nC_8H_{17}$, Ph, $CH_2Ph$, $CH_2CH_2Ph$, $C_6H_4$—4-Me, $C_6H_4$—4-OMe, $CH_2{}^cC_6H_{11}$, $CH_2OPh$, $C_4H_3O$, $C_4H_2OBr$) by treatment of $K_2[HgI_4]$ with $RC\equiv CH$ in presence of KOH. Caution is advised, since these compounds do not melt below the temperature of decomposition or even explosion. In 1964, Nast described the synthesis of the explosive colorless mercury alkynide $Ba[Hg(C\equiv CH)_4]$ and the more stable derivative $Ba[Hg(C\equiv CPh)_4]$ [251]. These molecules have been synthesized by reacting the mercury salt $[Hg(SCN)_2]$ with $KC\equiv CR$ (R = H, Ph) and $Ba(SCN)_2$ in liquid ammonia. Their characterization is based mainly on IR spectroscopy and elemental analysis. Upon protolysis, $Ba[Hg(C\equiv CH)_4]$ completely decomposed to give acetylene along with mercury(II), while the corresponding $Ba[Hg(C\equiv CPh)_4]$ derivative gave hydrophobic insoluble $[Hg(C\equiv CPh)_2]$ and phenyl acetylene [251].

Hill and coworkers used diverse mercury(II) alkynyls $[Hg(C\equiv CR)_2]$ (R = Ph, $C_6H_4$—4-Me, Fc) for the convenient synthesis of alkynyl aryl chalcogenoethers by reacting the bis(alkynyl) mercurials with diaryl dichalogenides (R'EER'; E = Se, Te; R' = Ph, $C_6H_4$—4-Cl) [252]. Mechanistic investigations of this reaction were also undertaken and are summarized in Scheme 16. In 2006, the same author discussed the hazardous properties of homoleptic $[Hg(C\equiv C^iC_3H_7)_2]$, which spontaneously detonates producing finely divided mercury [253].

In recent studies a large number of homoleptic mercury alkynides $[Hg(C\equiv CR)_2]$ with different organic groups R have been identified, and are summarized in Table 7. The use of bifunctional building blocks leads to the formation of organomercury polyynes (Table 8). To discuss all these compounds in detail would go beyond the scope of this article. Rather the interested reader is referred to the original literature given in Tables 7 and 8 and to the review written by W.-Y. Wong in 2007 joining the above discussed homoleptic mercury alkynyls and their heteroleptic counterparts as versatile templates for new organometallic materials and polymers [14].

A series of heterometallic mercury bis(diyndiyl) compounds of type $Hg\{C\equiv C-C\equiv C[ML_n]\}_2$ bearing different σ-bonded transition metal complex fragments, such as $CpW(CO)_3$ [269], $Cp^*Ru(dppe)$ [270], $AuPR_3$ [271], and $C[Co_3(\mu-dppm)(CO)_7]$ (dppm = $Ph_2PCH_2PPh_2$) [272] was synthesized by Bruce et al. The



**Scheme 15.** Synthesis and decomposition of $[Cd(C\equiv CFc)_2]$ [249].
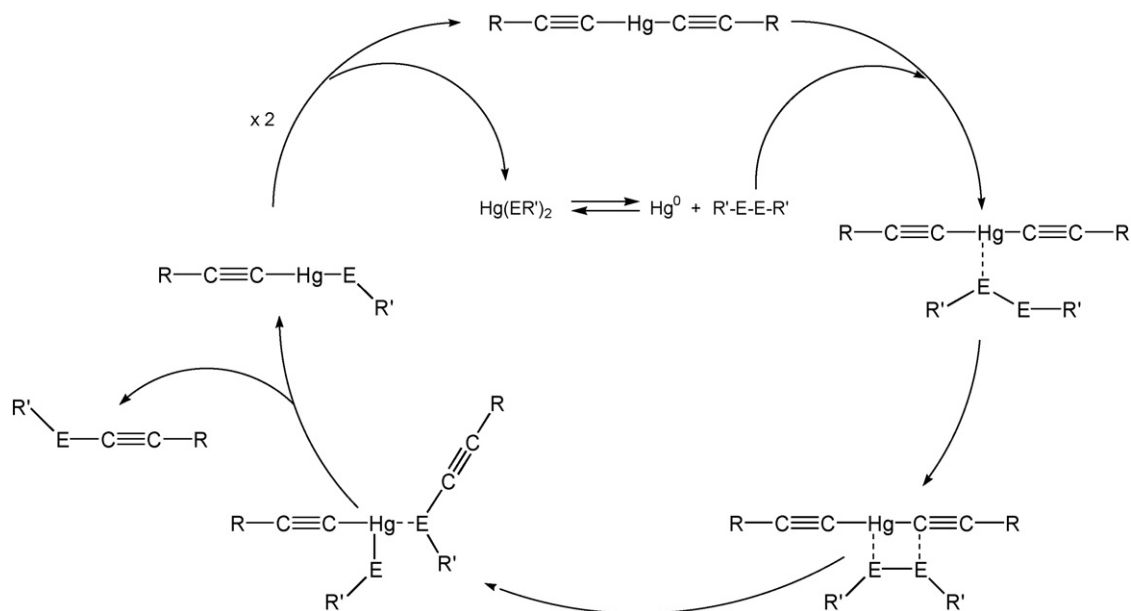
**Scheme 16.** Mechanism of alkynyl aryl chalcogenoether synthesis starting from homoleptic [Hg(C≡CR)$_2$] [252].
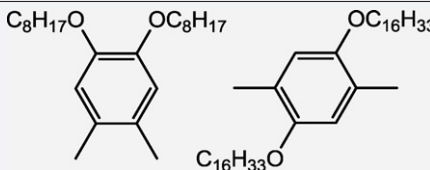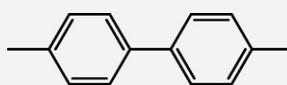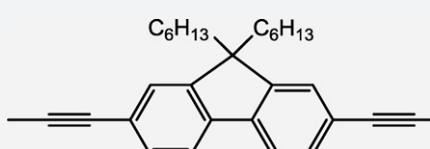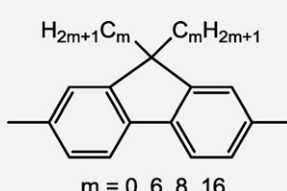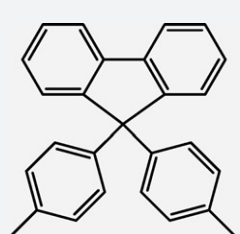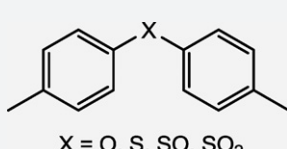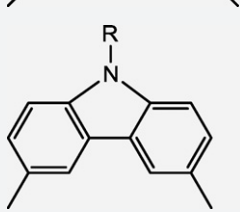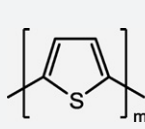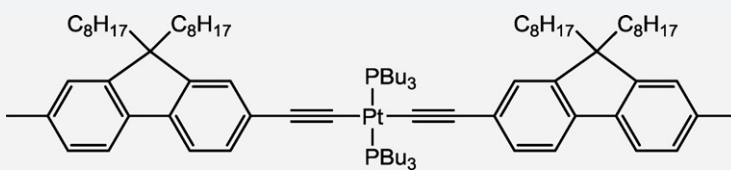
**Table 7**
Homoleptic mercury alkynides of type [Hg(C≡CR)$_2$] bearing different organic groups R.

| R | Ref. |
|---|---|
|  | [254] |
|  | [255] |
| | [256] |
|  | [171] |
|  | [257] |
|  | [258] |
|  | [259] |

**Table 8**
Homoleptic mercury polyynes of type [-HgC≡C-E-C≡C-]$_n$ with different connecting units E.

| E | Ref. | E | Ref. |
|---|---|---|---|
|  | [260] |  | [261] |
|  | [262] |  | [263] |
|  | [264] |  | [265] |
|  | [266,267] |  | [268] |
|  | | | [257] |

preparation of these rod-like molecules were realized by the reaction of [Hg(OAc)$_2$] with the respective diynyl metal complex. X-ray results showed in the molecular structure of the ruthenium compound an unusual large bending at the carbon atoms attached to mercury (C≡C-Hg 166.5(3)°) [270]. DFT calculations were employed to explain this phenomenon with the result that no electronic source is responsible for this feature. It must be caused by lattice forces [270]. This contrasts to the single crystal X-ray structures of [Hg{(C≡C)$_x$C[Co$_3$($\mu$-dppm)(CO)$_7$]}$_2$] ($x$ = 1, 2) where no conspicuous angles around the mercury centre are observed [272]. Bruce succeeded also in the preparation of homoleptic [Hg{(C≡C)$_4$[CCo$_3$($\mu$-dppm)(CO)$_7$]}$_2$] containing

even longer alkynyl chains with cobalt cluster end groups [273].

The first ferrocenyl-functionalized bis(alkynyl) mercury compound was reported by Bassetti et al. [274] who demonstated that quenching the reaction of [Hg(OAc)$_2$] and HC≡CFc with an iodine solution, immediately after addition of the mercury acetate, led to an orange precipitate, which could be identified as [Hg(C≡CFc)$_2$]. This molecule was formed in quantitative yield. However, when longer reaction times (up to three days) were used then acetyl ferrocene was obtained quantitatively via intermediates including FcC(OMe)=CH$_2$ [274]. A similar compound featuring a diphenylthiophosphoryl group at ferrocene
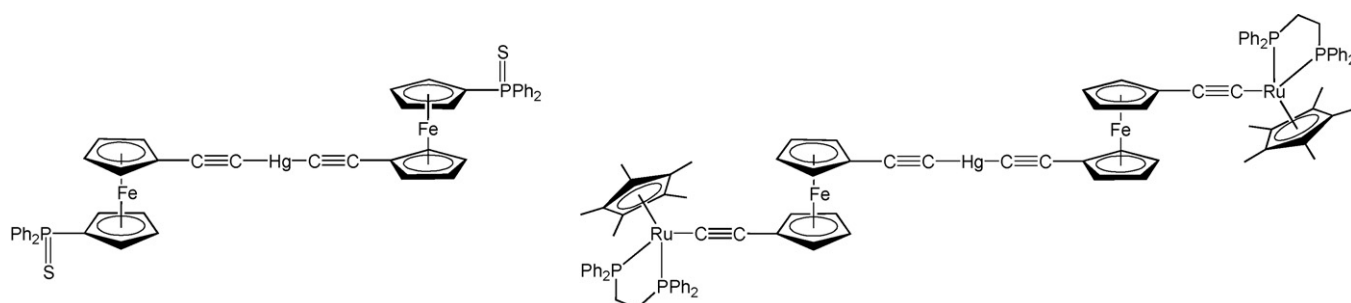


**Fig. 39.** Heterometallic Complexes [Hg{C≡C-fc-P(S)Ph$_2$}$_2$] (left) [275] and [Hg{C≡C-fc-C≡CRu(dppe)(Cp$^*$)}$_2$] (right) [276].

was recently published according to the synthesis method reported by Kutscheroff (see above) [275]. Complex [Hg{C≡C-fc-P(S)Ph$_2$}$_2$] (fc = ($\eta^5$-C$_5$H$_4$)($\eta^5$-C$_5$H$_4$)Fe) (Fig. 39, left) was obtained as an orange, very poorly soluble material. Heterotrimetallic [Hg{C≡C-fc-C≡CRu(dppe)(Cp$^*$)}$_2$] could be isolated from the reaction of [Hg(OAc)$_2$] with [HC≡C-fc-C≡CRu(dppe)(Cp$^*$)] in refluxing tetrahydrofuran as described by Bruce (Fig. 39, right) [276].

The electrochemical response of the latter molecule was examined by cyclic voltammetry. Typical one-electron oxidations occur between 0.60 and 0.67 V for the ferrocenyl and the ruthenium half-sandwich fragments [276]. Comparing these values with the redox potentials of FcC≡CH and [(dppe)(Cp$^*$)RuC≡CPh] leads to the conclusion that an interaction between both redox-centers through the acetylide link exists.

## 9. Conclusion

This review describes the current trends in homoleptic transition metal alkynide chemistry, a family of compounds which was first identified in literature more than one century ago. The renaissance in this area took place in the early 1950s with Nast's pioneering contributions. Since that time, a wide range of such complexes, especially from group 10–12 metals, have been prepared and studied. Their synthesis, structure, bonding motifs, reaction chemistry, reactivity, and their application potential is well understood and documented, nevertheless, the characterization of the molecules synthesized in the nineteen-fifties and -sixties are limited by modern standards.

The large quantity of work carried out so far in this field of chemistry opens the possibility, for example, to use transition metal acetylides as building blocks for the preparation of nowadays fascinating heteromultimetallic transition metal complexes [277–282] allowing to study electron transfer processes between different redox-active metal centers *via* alkynide connectivities. It will be of interest to see if the applications of homoleptic alkynide complexes reach a comparable level to the broad variety of heteroleptic transition metal alkynide and cyanide systems.

## References

[1] A.G. Sharpe, The Chemistry of Cyano Complexes of the Transition Metals, Academic Press, London, 1976.
[2] J. Bartoll, B. Jackisch, M. Most, E. Wenders de Calisse, C.M. Vogtherr, Techne 25 (2007) 39.
[3] M. Kutscheroff, Ber. dt. chem. Ges. 17 (1884) 13.
[4] J.A. Mathews, L.L. Watters, J. Am. Chem. Soc. 22 (1900) 108.
[5] R. Nast, Z. Naturforsch. Teil B 8 (1953) 381.
[6] R. Nast, Angew. Chem. 72 (1960) 26.
[7] R. Nast, Coord. Chem. Rev. 47 (1982) 89.
[8] J.R. Berenguer, E. Lalinde, M.T. Moreno, Coord. Chem. Rev. 254 (2010) 832.
[9] J.R. Berenguer, A. Díez, J. Fernández, J. Forniés, A. García, B. Gil, E. Lalinde, M.T. Moreno, Inorg. Chem. 47 (2008) 7703.
[10] A. Díez, J. Fernández, E. Lalinde, M.T. Moreno, S. Sanchez, Dalton Trans. 36 (2008) 4926.
[11] B. Gil, J. Forniés, J. Gómez, E. Lalinde, A. Martin, M.T. Moreno, Inorg. Chem. 45 (2006) 7788.
[12] V.W.-W. Yam, C.-K. Hui, S.-Y. Yu, N. Zhu, Inorg. Chem. 43 (2004) 812.
[13] L.A. Berben, J.R. Long, Inorg. Chem. 44 (2005) 8459.
[14] W.-Y. Wong, Coord. Chem. Rev. 251 (2007) 2400.
[15] H. Lang, D.S.A. George, G. Rheinwald, Coord. Chem. Rev. 206–207 (2000) 101.
[16] U. Rosenthal, Angew. Chem. 115 (2003) 1838.
[17] D. Rais, J. Yau, D.M.P. Mingos, R. Vilar, A.J.P. White, D.J. Williams, Angew. Chem. Int. Ed. 40 (2001) 3464.
[18] D.M.P. Mingos, J. Yau, S. Menzer, D.J. Williams, Angew. Chem. Int. Ed. Engl. 34 (1995) 1894.
[19] B.C. Guo, K.P. Kerns, A.W. Castleman Jr., Science 223 (1992) 1411.
[20] S. Wei, B.C. Guo, J. Purnell, S.A. Buzza, A.W. Castleman Jr., J. Phys. Chem. 96 (1992) 4166.
[21] B.D. Leskiw, A.W. Castleman Jr., C. R. Physique 3 (2002) 251.
[22] M.-M. Rohmer, M. Benard, J.-M. Poblet, Chem. Rev. 100 (2000) 495.
[23] I. Dance, E. Wenger, H. Harris, Chem. Eur. J. 8 (2002) 3497.
[24] V.V. Ivanovskaya, A.A. Sofronov, Y.N. Makurin, A.L. Ivanovskii, J. Mol. Struct. 594 (2002) 31.
[25] Z.Y. Chen, G.J. Walder, A.W. Castleman Jr., Phys. Rev. B 49 (1994) 2739.
[26] A.A. Sofronov, V.V. Ivanovskaya, Y.N. Makurin, A.L. Ivanovskii, Russ. J. Coord. Chem. 28 (2002) 618.
[27] P. Liu, J.A. Rodriguez, J.T. Muckerman, J. Chem. Phys. B 108 (2004) 18796.
[28] M.A. Sobhy, A.W. Castleman Jr., J.O. Sofo, J. Chem. Phys. 123 (2005) 154106.
[29] H. Hou, J.T. Muckerman, P. Liu, J.A. Rodriguez, J. Phys. Chem. A 107 (2003) 9344.
[30] P. Liu, J.A. Rodriguez, J.T. Muckerman, J. Chem. Phys. 121 (2004) 10321.
[31] J. Muñoz, C. Pujol, C. Bo, J.-M. Poblet, M.-M. Rohmer, M. Benard, J. Phys. Chem. A 101 (1997) 8345.
[32] M.-M. Rohmer, P. De Vaal, M. Benard, J. Am. Chem. Soc. 114 (1992) 9696.
[33] M.-M. Rohmer, M. Benard, C. Bo, J.-M. Poblet, J. Am. Chem. Soc. 117 (1995) 508.
[34] M. Benard, M.-M. Rohmer, J.-M. Poblet, C. Bo, J. Phys. Chem. 99 (1995) 16913.
[35] J. Devemy, M.-M. Rohmer, M. Benard, Int. J. Quant. Chem. 58 (1996) 267.
[36] I. Dance, J. Am. Chem. Soc. 118 (1996) 6309.
[37] I. Dance, Chem. Commun. (1998) 523.
[38] R.W. Grimes, J.D. Gale, J. Phys. Chem. 97 (1993) 4616.
[39] B.V. Reddy, S.N. Khanna, J. Phys. Chem. 98 (1994) 9446.
[40] S.N. Khanna, Phys. Rev. B 51 (1995) 10965.
[41] B. Todorović-Marković, Z. Marković, T. Nenadović, Fullerene Sci. Technol. 8 (2000) 27.
[42] B.C. Guo, S. Wei, J. Purnell, S.A. Buzza, A.W. Castleman Jr., Science 256 (1992) 515.
[43] L.-S. Wang, H. Cheng, Phys. Rev. Lett. 78 (1997) 2983.
[44] S. Wei, B.C. Guo, J. Purnell, S.A. Buzza, A.W. Castleman Jr., J. Phys. Chem. 97 (1993) 9559.
[45] S.F. Cartier, B.D. May, B.J. Toleno, J. Purnell, S. Wei, A.W. Castleman Jr., Chem. Phys. Lett. 220 (1994) 23.
[46] H.T. Deng, B.C. Guo, K.P. Kerns, A.W. Castleman Jr., J. Phys. Chem. 98 (1994) 13378.
[47] B.D. May, S.F. Cartier, A.W. Castleman Jr., Chem. Phys. Lett. 242 (1995) 265.
[48] H.T. Deng, K.P. Kerns, A.W. Castleman Jr., J. Chem. Phys. 104 (1996) 4862.
[49] S.F. Cartier, B.D. May, A.W. Castleman Jr., J. Phys. Chem. 100 (1996) 8175.
[50] S.E. Kooi, A.W. Castleman Jr., J. Chem. Phys. 108 (1998) 8864.
[51] H. Sakurai, A.W. Castleman Jr., J. Chem. Phys. 111 (1999) 1462.
[52] K.J. Auberry, Y.G. Byun, D.B. Jacobson, B.S. Freiser, J. Phys. Chem. 103 (1999) 9029.
[53] R. Selvan, T. Pradeep, Chem. Phys. Lett. 309 (1999) 149.
[54] S. Li, H. Wu, L.-S. Wang, J. Am. Chem. Soc. 119 (1997) 7417.
[55] V.V. Ivanovskaya, A.A. Sofronov, A.L. Ivanovskii, Phys. Lett. A 297 (2002) 436.
[56] L. Gao, M.E. Lyn, D.E. Bergeron, A.W. Castleman Jr., Int. J. Mass Spectrom. 229 (2003) 11.
[57] G.S. McCarty, J.C. Love, J.G. Kushmerick, L.F. Charles, C.D. Keating, B.J. Toleno, M.E. Lyn, A.W. Castleman Jr., M.J. Natan, P.S. Weiss, J. Nanopart. Res. 1 (1999) 459.
[58] C.S. Yeh, S. Afzaal, S.A. Lee, Y.G. Byun, B.S. Freiser, J. Am. Chem. Soc. 116 (1994) 8806.
[59] H. Harris, I. Dance, J. Phys. Chem. A 105 (2001) 3340.
[60] S. Wei, B.C. Guo, H.T. Deng, K. Kerns, J. Purnell, S.A. Buzza, A.W. Castleman Jr., J. Am. Chem. Soc. 116 (1994) 4475.
[61] Y.G. Byun, S.A. Lee, S.Z. Kan, B.S. Freiser, J. Phys. Chem. 100 (1996) 14281.
[62] S.-G. He, Y. Xie, F. Dong, E.R. Bernstein, J. Chem. Phys. 125 (2006) 164306.
[63] J.S. Pilgrim, M.A. Duncan, J. Am. Chem. Soc. 115 (1993) 6958.
[64] J.M. Lightstone, H.A. Mann, M. Wu, P.M. Johnson, M.G. White, J. Phys. Chem. B 107 (2003) 10359.
[65] H.H. Harris, I.G. Dance, Polyhedron 26 (2007) 250.
[66] H.T. Deng, B.C. Guo, K.P. Kerns, A.W. Castleman Jr., Int. J. Mass Spectr. Ion Proc. 138 (1994) 275.
[67] S.F. Cartier, B.D. May, A.W. Castleman Jr., J. Am. Chem. Soc. 116 (1994) 5295.
[68] S.F. Cartier, B.D. May, A.W. Castleman Jr., J. Chem. Phys. 100 (1994) 5384.
[69] S.F. Cartier, B.D. May, A.W. Castleman Jr., J. Chem. Phys. 104 (1996) 3423.
[70] B.D. May, S.E. Kooi, B.J. Toleno, A.W. Castleman Jr., J. Chem. Phys. 106 (1997) 2231.
[71] S.F. Cartier, Z.Y. Chen, G.J. Walder, C.R. Sleppy, A.W. Castleman Jr., Science 260 (1993) 195.
[72] B.V. Reddy, S.N. Khanna, P. Jena, Science 258 (1992) 1640.
[73] Z.Q. Li, B.L. Gu, R.S. Han, Q.Q. Zheng, Z. Phys. D 27 (1993) 275.
[74] L.R. Brock, M.A. Duncan, J. Phys. Chem. 100 (1996) 5654.
[75] J.-M. Poblet, C. Bo, M.-M. Rohmer, M. Bénard, Chem. Phys. Lett. 260 (1996) 577.
[76] A. Rubio, J.A. Alonso, J.M. López, An. Fis. 89 (1993) 174.
[77] U. Ruschewitz, Coord. Chem. Rev. 244 (2003) 115.
[78] U. Cremer, W. Kockelmann, M. Bertmer, U. Ruschewitz, Solid State Sci. 4 (2002) 247.
[79] W. Kockelmann, U. Ruschewitz, Angew. Chem. Int. Ed. 38 (1999) 3492.
[80] J. Offermanns, U. Ruschewitz, Z. Anorg. Allg. Chem. 626 (2000) 649.
[81] U. Ruschewitz, Z. Anorg. Allg. Chem. 632 (2006) 705.
[82] R. Ahlers, U. Ruschewitz, Z. Anorg. Allg. Chem. 631 (2005) 1241.
[83] R. Nast, H. Schindel, Z. Anorg. Allg. Chem. 326 (1963) 201.
[84] U. Cremer, U. Ruschewitz, Z. Anorg. Allg. Chem. 630 (2004) 161.
[85] M. Weiß, U. Ruschewitz, Z. Anorg. Allg. Chem. 623 (1997) 1208.
[86] S. Hemmersbach, B. Zibrowius, W. Kockelmann, U. Ruschewitz, Chem. Eur. J. 7 (2001) 1951.
[87] U. Ruschewitz, Z. Anorg. Allg. Chem. 627 (2001) 1231.
[88] U. Ruschewitz, C. Bähtz, M. Knapp, Z. Anorg. Allg. Chem. 629 (2003) 1581.
[89] H. Lang, K. Köhler, S. Blau, Coord. Chem. Rev. 143 (1995) 113.

[90] W.J. Evans, A.L. Wayda, J. Organomet. Chem. 202 (1980) C6.
[91] W.J. Evans, D.K. Drummond, T.P. Hanusa, J.M. Olofson, J. Organomet. Chem. 376 (1989) 311.
[92] R. Duchateau, T. Tuinstra, E.A.C. Brussee, A. Meetsma, P.T. van Duijnen, J.H. Teuben, Organometallics 16 (1997) 3511.
[93] T.P. Vaid, A.S. Veige, E.B. Lobkovsky, W.V. Glassey, P.T. Wolczanski, L.M. Liable Sands, A.L. Rheingold, T.R. Cundari, J. Am. Chem. Soc. 120 (1998) 10067.
[94] H. Kawaguchi, K. Tatsumi, Organometallics 14 (1995) 4294.
[95] R. Nast, E. Sirtl, Chem. Ber. 88 (1955) 1723.
[96] R. Nast, H. Griesshammer, Chem. Ber. 90 (1957) 1315.
[97] R. Nast, H.P. Müller, Chem. Ber. 111 (1978) 415.
[98] R. Nast, A. Santos, Z. Natur. B 35 (1980) 248.
[99] R. Nast, F. Urban, Z. Anorg. Allg. Chem. 287 (1956) 17.
[100] E. Rojas, A. Santos, V. Moreno, C. Del Pino, J. Organomet. Chem. 181 (1979) 365.
[101] R. Nast, H. Lewinsky, Z. Anorg. Allg. Chem. 282 (1955) 210.
[102] R. Nast, K. Fock, Chem. Ber. 109 (1976) 455.
[103] R. Nast, H. Kasperl, Z. Anorg. Allg. Chem. 295 (1958) 227.
[104] R. Nast, H.P. Müller, V. Pank, Chem. Ber. 111 (1978) 1627.
[105] R. Nast, W.D. Heinz, Chem. Ber. 95 (1962) 1478.
[106] A.T. Casey, A.M. Vecchio, Appl. Organomet. Chem. 4 (1990) 513.
[107] R. Nast, W. Hoerl, Chem. Ber. 95 (1962) 1470.
[108] R. Nast, K. Vester, Z. Anorg. Allg. Chem. 279 (1955) 146.
[109] B.D. Chandler, A.B. Schabel, L.H. Pignolet, J. Phys. Chem. B 105 (2001) 149.
[110] Q.-H. Wei, G.-Q. Yin, Z. Ma, L.-X. Shi, Z.-N. Chen, Chem. Commun. (2003) 2188.
[111] G.-Q. Yin, Q.-H. Wei, L.-Y. Zhang, Z.-N. Chen, Organometallics 25 (2006) 580.
[112] J.R. Berenguer, J. Forniés, B. Gil, E. Lalinde, Chem. Eur. J. 12 (2006) 785.
[113] V.W.-W. Yam, K.-L. Yu, K.-K. Cheung, J. Chem. Soc., Dalton Trans.: Inorg. Chem. 17 (1999) 2913.
[114] J.P.H. Charmant, J. Forniés, J. Gomez, E. Lalinde, R.I. Merino, M.T. Moreno, A.G. Orpen, Organometallics 18 (1999) 3353.
[115] I. Ara, J. Forniés, J. Gómez, E. Lalinde, R.I. Merino, M.T. Moreno, Inorg. Chem. Commun. 2 (1999) 62.
[116] I. Ara, J. Forniés, J. Gómez, E. Lalinde, M.T. Moreno, Organometallics 19 (2000) 3137.
[117] J.W. Eastes, W.M. Burgess, J. Am. Chem. Soc. 64 (1942) 1187.
[118] R. Nast, H.D. Moerler, Chem. Ber. 99 (1966) 3787.
[119] L. Ballester, M. Cano, A. Santos, J. Organomet. Chem. 229 (1982) 101.
[120] M.C. Barral, R. Jimenez, E. Royer, V. Moreno, A. Santos, Inorg. Chim. Acta 31 (1978) 165.
[121] Y. Zhou, A.M. Arif, J.S. Miller, Chem. Commun. 16 (1996) 1881.
[122] R. Taube, G. Honymus, Angew. Chem. 87 (1975) 291.
[123] R. Nast, K. Vester, H. Griesshammer, Chem. Ber. 90 (1957) 2678.
[124] E. Negishi, K. Akiyoshi, T. Takahashi, J. Chem. Soc., Chem. Commun. 6 (1987) 477.
[125] P. Espinet, J. Forniés, F. Martinez, M. Tomas, E. Lalinde, M.T. Moreno, A. Ruiz, A.J. Welch, J. Chem. Soc., Dalton Trans.: Inorg. Chem. 3 (1990) 791.
[126] J. Forniés, E. Lalinde, A. Martin, M.T. Moreno, J. Chem. Soc., Dalton Trans.: Inorg. Chem. 2 (1994) 135.
[127] J. Benito, J.R. Berenguer, J. Forniés, B. Gil, J. Gómez, E. Lalinde, Dalton Trans. 22 (2003) 4331.
[128] L.R. Falvello, J. Forniés, J. Gómez, E. Lalinde, A. Martin, M.T. Moreno, J. Sacristan, Chem. Eur. J. 5 (1999) 474.
[129] H. Lang, M. Leschke, Heteroatom Chem. 13 (2002) 521.
[130] I. Ara, J.R. Berenguer, J. Forniés, E. Lalinde, Inorg. Chim. Acta 264 (1997) 199.
[131] I. Ara, J.R. Berenguer, J. Forniés, E. Lalinde, Organometallics 16 (1997) 3921.
[132] N. Mansilla, G. Rheinwald, H. Lang, unpublished.
[133] I. Ara, J.R. Berenguer, E. Eguizabal, J. Forniés, E. Lalinde, Organometallics 20 (2001) 2686.
[134] J.R. Berenguer, E. Eguizabal, L.R. Falvello, J. Forniés, E. Lalinde, A. Martin, Organometallics 19 (2000) 490.
[135] J.R. Berenguer, J. Forniés, E. Lalinde, F. Martinez, Organometallics 15 (1996) 4537.
[136] J.R. Berenguer, J. Forniés, E. Lalinde, A. Martin, M.T. Moreno, J. Chem. Soc., Dalton Trans.: Inorg. Chem. 23 (1994) 3343.
[137] J. Forniés, J. Gómez, E. Lalinde, M.T. Moreno, Inorg. Chem. 40 (2001) 5415.
[138] J.P.H. Charmant, J. Gómez, A.G. Orpen, L.R. Falvello, J. Forniés, A. Rueda, J. Gómez, E. Lalinde, M.T. Moreno, Commun. 20 (1999) 2045.
[139] J.R. Berenguer, J. Fernández, B. Gil, E. Lalinde, S. Sánchez, Inorg. Chem. 49 (2010) 4232.
[140] J. Forniés, E. Lalinde, A. Martin, M.T. Moreno, J. Organomet. Chem. 490 (1995) 179.
[141] S. Tanaka, T. Yoshida, T. Adachi, T. Yoshida, K. Onitsuka, K. Sonogashira, Chem. Lett. (1994) 877.
[142] E. Bus, J.A. van Bokhoven, J. Phys. Chem. C 111 (2007) 9761.
[143] J.R. Berenguer, J. Forniés, J. Gómez, E. Lalinde, M.T. Moreno, Organometallics 20 (2001) 4847.
[144] J.K. Nagle, A.L. Balch, M.M. Olmstead, J. Am. Chem. Soc. 110 (1988) 319.
[145] D. Zhang, D.B. McConville, C.A. Tessier, W.J. Youngs, Organometallics 16 (1997) 824.
[146] O.M. Abu-Salah, J. Organomet. Chem. 565 (1998) 211.
[147] J.G. Noltes, G. van Koten, in: G. Wilkinson, F.G.A. Stone, E.W. Abel (Eds.), Comprehensive Organometallic Chemistry, vol. 2, Pergamon, New York, 1982, p. 709.

[148] H. Bauer, J. Faust, R. Fröböse, J. Füssel, Gmelin Handbook of Inorganic Chemistry, Cu, Organocopper Compounds, Part 3, 8th ed., Springer, Berlin, 1986.
[149] G.E. Coates, M.L.H. Green, K. Wade, Organometallic Compounds—Transition Elements, vol. 2, 3rd ed., Methuen, London, 1968, p. 271.
[150] P.P. Power, Prog. Inorg. Chem. 39 (1991) 75.
[151] D.M.P. Mingos, R. Vilar, D. Rais, J. Organomet. Chem. 641 (2002) 126.
[152] N. Krause (Ed.), Modern Organocopper Chemistry, Wiley-VCH, New York, 2002.
[153] C.E. Castro, R.D. Stephens, J. Org. Chem. 28 (1963) 2163.
[154] R.D. Stephens, C.E. Castro, J. Org. Chem. 28 (1963) 3313.
[155] C.E. Castro, E.J. Caughan, D.C. Owsley, J. Org. Chem. 31 (1966) 4071.
[156] C.J. Woltermann, H. Schechter, Helv. Chim. Acta 109 (2005) 562.
[157] T. Kitamura, T. Tanaka, H. Taniguchi, P.J. Stang, J. Chem. Soc., Perkin Trans. 1 (1991) 2892.
[158] S. Murata, C. Seo, M. Kujime, T. Sugimoto, Heterocycles 53 (2000) 1259.
[159] T.S. Chou, S.C. Hung, H.H. Tso, J. Org. Chem. 52 (1987) 3394.
[160] M.-H. Cheng, Y.-H. Ho, C.-C. Chen, G.-H. Lee, S.-M. Peng, S.-Y. Chu, R.-S. Liu, Organometallics 13 (1994) 4082.
[161] D. Daia, C.D. Gabbutt, B.M. Heron, J.D. Hepworth, M.B. Hursthouse, K.M.A. Malik, Tetrahedron Lett. 44 (2003) 1461.
[162] E.U. Wuerthwein, R. Weigmann, Angew. Chem. 99 (1987) 918.
[163] B.F. Straub, Chem. Commun. (2007) 3868.
[164] M. Ahlquist, V.V. Fokin, Organometallics 26 (2007) 4389.
[165] S.S.Y. Chui, M.F.Y. Ng, C.-M. Che, Chem. Eur. J. 11 (2005) 1739.
[166] I.O. Koshevoy, L. Koskinen, M. Haukka, S.P. Tunik, Yu.P. Serdobintsev, A.S. Melnikov, T.A. Pakkanen, Angew. Chem. Int. Ed. 47 (2008) 3942.
[167] S.-K. Yip, C.-L. Chan, W.H. Lam, K.-K. Cheung, V.W.-W. Yam, Photochem. Photobiol. Sci. 6 (2007) 365.
[168] Q.H. Wei, G.Q. Yin, L.Y. Zhang, L.X. Shi, Z.W. Mao, Z.N. Chen, Inorg. Chem. 43 (2004) 3484.
[169] Y. Yamamoto, M. Shiotsuka, S. Okuno, S. Onaka, Chem. Lett. 33 (2004) 210.
[170] S.-K. Yip, E.C.-C. Cheng, L.-H. Yuan, N. Zhu, V.W.-W. Yam, Angew. Chem. Int. Ed. 43 (2004) 4954.
[171] M. Ferrer, L. Rodriguez, O. Rossell, F. Pina, J.C. Lima, M.F. Bardia, X. Solans, J. Organomet. Chem. 678 (2003) 82.
[172] B.W. Ticknor, B. Bandyopadhyay, M.A. Duncan, J. Phys. Chem. A 112 (2008) 12355.
[173] A.N. Alexandrova, A.I. Boldyrev, H.-J. Zhai, L.-S. Wang, J. Phys. Chem. A 109 (2005) 562.
[174] R. Nast, P. Schneller, A. Hengefeld, J. Organomet. Chem. 214 (1981) 273.
[175] R. Nast, U. Kirner, Z. Anorg. Allorg. Chem. 330 (1964) 311.
[176] M.I. Bruce, P.J. Low, Adv. Organomet. Chem. 50 (2004) 179.
[177] T.C.W. Mak, X.L.Z.Q.M. Wang, G.C. Guo, Coord. Chem. Rev. 251 (2007) 2311.
[178] T.C.W. Mak, L. Zhao, Chem. Asian J. 2 (2007) 456.
[179] J. Vicente, J. Gil-Rubio, N. Barquero, P.G. Jones, D. Bautista, Organometallics 27 (2008) 646.
[180] R.N. Haszeldine, J. Chem. Soc. (1951) 588.
[181] G.E. Parkin, C. Parkin, J. Inorg. Nucl. Chem. 22 (1961) 59.
[182] G.E. Coates, C. Parkin, J. Chem. Soc. (1962) 3220.
[183] D. Blake, G. Calvin, G.E. Coates, Proc. Chem. Soc. (1959) 396.
[184] P.W.R. Corfield, M.M. Harrison, Acta Cryst. 21 (1966) 957.
[185] M.I. Bruce, Chem. Rev. 91 (1991) 197.
[186] S. Lotz, P.H. van Rooyen, R. Meyer, Adv. Organomet. Chem. 37 (1995) 219.
[187] F. Olbrich, J. Kopf, E. Weiss, Angew. Chem., Int. Ed. Engl. 32 (1993) 1077.
[188] D. Rais, D.M.P. Mingos, R. Vilar, A.J.P. White, D.J. Williams, J. Organomet. Chem. 652 (2002) 87.
[189] Q.-H. Wei, G.-Q. Yin, L.-Y. Zhang, Z.-N. Chen, Organometallics 25 (2006) 4941.
[190] O.M. Abu-Salah, M.H. Ja'far, A.R. Al-Ohaly, K.A. Al-Farhan, H.S. Al-Enzi, O.V. Dolomanov, J.A.K. Howard, Eur. J. Inorg. Chem. (2006) 2353.
[191] J. Nishijo, O. Oishi, K. Judai, N. Nishi, Chem. Mater. 19 (2007) 4627.
[192] K. Judai, J. Nishijo, N. Nishi, Adv. Mater. 18 (2006) 2842.
[193] K. Judai, S. Numaro, A. Furuya, J. Nishijo, N. Nishi, J. Am. Chem. Oc. 130 (2008) 1142.
[194] F. Cataldo, C.S. Casari, J. Inorg. Organomet. Polym. 17 (2007) 641.
[195] G. Grasso, L. D'Urso, E. Messina, F. Cataldo, O. Puglisi, G. Spoto, G. Compagnini, Carbon 47 (2009) 2611.
[196] F. Cataldo, G. Compagnini, A. Scandurra, G. Strazzulla, Fuller. Nanotub. Car. N. 16 (2008) 126.
[197] R. Nast, W.H. Lepel, Z. Naturforsch, Teil B 34 (1979) 856.
[198] J. Vicente, M.-T. Chicote, M.M. Alvarez-Falcón, Organometallics 24 (2005) 4666.
[199] T. Zhang, H. Song, Z. Dai, X. Meng, Dalton Trans. (2009) 7688.
[200] P. Espinet, J. Fornies, F. Martinez, M. Sotes, E. Lalinde, M.T. Moreno, A. Ruiz, A.J. Welch, J. Organomet. Chem. 403 (1991) 253.
[201] M.I. Bruce, M.G. Humphrey, J.G. Matisons, S.K. Roy, A.G. Swincer, Aust. J. Chem. 37 (1984) 1955.
[202] R. Nast, W. Pfab, Chem. Ber. 89 (1956) 415.
[203] O.M. Abu-Salah, A.R. Al-Ohaly, J. Organomet. Chem. 270 (1983) C39.
[204] O.M. Abu-Salah, A.R. Al-Ohaly, J. Chem. Soc., Dalton Trans. (1988) 2297.
[205] O.M. Abu-Salah, J. Organomet. Chem. 387 (1990) 123.
[206] O.M. Abu-Salah, A.R. Al-Ohaly, H.A. Al-Qahtani, Inorg. Chim. Acta (1986) L29.
[207] C.M.P. Kronenburg, J.T.B.H. Jastrzebski, M. Lutz, A.L. Spek, G. van Koten, Organometallics 22 (2003) 2312.
[208] R. Nast, P.-G. Kirst, G. Beck, J. Gremm, Chem. Ber. 96 (1963) 3302.
[209] O.M. Abu-Salah, A.A. Al-Ohaly, Z.F. Mutter, J. Organomet. Chem. 389 (1990) 427.

[210] U. Cremer, S. Disch, U. Ruschewitz, Z. Anorg. Allorg. Chem. 630 (2004) 2304.
[211] O. Schuster, H. Schmidbaur, Organometallics 24 (2005) 2289.
[212] F.-Q. Wang, G.N. Khairallah, G.A. Koutsantonis, C.M. Williams, D.L. Callahan, R.A.J. O'Hair, Phys. Chem. Chem. Phys. 11 (2009) 4132.
[213] K.A. Al-Farhan, M.H. Ja'far, O.M. Abu-Salah, J. Organomet. Chem. 579 (1999) 59.
[214] S.-D. Bian, J.-H. Jia, Q.-M. Wang, J. Am. Chem. Soc. 131 (2009) 3422.
[215] O.M. Abu-Salah, J. Organomet. Chem. 270 (1984) C26.
[216] O.M. Abu-Salah, A.R. Al-Ohaly, C.B. Knobler, J. Chem. Soc., Chem. Commun. (1985) 1502.
[217] M. Ul-Haque, W. Horne, O.M. Abu-Salah, J. Crystallogr. Spectrosc. Res. 22 (1992) 421.
[218] M.S. Hussain, M. Ul-Haque, O.M. Abu-Salah, J. Cluster Sci. 7 (1996) 167.
[219] K.A. Al-Farhan, O.M. Abu-Salah, M. Mukhalalati, M. Jaafar, Acta Cryst. C C51 (1995) 1089.
[220] O.M. Abu-Salah, Polyhedron 11 (1992) 951.
[221] O.M. Abu-Salah, A.R. Al-Ohaly, Z.F. Mutter, J. Organomet. Chem. 391 (1990) 267.
[222] O.M. Abu-Salah, M.S. Hussain, E.O. Schlemper, J. Chem. Soc., Chem. Commun. (1988) 212.
[223] M.S. Hussain, O.M. Abu-Salah, J. Organomet. Chem. 445 (1993) 295.
[224] A. Vega, V. Calvo, E. Spodine, A. Zárate, V. Fuenzalida, J.-Y. Saillard, Inorg. Chem. 41 (2002) 3389.
[225] L. Zhao, W.-Y. Wong, T.C.W. Mak, Chem. Eur. J. 12 (2006) 4865.
[226] L. Zha, X.-L. Zhao, T.C.W. Mak, Chem. Eur. J. 13 (2007) 5927.
[227] L. Zhao, T.C.W. Mak, J. Am. Chem. Soc. 127 (2005) 14966.
[228] L. Zhao, X.D. Chen, T.C.W. Mak, Organometallics 27 (2008) 2483.
[229] S.Q. Zang, T.C.W. Mak, Inorg. Chem. 47 (2008) 7094.
[230] S.M.J. Wang, L. Zhao, T.C.W. Mak, Dalton Trans. 39 (2010) 2108.
[231] S.M.J. Wang, T.C.W. Mak, Polyhedron 28 (2009) 2684.
[232] L. Zhao, T.C.W. Mak, Inorg. Chem. 48 (2009) 6480.
[233] S.Q. Zang, P.S. Cheng, T.C.W. Mak, Cryst. Eng. Commun. 11 (2009) 1061.
[234] P. Knochel, R.D. Singer, Chem. Rev. 93 (1993) 2117.
[235] E.M. Cano, M.A. Santos, R.L. Ballester, Anal. Quim. 73 (1977) 1051.
[236] J.V. Nef, Justus Liebigs Ann. Chem. 308 (1899) 264.
[237] R. Nast, R. Müller, Chem. Ber. 91 (1958) 2861.
[238] E. Weiss, H. Plass, J. Organomet. Chem. 14 (1968) 21.
[239] U. Cremer, I. Pantenburg, U. Ruschewitz, Inorg. Chem. 42 (2003) 7716.
[240] E.A. Jeffrey, T. Mole, J. Organomet. Chem. 11 (1968) 393.
[241] R.M. Fabricon, M. Parvez, H.G. Richey Jr., Organometallics 18 (1999) 5163.
[242] O.Y. Okhlobystin, L.I. Zakharkin, J. Organomet. Chem. 3 (1965) 257.
[243] M.A. Putzer, B. Neumüller, K. Dehnicke, Z. Anorg. Allg. Chem. 623 (1997) 539.
[244] A.J. Edwards, A. Fallaize, P.R. Raithby, M.-A. Rennie, A. Steiner, K.L. Verhorevoort, D.S. Wright, J. Chem. Soc., Dalton Trans. (1996) 133.
[245] M.J. Dabdoub, V.B. Dabdoub, J.P. Marino, Tetrahedr. Lett. 41 (2000) 437.
[246] J.F. Traverse, A.H. Hoveyda, M.L. Snapper, Organic Lett. 5 (2003) 3273.
[247] R. Nast, C. Richers, Z. Anorg. Allg. Chem. 319 (1963) 320.
[248] U. Cremer, U. Ruschewitz, Z. Anorg. Allg. Chem. 630 (2004) 337.
[249] N. Wetzold, Thesis, TU Chemnitz, 2007.
[250] J.R. Johnson, W.L. McEwen, J. Am. Chem. Soc. 48 (1926) 469.
[251] R. Nast, C. Richers, Chem. Ber. 97 (1964) 3317.
[252] D.J. Cook, A.F. Hill, D.J. Wilson, J. Chem. Soc., Dalton Trans. (1998) 1171.
[253] R.D. Dewhurst, A.F. Hill, M.K. Smith, Organometallics 25 (2006) 2388.
[254] E.A. Dikusar, V.I. Potkin, E.V. Vashkevich, N.G. Kozlov, R.V. Kaberdin, Russ. J. Gen. Chem. 74 (2004) 578.
[255] E.A. Dikusar, N.G. Kozlov, S.S. Koval'skaya, L.A. Popova, K.L. Moiseichuk, Russ. J. Gen. Chem. 71 (2001) 290.
[256] B.F. Hoskins, R. Robson, E.E. Sutherland, J. Organomet. Chem. 515 (1996) 259.
[257] G.-J. Zhou, W.-Y. Wong, Z. Lin, C. Ye, Angew. Chem. Int. Ed. 45 (2006) 6189.
[258] L. Liu, W.-Y. Wong, Y.-W. Lam, W.-Y. Tam, Inorg. Chim. Acta 360 (2007) 109.
[259] L. Liu, Y.-W. Lam, W.-Y. Wong, J. Organomet. Chem. 691 (2006) 1092.
[260] L. Liu, M.-X. Li, W.-Y. Wong, Aust. J. Chem. 58 (2005) 799.
[261] L. Liu, S.-Y. Poon, W.-Y. Wong, J. Organomet. Chem. 690 (2005) 5036.
[262] L. Liu, W.-Y. Wong, S.-Y. Poon, J.-X. Shi, K.-W. Cheah, Z. Lin, Chem. Mater. 18 (2006) 1369.
[263] U.H.F. Bunz, Chem. Rev. 100 (2000) 1605.
[264] W.-Y. Wong, L. Liu, S.-Y. Poon, K.-H. Choi, K.-W. Cheah, J.-X. Shi, Macromolecules 37 (2004) 4496.
[265] S.-Y. Poon, W.-Y. Wong, K.-W. Cheah, J.-X. Shi, Chem. Eur. J. 12 (2006) 2550.
[266] L. Liu, W.-Y. Wong, J.-X. Shi, K.-W. Cheah, J. Polym. Sci. Part A: Polym. Chem. 44 (2006) 5588.
[267] L. Liu, W.-Y. Wong, J.-X. Shi, K.-W. Cheah, T.-H. Lee, L.-M. Leung, J. Organomet. Chem. 691 (2006) 4028.
[268] W.-Y. Wong, K.-H. Choi, G.-L. Lu, Organometallics 21 (2002) 4475.
[269] M.I. Bruce, B.C. Hall, P.J. Low, M.E. Smith, B.W. Skelton, A.H. White, Inorg. Chim. Acta 300–302 (2000) 633.
[270] M.I. Bruce, J.-F. Halet, B. Le Guennic, B.W. Skelton, M.E. Smith, A.H. White, Inorg. Chim. Acta 350 (2003) 175.
[271] M.I. Bruce, M. Jevric, B.W. Skelton, M.E. Smith, A.H. White, N.N. Zaitseva, J. Organomet. Chem. 691 (2006) 361.
[272] M.I. Bruce, N.N. Zaitseva, B.K. Nicholson, B.W. Skelton, A.H. White, J. Organomet. Chem. 693 (2008) 2887.
[273] M.I. Bruce, B.K. Nicholson, N.N. Zaitseva, C. R. Chimie 12 (2009) 1280.
[274] M. Bassetti, B. Floris, G. Illuminati, Organometallics 4 (1985) 617.
[275] P. Štěpnička, I. Císařová, J. Organomet. Chem. 691 (2006) 2863.
[276] M.I. Bruce, P.A. Humphrey, M. Jevric, G.J. Perkins, B.W. Skelton, A.H. White, J. Organomet. Chem. 692 (2007) 1748.
[277] H. Lang, R. Packheiser, B. Walfort, Organometallics 25 (2006) 1836.
[278] R. Packheiser, H. Lang, Europ. J. Inorg. Chem. (2007) 3786.
[279] R. Packheiser, P. Ecorchard, T. Rüffer, B. Walfort, H. Lang, Europ. J. Inorg. Chem. (2008) 4152.
[280] R. Packheiser, P. Ecorchard, T. Rüffer, H. Lang, Organometallics 27 (2008) 3534.
[281] R. Packheiser, P. Ecorchard, T. Rüffer, H. Lang, Chem. Eur. J. 14 (2008) 4948.
[282] R. Packheiser, A. Jakob, P. Ecorchard, B. Walfort, H. Lang, Organometallics 27 (2008) 1214.